SEPARATION PROCESS PRINCIPLES

Second Edition

J. D. SEADER / ERNEST J. HENLEY

Chapter 8

Liquid–Liquid Extraction with Ternary Systems

In *liquid–liquid extraction,* a liquid feed of two or more components to be separated is contacted with a second liquid phase, called the *solvent,* which is immiscible or only partly miscible with one or more components of the liquid feed and completely or partially miscible with one or more of the other components of the liquid feed. Thus, the solvent, which is a single chemical species or a mixture, partially dissolves certain components of the liquid feed, effecting at least a partial separation of the feed. Liquid–liquid extraction is sometimes called *extraction, solvent extraction,* or *liquid extraction.* These, as well as the term *solid–liquid extraction,* are also applied to the recovery of substances from a solid by contact with a liquid solvent, such as the recovery of oil from seeds by an organic solvent. Solid–liquid extraction (leaching) is covered in Chapter 16.

According to Derry and Williams [1], liquid extraction has been practiced since at least the time of the Romans, who separated gold and silver from molten copper by extraction using molten lead as a solvent. This was followed by the discovery that sulfur could selectively dissolve silver from an alloy with gold. However, it was not until the early 1930s that the first large-scale liquid–liquid extraction process began operation. In that industrial process, named after its inventor L. Edeleanu, aromatic and sulfur compounds were selectively removed from liquid kerosene by liquid–liquid extraction with liquid sulfur dioxide at 10 to 20°F. Removal of aromatic compounds resulted in a cleaner-burning kerosene. Liquid–liquid extraction has grown in importance in recent years because of the growing demand for temperature-sensitive products, higher-purity requirements, more efficient equipment, and availability of solvents with higher selectivity.

The simplest liquid–liquid extraction involves only a ternary system. The feed consists of two miscible components, the *carrier, C,* and the *solute, A.* Solvent, *S,* is a pure compound. Components *C* and *S* are at most only partially soluble in each other. Solute *A* is soluble in *C* and completely or partially soluble in *S.* During the extraction process, mass transfer of *A* from the feed to the solvent occurs, with less transfer of *C* to the solvent, or *S* to the feed. However, complete or nearly complete transfer of *A* to the solvent is seldom achieved in just one stage, as discussed in Chapter 4. In practice, a number of stages are used in one- or two-section, countercurrent cascades, as discussed in Chapter 5.

8.0 INSTRUCTIONAL OBJECTIVES

After completing this chapter, you should be able to:

- Explain differences among liquid–liquid extraction, stripping, and distillation.
- List situations where liquid–liquid extraction might be preferred to distillation.
- Explain why so many different types of equipment are used for liquid–liquid extraction.
- List major types of equipment used for liquid–liquid extraction and compare their advantages and disadvantages.
- List major factors involved in the selection of extraction equipment.
- List factors that influence liquid–liquid extraction.
- List characteristics of an ideal solvent.
- Define the distribution coefficient and show its relationship to activity coefficients and relative selectivity of a solute between carrier and solvent.
- Make a preliminary selection of a solvent using group-interaction rules.
- Distinguish, for ternary mixtures, between Type I and Type II systems.
- For a specified recovery of a solute, calculate with the Hunter and Nash method, using a triangular diagram, minimum solvent requirement and number of equilibrium stages for ternary liquid–liquid extraction in a countercurrent cascade.

- Determine usefulness of extract reflux and carry out calculations with the Maloney and Schubert graphical method for a two-section extraction cascade that uses extract reflux.
- Design a cascade of mixer-settler units based on mass-transfer considerations.
- Determine the size of multicompartment extraction columns, including consideration of the effect of axial dispersion.

Industrial Example

Acetic acid is produced by methanol carbonylation or oxidation of acetaldehyde, or as a by-product of cellulose-acetate manufacture. In all three cases, a mixture of acetic acid (normal b.p. = 118.1°C) and water (normal b.p. = 100°C) must be separated to give glacial acetic acid (99.8 wt% min). When the mixture contains less than 50% acetic acid, separation by distillation is expensive because of the need to vaporize large amounts of the more volatile water, with its very high heat of vaporization. Accordingly, an alternative liquid–liquid extraction process is often considered. A typical implementation is shown in Figure 8.1. In this process, it is important to note that two additional distillation separation steps are required to recover the solvent for recycle to the extractor. These additional separation steps are common to almost all extraction processes.

In the process of Figure 8.1, a feed of 30,260 lb/h, of 22 wt% acetic acid in water, is sent to a single-section extraction column, operating at near-ambient conditions, where the feed is countercurrently contacted with 71,100 lb/h of

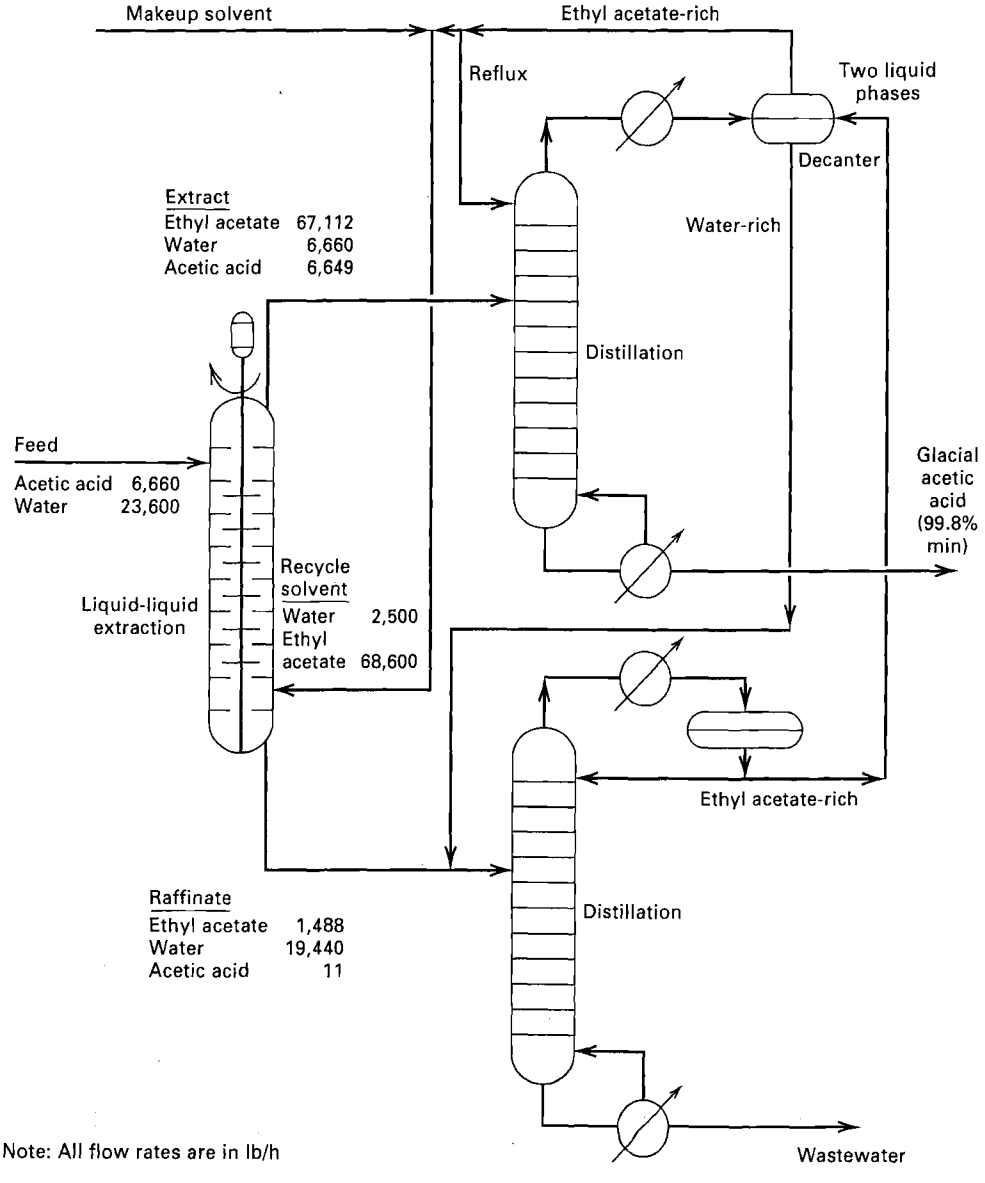

Figure 8.1 Typical liquid–liquid extraction process.

ethyl-acetate solvent (normal b.p. = 77.1°C), saturated with water. The extract (solvent-rich product), being the low-density liquid phase, exits from the top of the extractor with 99.8% of the acetic acid originally contained in the feed. The raffinate (carrier-rich product), being the high-density liquid phase, exits from the bottom of the extractor and contains only 0.05 wt% acetic acid. The extract is sent to a distillation column, where glacial acetic acid is the bottoms product. The overhead vapor, which is rich in ethyl acetate but which also contains appreciable water vapor, splits into two liquid phases upon condensation. The two phases are separated by gravity in the decanter. The lighter ethyl-acetate-rich phase is divided into two streams. One is used for reflux for the distillation operation and the other is used for solvent recycle to the extractor.

The water-rich phase from the decanter is sent, together with the raffinate from the extractor, to a second distillation column, where wastewater is removed from the bottom and the ethyl-acetate-rich overhead distillate is recycled to the decanter. Makeup ethyl-acetate solvent is provided for solvent losses to the glacial acetic acid and wastewater products.

At an average extraction temperature of 100°F, six equilibrium stages are required to transfer 99.8% of the acetic acid from the feed to the extract using a solvent-to-feed ratio of 2.35 on a weight basis, where the recycled solvent is saturated with water. For six theoretical stages, a mechanically assisted extractor is preferred and a rotating-disk contactor (RDC), in a column configuration, is shown in Figure 8.1. The organic-rich phase is dispersed into droplets by rotating disks, while the water-rich phase is a continuous phase throughout the column. Dispersion and subsequent coalescence and settling takes place easily because at extractor operating conditions, liquid-phase viscosities are less than 1 cP, the phase-density difference is more than 0.08 g/cm^3, and the interfacial tension between the two phases is appreciable, at more than 30 dyne/cm.

The column has an inside diameter of 5.5 ft and a total height from the tangent of the top head to the tangent of the bottom head of 28 ft. The column is divided into 40 compartments, each 7.5 in. high and each containing a 40-in.-diameter rotor disk located between a pair of stator (donut) rings of 46-in. inside diameter. Above the top stator ring and below the bottom stator ring are settling zones. Because the light liquid phase is dispersed, the liquid–liquid interface is maintained near the top of the column. The rotors are mounted on a centrally located single shaft driven at a nominal 60 rpm by a 5-hp motor, equipped with a speed changer, the optimal disk speed being determined during plant operation. The HETP for the extractor is 50 in., equivalent to 6.67 compartments per theoretical stage. The HETP would be only 33 in. if axial (longitudinal) mixing did not occur. Because of the corrosive nature of aqueous acetic acid solutions, the extractor is constructed of stainless steel. Since 1948, hundreds of extraction columns similar to that of Figure 8.1, with diameters ranging up to at least 25 ft, have been built. As discussed in Section 8.1, a number of other extraction devices are suitable for the process in Figure 8.1.

Liquid–liquid extraction is a reasonably mature separation operation, although not as mature or as widely applied as distillation, absorption, and stripping. Since the 1930s, more than 1,000 laboratory, pilot-plant, and industrial extractors have been installed. Procedures for determining the number of theoretical stages to achieve a desired solute recovery are well established. However, in the thermodynamics of liquid–liquid extraction, no simple limiting theory, such as that of ideal solutions for vapor–liquid equilibrium, exists. In many cases, experimental equilibrium data are preferred over predictions based on activity-coefficient correlations. However, such data can often be correlated well by semi-theoretical activity-coefficient equations such as the NRTL or UNIQUAC equations discussed in Chapter 2. Also, considerable laboratory effort may be required just to find an acceptable and efficient solvent. Furthermore, as will be discussed in the next section, a wide variety of industrial extraction equipment is available, making it necessary to consider many alternatives before making a final selection. Unfortunately, no generalized capacity and efficiency correlations are available for all equipment types. Often, equipment vendors must be relied upon to determine equipment size, or pilot-plant tests must be performed, followed by application of scale-up procedures recommended by the vendor or taken from sources such as this textbook.

Since the introduction of industrial liquid–liquid extraction processes, a large number of applications have been proposed and developed. The petroleum industry represents the largest-volume application for liquid–liquid extraction. By the late 1960s, more than 100,000 m^3/day of liquid feedstocks were being processed with physically selective solvents [2]. Extraction processes are well suited to the petroleum industry because of the need to separate heat-sensitive liquid feeds according to chemical type (e.g., aliphatic, aromatic, naphthenic) rather than by molecular weight or vapor pressure. Table 8.1 shows some representative, industrial extraction processes. Other major applications exist in the biochemical industry, where emphasis is on the separation of antibiotics and protein recovery from natural substrates; in the recovery of metals, such as copper from ammoniacal leach liquors, and in separations involving rare metals and radioactive isotopes from spent-fuel elements; and in the inorganic chemical industry, where high-boiling constituents

Table 8.1 Representative Industrial Liquid–Liquid Extraction Processes

Solute	Carrier	Solvent
Acetic acid	Water	Ethyl acetate
Acetic acid	Water	Isopropyl acetate
Aconitic acid	Molasses	Methyl ethyl ketone
Ammonia	Butenes	Water
Aromatics	Paraffins	Diethylene glycol
Aromatics	Paraffins	Furfural
Aromatics	Kerosene	Sulfur dioxide
Aromatics	Paraffins	Sulfur dioxide
Asphaltenes	Hydrocarbon oil	Furfural
Benzoic acid	Water	Benzene
Butadiene	1-Butene	*aq.* Cuprammonium acetate
Ethylene cyanohydrin	Methyl ethyl ketone	Brine liquor
Fatty acids	Oil	Propane
Formaldehyde	Water	Isopropyl ether
Formic acid	Water	Tetrahydrofuran
Glycerol	Water	High alcohols
Hydrogen peroxide	Anthrahydroquinone	Water
Methyl ethyl ketone	Water	Trichloroethane
Methyl borate	Methanol	Hydrocarbons
Naphthenes	Distillate oil	Nitrobenzene
Naphthenes/ aromatics	Distillate oil	Phenol
Phenol	Water	Benzene
Phenol	Water	Chlorobenzene
Penicillin	Broth	Butyl acetate
Sodium chloride	*aq.* Sodium hydroxide	Ammonia
Vanilla	Oxidized liquors	Toluene
Vitamin A	Fish-liver oil	Propane
Vitamin E	Vegetable oil	Propane
Water	Methyl ethyl ketone	*aq.* Calcium chloride

such as phosphoric acid, boric acid, and sodium hydroxide need to be recovered from aqueous solutions.

In general, extraction is preferred to distillation for the following applications:

1. In the case of dissolved or complexed inorganic substances in organic or aqueous solutions.
2. The removal of a component present in small concentrations, such as a color former in tallow or hormones in animal oil.
3. When a high-boiling component is present in relatively small quantities in an aqueous waste stream, as in the recovery of acetic acid from cellulose acetate. Extraction becomes competitive with distillation because of the expense of evaporating large quantities of water with its very high heat of vaporization.
4. The recovery of heat-sensitive materials, where extraction may be less expensive than vacuum distillation.
5. The separation of a mixture according to chemical type rather than relative volatility.
6. The separation of close-melting or close-boiling liquids, where solubility differences can be exploited.
7. Mixtures that form azeotropes.

The key to an effective extraction process is the discovery of a suitable solvent. In addition to being stable, nontoxic, inexpensive, and easily recoverable, a good solvent should be relatively immiscible with feed components(s) other than the solute and have a different density from the feed to facilitate phase separation. Also, it must have a very high affinity for the solute, from which it should be easily separated by distillation, crystallization, or other means. Ideally, the distribution coefficient for the solute between the two liquid phases should be greater than 1; otherwise a large solvent-to-feed ratio is required. When the degree of solute extraction is not particularly high and/or when a large extraction factor can be achieved, an extractor will not require many stages. This is fortunate because mass-transfer resistance in liquid–liquid systems is often high and stage efficiency is low in commercial contacting devices, unless mechanical agitation is provided.

In this chapter, equipment for conducting liquid–liquid extraction operations is discussed and fundamental equilibrium-based and rate-based calculation procedures are presented mainly for extraction in ternary systems. The use of graphical methods is emphasized. Except for systems dilute in solute(s), calculations for higher-order multicomponent systems are best conducted with computer-aided methods discussed in Chapter 10.

8.1 EQUIPMENT

Given the wide diversity of applications, one might expect a correspondingly large variety of liquid–liquid extraction devices. Indeed, such is the case. Equipment similar to that used for absorption, stripping, and distillation is sometimes used, but such devices are inefficient unless liquid viscosities are low and the difference in phase density is high. For that reason, centrifugal and mechanically agitated devices are often preferred. Regardless of the type of equipment, the necessary number of theoretical stages is computed. Then the size of the device for a continuous, countercurrent process is obtained from experimental HETP or mass-transfer-performance-data characteristic of the particular piece of equipment. In extraction, some authors use the acronym HETS, height equivalent to a theoretical stage, rather than HETP. Also, the dispersed phase is sometimes referred to as the *discontinuous phase,* the other phase being the *continuous phase.*

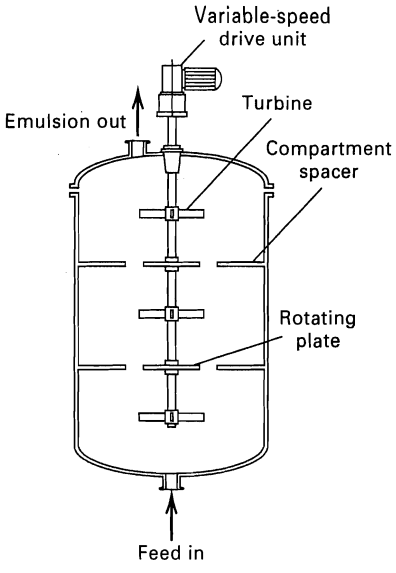

Figure 8.2 Compartmented mixing vessel with variable-speed turbine agitators.

[Adapted from R.E. Treybal, *Mass Transfer,* 3rd ed., McGraw-Hill, New York (1980).]

Mixer-Settlers

In mixer-settlers, the two liquid phases are first mixed (Figure 8.2) and then separated by settling (Figure 8.4). Any number of mixer-settler units may be connected together to form a multistage, countercurrent cascade. During mixing, one of the liquids is dispersed in the form of small droplets into the other liquid phase. The dispersed phase may be either the heavier or the lighter of the two phases. The mixing

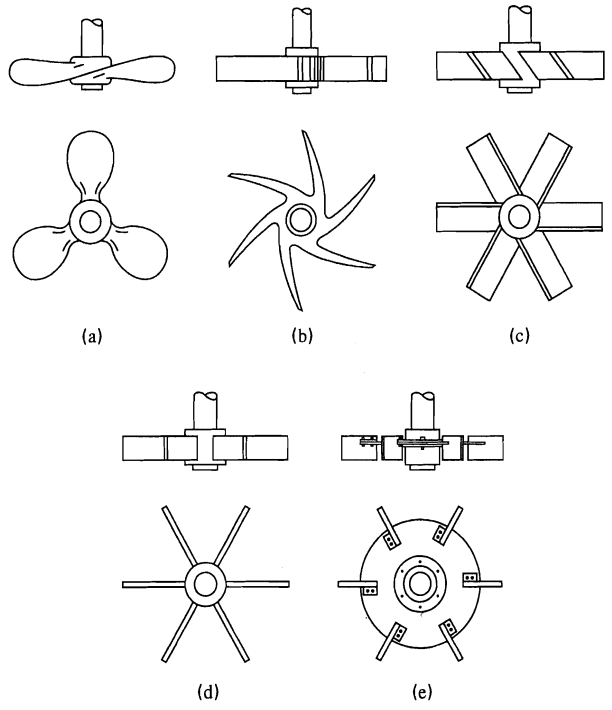

Figure 8.3 Some common types of mixing impellers: (a) marine-type propeller; (b) centrifugal turbine; (c) pitched-blade turbine; (d) flat-blade paddle; (e) flat-blade turbine.

[From R.E. Treybal, *Mass Transfer,* 3rd ed., McGraw-Hill, New York (1980) with permission.]

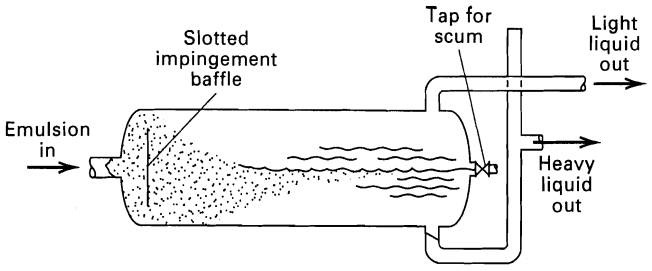

Figure 8.4 Horizontal gravity-settling vessel.

[Adapted from R.E. Treybal, *Liquid Extraction,* 2nd ed., McGraw-Hill, New York (1963) with permission.]

step is commonly conducted in an agitated vessel, with sufficient agitation and residence time so that a reasonable approach to equilibrium (e.g., 80% to 90% of a theoretical stage) is attained. The vessel may be compartmented as shown in Figure 8.2, and is usually agitated by means of impellers of the type shown in Figure 8.3. If dispersion is easily achieved and equilibrium is rapidly approached, as with liquids of low interfacial tension and viscosity, the mixing step can be carried out by impingement in a jet mixer; by turbulence in a nozzle mixer, orifice mixer, or other in-line mixing device; by shearing action if both phases are fed simultaneously into a centrifugal pump; or by injectors, wherein the flow of one liquid is induced by another.

The settling step is by gravity in a second vessel called a settler or decanter. In the configuration shown in Figure 8.4, a horizontal vessel, with an impingement baffle to prevent the jet of the entering two-phase dispersion (emulsion) from disturbing the gravity-settling process, is used. Vertical and inclined vessels are also used. A major problem in settlers is the emulsification in the mixing vessel, which may occur if the agitation is so intense that the dispersed droplet size falls below 1 to 1.5 micrometers. When this happens, coalescers, separator membranes, meshes, electrostatic forces, ultrasound, chemical treatment, or other ploys are required to speed settling. The rate of settling can also be increased by substituting centrifugal for gravitational force. This may be necessary if the phase-density difference is small.

A large number of commercial single- and multi-stage mixer-settler units are available, many of which are described by Bailes, Hanson, and Hughes [3] and by Lo, Baird, and Hanson [4]. Particularly worthy of mention is the Lurgi extraction tower [4], which was originally developed for extracting aromatics from hydrocarbon mixtures. In this device, the phases are mixed by centrifugal mixers stacked vertically outside the column and driven from a single shaft. Settling takes place in the column, with phases flowing interstagewise, guided by a complex baffle design located within the settling zones.

Spray Columns

The simplest and one of the oldest extraction devices is the spray column. Either the heavy phase or the light phase can be dispersed, as shown in Figure 8.5. The droplets of the

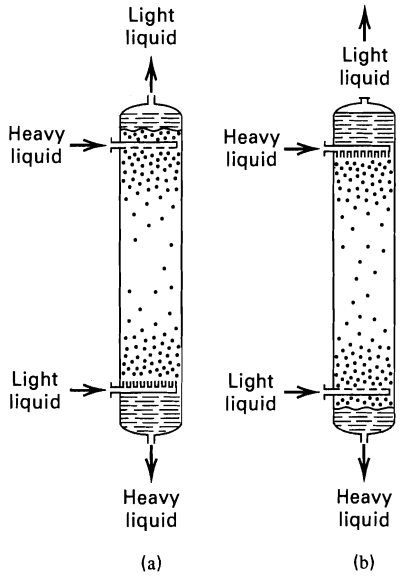

Figure 8.5 Spray columns: (a) light liquid dispersed, heavy liquid continuous; (b) heavy liquid dispersed, light liquid continuous.

dispersed phase are generated only at the inlet, usually by spray nozzles. Because of lack of column internals, throughputs are large, depending upon phase-density difference and phase viscosities. As in gas absorption, *axial dispersion* (*backmixing*) in the continuous phase limits these devices to applications where only one or two stages are required. Axial dispersion is so serious for columns with large diameter-to-length ratio that the continuous phase may be completely mixed. Therefore, spray columns are rarely used, despite their very low cost.

Packed Columns

Axial mixing in a spray column can be substantially reduced, but not eliminated, by packing the column. The packing also improves mass transfer by breaking up large drops to increase interfacial area and promotes mixing in drops by distorting droplet shape. With the exception of Raschig rings [5], the same packings used in distillation and absorption are employed for liquid–liquid extraction. The choice of packing material, however, is somewhat more critical. A material preferentially wetted by the continuous phase is preferred. Figure 8.6 shows performance data, in terms of HTU, for Intalox saddles in an extraction service as a function of continuous, U_C, and discontinuous, U_D, phase superficial velocities. Because of backmixing, the HETP is generally larger than for staged devices. For that reason, packed columns are used only where few stages are needed.

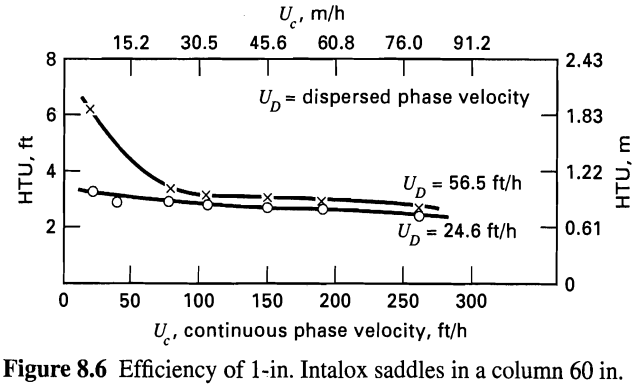

Figure 8.6 Efficiency of 1-in. Intalox saddles in a column 60 in. high with MEK–water–kerosene.

[From R.R. Neumatis, J.S. Eckert, E.H. Foote, and L.R. Rollinson, *Chem. Eng. Progr.*, *67*(1), 60 (1971) with permission.]

Plate Columns

Sieve plates in a column also reduce axial mixing and achieve a more stagewise type of contact. The dispersed phase may be the light or the heavy phase. In the former case, the dispersed phase, analogous to vapor bubbles in distillation, flows vertically up the column, with redispersion at each tray. The heavy phase is the continuous phase, flowing at each stage through a *downcomer* and then across the tray the way a liquid does in a trayed distillation tower. If the heavy phase is dispersed, *upcomers* are used for the light phase. Columns have been built and successfully operated for diameters larger than 4.5 m. Holes from 0.64 to 0.32 cm in diameter and 1.25 to 1.91 cm apart are commonly used. Tray spacings are much closer than in distillation—10 to 15 cm in most applications involving low-interfacial-tension liquids. Plates are usually built without outlet weirs on the downspouts. A variation of the simple sieve column is the Koch Kascade Tower, where perforated plates are set in vertical arrays of complex designs.

If operated in the proper hydrodynamic flow regime, extraction rates in sieve-plate columns are high because the dispersed-phase droplets coalesce and re-form on each stage. This helps destroy concentration gradients, which develop if a droplet passes through the entire column without disturbance. Sieve-plate columns in extraction service are subject to the same limitations as distillation columns: flooding, entrainment, and, to a lesser extent, weeping. Additional problems, such as scum formation at interfaces due to small amounts of impurities, are frequently encountered in all types of extraction devices.

Columns with Mechanically Assisted Agitation

If the surface tension is high, and/or the density difference between the two liquid phases is low, and/or liquid viscosities are high, gravitational forces are inadequate for proper phase dispersal and the creation of turbulence. In that case, some type of mechanical agitation is necessary to increase interfacial area per unit volume and/or decrease mass-transfer resistance. For packed and plate columns, agitation is provided by an oscillating pulse to the liquid, either by mechanical or pneumatic means. Pulsed, perforated-plate columns found considerable application in the nuclear

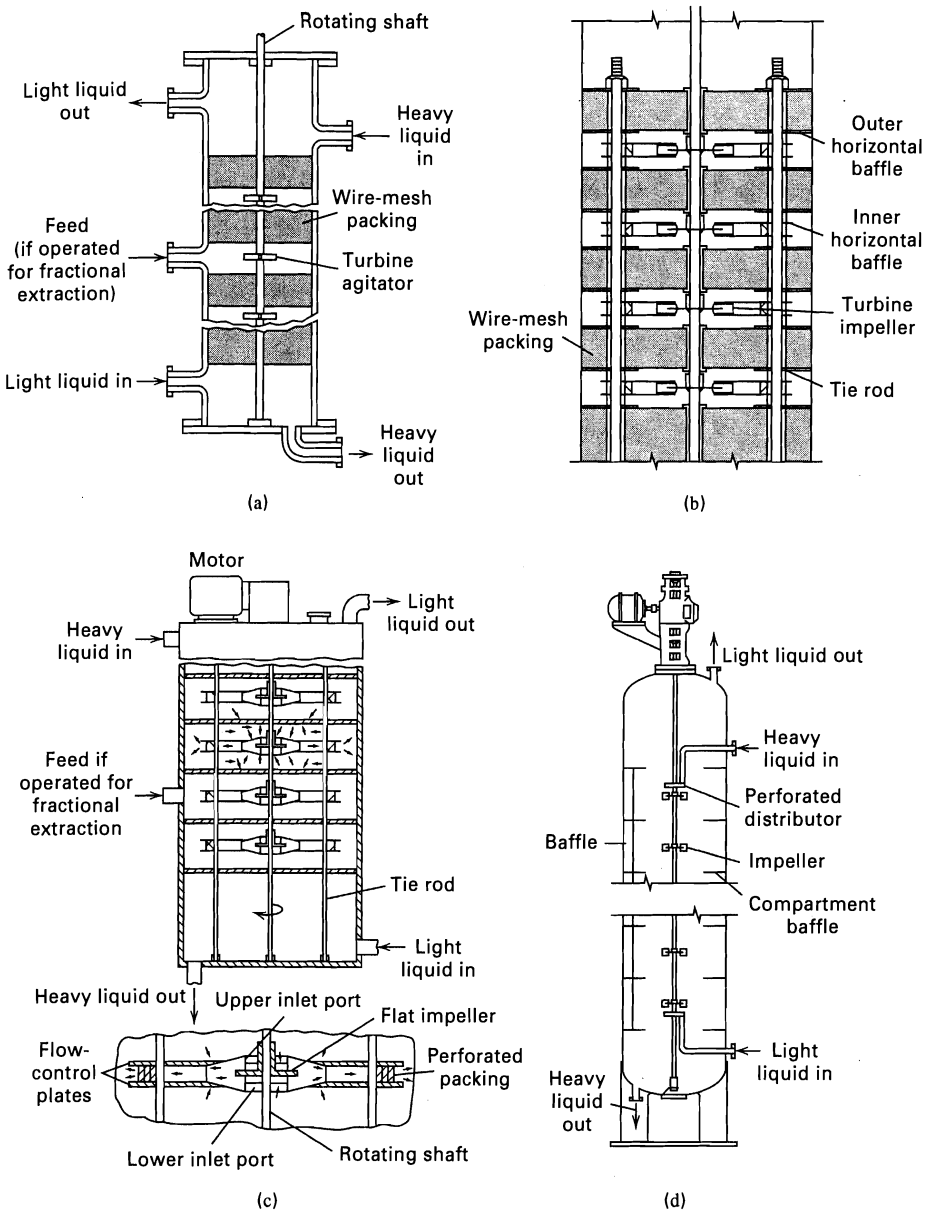

Figure 8.7 Commercial extractors with mechanically assisted agitation: (a) Scheibel column—first design; (b) Scheibel column—second design; (c) Scheibel column—third design; (d) Oldshue–Rushton (Mixco) column; (*continued*)

industry in the 1950s, but their popularity declined because of mechanical problems and the difficulty of propagating a pulse through a large volume [6]. The most important mechanically agitated columns are those that employ rotating agitators, driven by a shaft that extends axially through the column. The agitators create shear mixing zones, which alternate with settling zones in the column. Differences among the various agitated columns lie primarily in the mixers and settling chambers used. Nine of the more popular arrangements are shown in Figure 8.7. Agitation can also be induced in a column by moving the plates back and forth in a reciprocating motion (Figure 8.7j) or in a novel horizontal contactor (Figure 8.7k). Such devices are also included in Figure 8.7. These devices answer the plea of Fenske, Carlson, and Quiggle [7] in 1947 for equipment that can efficiently provide large numbers of equilibrium stages in a compact device without large numbers of pumps and motors, and extensive piping. They stated, "Despite . . . advantages of liquid–liquid separational processes, the problems of accumulating twenty or more theoretical stages in a small compact and relatively simple countercurrent operation have not yet been fully solved." Indeed, in 1946 it was considered impractical to design for more than seven theoretical stages, which represented the number of mixer-settler units in the only large-scale, commercial, liquid-extraction process in use at that time.

Perhaps the first mechanically agitated column of importance was the Scheibel column [8] (Figure 8.7a), in which countercurrent liquid phases are contacted at fixed intervals by unbaffled, flat-bladed, turbine-type agitators (Figure 8.3) mounted on a vertical shaft. In the unbaffled separation or calming zones, located between the mixing zones, knitted wire-mesh packing is installed to prevent backmixing between mixing zones and to induce coalescence and

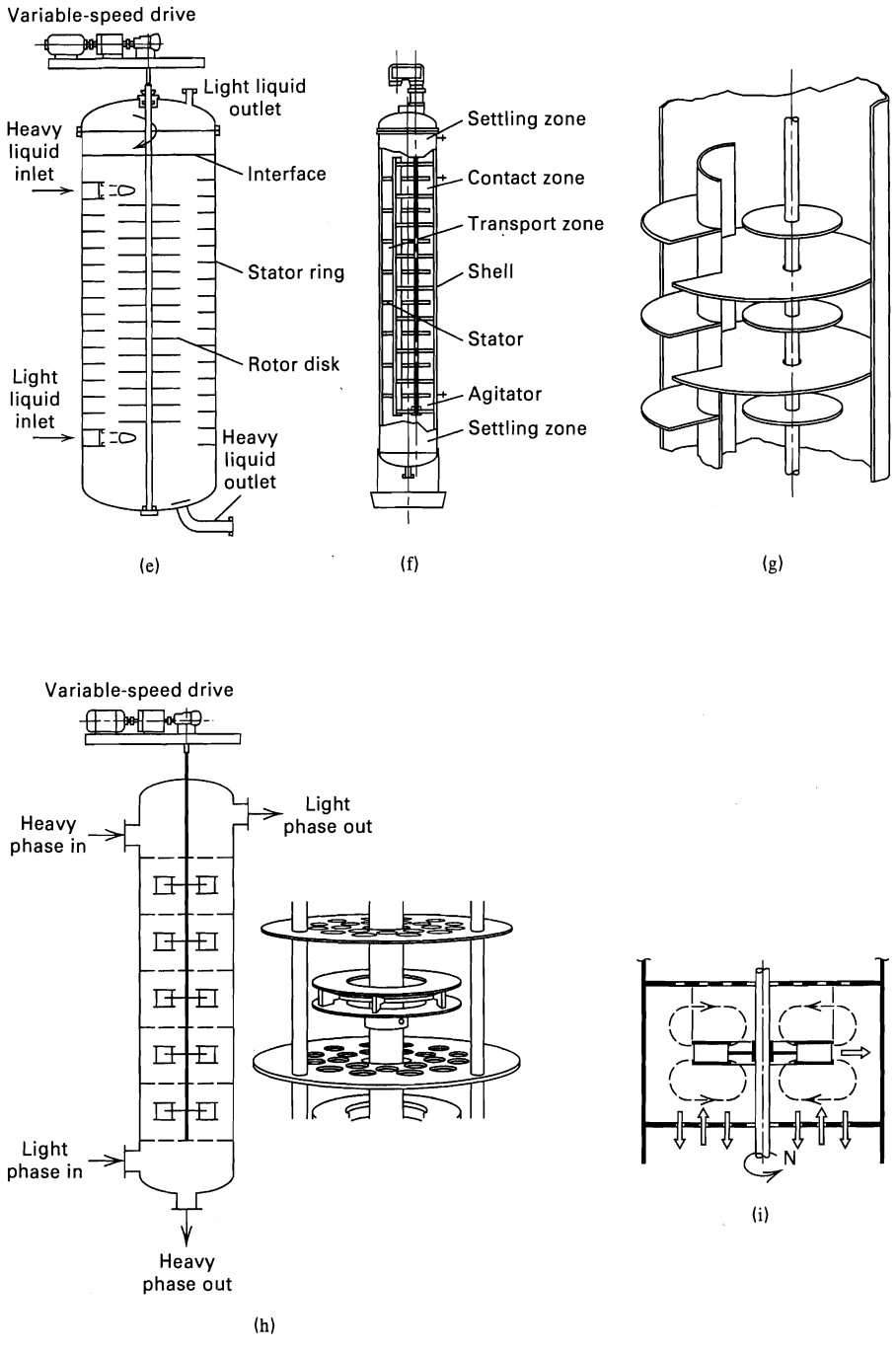

Figure 8.7 (*Continued*) (e) rotating-disk-contactor (RDC); (f) asymmetric rotating-disk contactor (ARD); (g) section of ARD contactor; (h) Kuhni column; (i) flow pattern in Kuhni column.

settling of drops. The mesh material must be wetted by the dispersed phase. For more economical designs for larger-diameter installations (>1 m), Scheibel [9] (Figure 8.7b) added outer and inner horizontal annular baffles to divert the vertical flow of the phases in the mixing zone and to ensure complete mixing. For systems with high interfacial surface tension and viscosities, the wire mesh is removed. The first two Scheibel designs did not permit removal of the agitator shaft for inspection and maintenance. Instead, the entire internal assembly (called the cartridge) had to be removed. To permit removal of just the agitator assembly shaft, especially for large-diameter columns (e.g., >1.5 m), and allow an access way through the column for any necessary inspection, cleaning, and repair, Scheibel [10] offered a third design, shown in Figure 8.7c. Here the agitator assembly shaft can be removed because it has a smaller diameter than the opening in the inner baffle.

The Oldshue–Rushton extractor [11] (Figure 8.7d) consists of a column with a series of compartments separated by annular outer stator-ring baffles, each with four vertical baffles attached to the wall. The centrally mounted vertical shaft drives a flat-bladed turbine impeller in each compartment.

A third type of column with rotating agitators that appeared about the same time as the Scheibel and Oldshue–Rushton columns is the rotating-disk contactor (RDC)

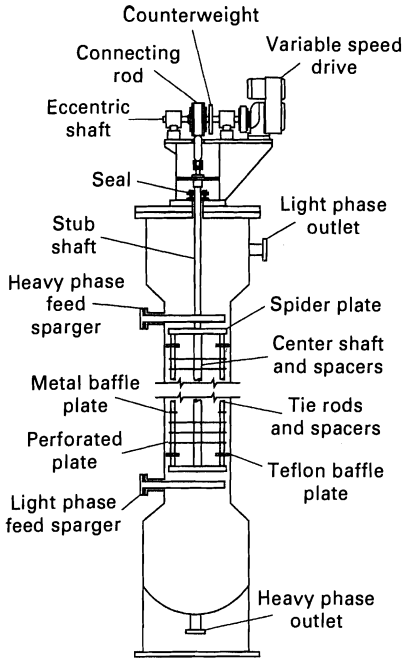

(j)

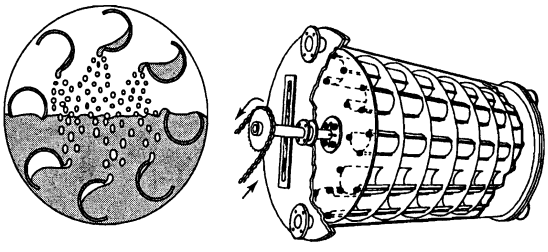

(k)

Figure 8.7 (*Continued*) (j) Karr reciprocating-plate column (RPC); (k) Graesser raining-bucket (RTL) extractor.

[12, 13] (Figure 8.7e), an example of which is described at the beginning of this chapter and shown in Figure 8.1. On a worldwide basis, it is probably the most extensively used liquid–liquid extraction device, with hundreds of units in use by 1983 [4]. Horizontal disks, mounted on a centrally located rotating shaft, are the agitation elements. Mounted at the column wall are annular stator rings with an opening larger than the agitator-disk diameter. Thus, the agitator assembly shaft is easily removed from the column. Because the rotational speed of the rotor controls the drop size, the rotor speed can be continuously varied over a wide range.

A modification of the RDC concept is the asymmetric rotating-disk contactor (ARD) [14], which has been in industrial use since 1965. As shown in Figure 8.7f, the contactor consists of a column, a baffled stator, and an offset multistage agitator fitted with disks. The asymmetric arrangement, shown in more detail in Figure 8.7g, provides contact and transport zones that are separated by a vertical baffle, to which is attached a series of horizontal baffles. Compared to the RDC, this design retains the efficient shearing action, but reduces backmixing because of the separate mixing and settling compartments.

Another extractor based on the Scheibel concept is the Kuhni extraction column [15]. As shown in Figure 8.7h, the column is compartmented by a series of stator disks made of perforated plates. On a centrally positioned shaft is mounted a series of double-entry, radial-flow, shrouded-turbine mixers, which promote, in each compartment, the circulation action shown in Figure 8.7i. For columns of diameter greater than 3 m, three turbine-mixer shafts on parallel axes are normally provided to preserve scale-up. Three hundred of these extractors were in use, mainly in Europe, by 1983 [4].

Rather than provide agitation by rotating impellers on a vertical shaft, or by pulsing the liquid phases, Karr [16, 17] devised a reciprocating, perforated-plate extractor, also called the Karr column, in which the plates move up and down approximately two times per second with a stroke length of 0.75 inch. As shown in Figure 8.7j, annular baffle plates are provided periodically in the plate stack to minimize axial mixing. The perforated plates use large holes (typically 9/16-in. diameter) and a high hole area (typically 58%). The central shaft, which supports both sets of plates, is reciprocated by a drive mechanism located at the top of the column. A modification of the Karr column is the vibrating-plate extractor (VPE) of Prochazka et al. [18], which uses perforated plates of smaller hole size and smaller percent hole area than the Karr column. The small holes provide passage for the dispersed phase, while one or more large holes on each plate provide passage for the continuous phase. Some VPE columns operate like the Karr column with uniform motion of all plates; others are provided with two shafts to obtain countermotion of alternate plates.

Another novel device for providing agitation is the Graesser raining-bucket contactor (RTL), which was developed in the late 1950s [4], primarily for extraction processes involving liquids of small density difference, low interfacial tension, and a tendency to form emulsions As shown in Figure 8.7k, a series of disks is mounted inside a shell on a central, horizontal, rotating shaft, with a series of horizontal, C-shaped buckets fitted between and around the periphery of the disks. An annular gap between the disks and the inside perphery of the shell allows countercurrent, longitudinal

flow of the phases. Dispersing action is very gentle, with each phase cascading through the other in opposite directions toward the two-phase interface, which is maintained close to the equatorial position.

A number of industrial centrifugal extractors have been available since 1944, when the Podbielniak (POD) extractor, with its short residence time, was successfully applied to penicillin extraction [19]. In the POD, several concentric sieve trays are arranged around a horizontal axis through which the two liquid phases flow countercurrently. Liquid inlet pressures of 4 to 7 atm are required to overcome pressure drop and centrifugal force. As many as five theoretical stages can be achieved in one unit.

Many of the commercial extractors described above have seen numerous industrial applications. Maximum loadings and sizes for column-type equipment, as given by Reissinger and Schroeter [5, 20] and Lo et al. [4], are listed in Table 8.2. As seen, the Lurgi tower, RDC, and Graesser extractors have been built in very large sizes. Throughputs per unit cross-sectional area are highest for the Karr extractor and lowest for the Graesser extractor.

The selection of an appropriate extractor is based on a large number of factors. Table 8.3 lists the advantages and disadvantages of the various types of extractors. Figure 8.8 shows a selection scheme for commercial extractors. For example, if only a small number of stages is required, a mixer-settler unit might be selected. If more than five theoretical stages, a high throughput, and a large load range (m^3/m^2-h) are needed, and floor space is limited, an RDC or ARD contactor should be considered.

Table 8.2 Maximum Size and Loading for Commercial Liquid–Liquid Extraction Columns

Column Type	Approximate Maximum Liquid Throughout, m^3/m^2-h	Maximum Column Diameter, m
Lurgi tower	30	8.0
Pulsed packed	40	3.0
Pulsed sieve tray	60	3.0
Scheibel	40	3.0
RDC	40	8.0
ARD	25	5.0
Kuhni	50	3.0
Karr	100	1.5
Graesser	<10	7.0

Above data apply to systems of:

1. High interfacial surface tension (30 to 40 dyne/cm).
2. Viscosity of approximately 1 cP.
3. Volumetric phase ratio of 1:1.
4. Phase-density difference of approximately 0.6 g/cm^3.

Table 8.3 Advantages and Disadvantages of Different Extraction Equipment

Class of Equipment	Advantages	Disadvantages
Mixer-settlers	Good contacting Handles wide flow ratio Low headroom High efficiency Many stages available Reliable scale-up	Large holdup High power costs High investment Large floor space Interstage pumping may be required
Continuous, counterflow contactors (no mechanical drive)	Low initial cost Low operating cost Simplest construction	Limited throughput with small density difference Cannot handle high flow ratio High headroom Sometimes low efficiency Difficult scale-up
Continuous, counterflow contactors (mechanical agitation)	Good dispersion Reasonable cost Many stages possible Relatively easy scale-up	Limited throughput with small density difference Cannot handle emulsifying systems Cannot handle high flow ratio
Centrifugal extractors	Handles low-density difference between phases Low holdup volume Short holdup time Low space requirements Small inventory of solvent	High initial costs High operating cost High maintenance cost Limited number of stages in single unit

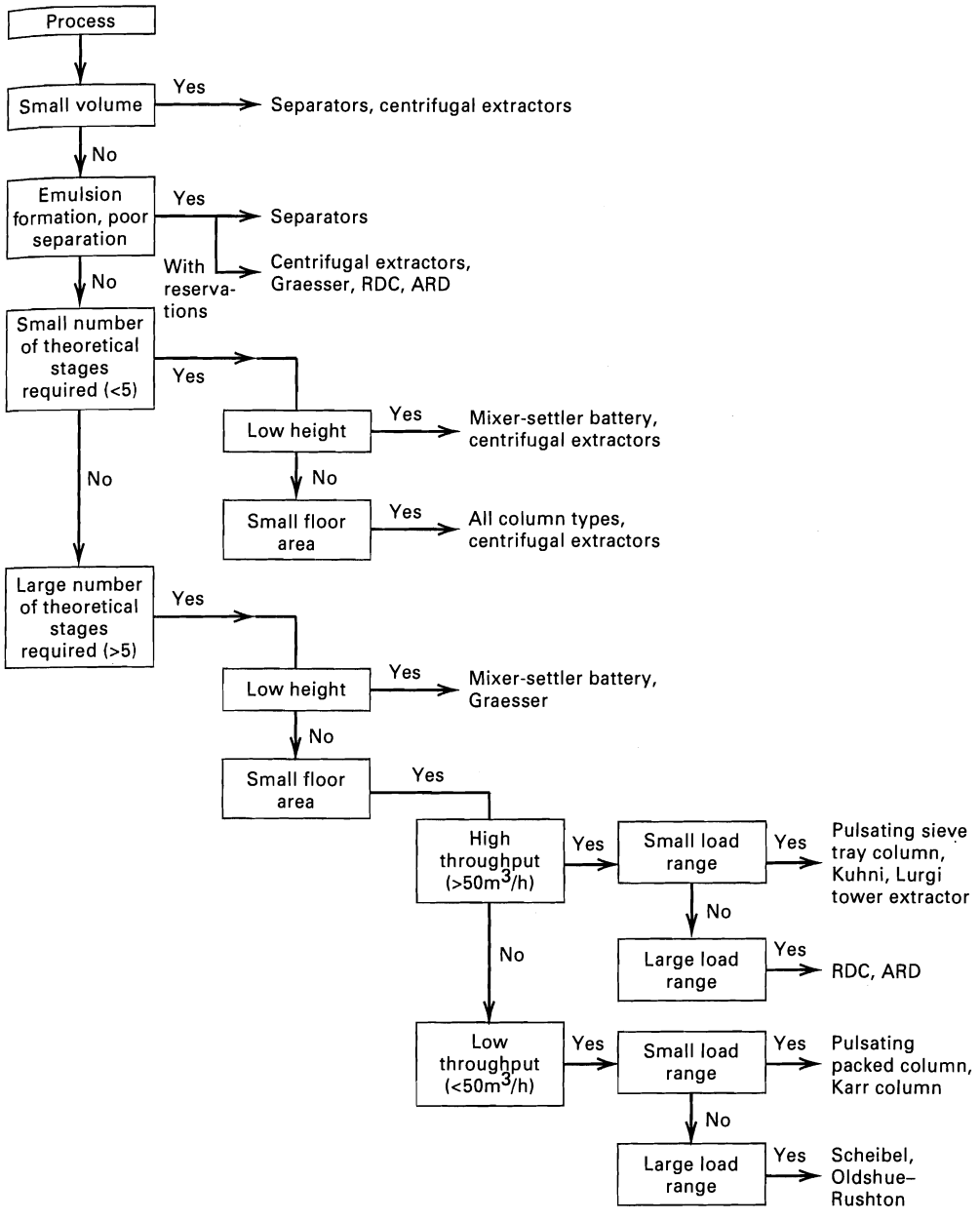

Figure 8.8 Scheme for selecting extractors.
[From K.-H. Reissinger and J. Schroeter, *I. Chem. E. Symp. Ser. No.* **54,** 33–48 (1978).]

8.2 GENERAL DESIGN CONSIDERATIONS

The design and analysis of a liquid–liquid extractor involves more factors than for vapor–liquid operations because of complications introduced by the two liquid phases. One of the three different cascade arrangements in Figure 8.9, or a more complex arrangement, must be selected. The single-section cascade of Figure 8.9a is similar to that used for absorption and stripping. It is designed to transfer to the solvent a certain percentage of the solute in the feed. The two-section cascade of Figure 8.9b is similar to distillation. Solvent enters at one end and reflux, derived from the extract, enters at the other end. The feed enters between the two sections. With two sections, depending on solubility considerations, it is sometimes possible to achieve a reasonably sharp separation between components of the feed; if not, a dual-solvent arrangement with two sections, as in Figure 8.9c, with or without reflux at the two ends, may be advantageous.

For the latter configuration, which involves a minimum of four components (two in the feed and two solvents), computer-aided calculations are preferred, as discussed in Chapter 10. Although the configurations in Figure 8.9 are shown with packed sections, any of the extractors discussed in Section 8.1 may be considered. The factors influencing extraction include:

1. Entering feed flow rate, composition, temperature, and pressure
2. Type of stage configuration (one-section or two-section)
3. Desired degree of recovery of one or more solutes for one-section cascades
4. Degree of separation of the feed for two-section cascades
5. Choice of liquid solvent(s)

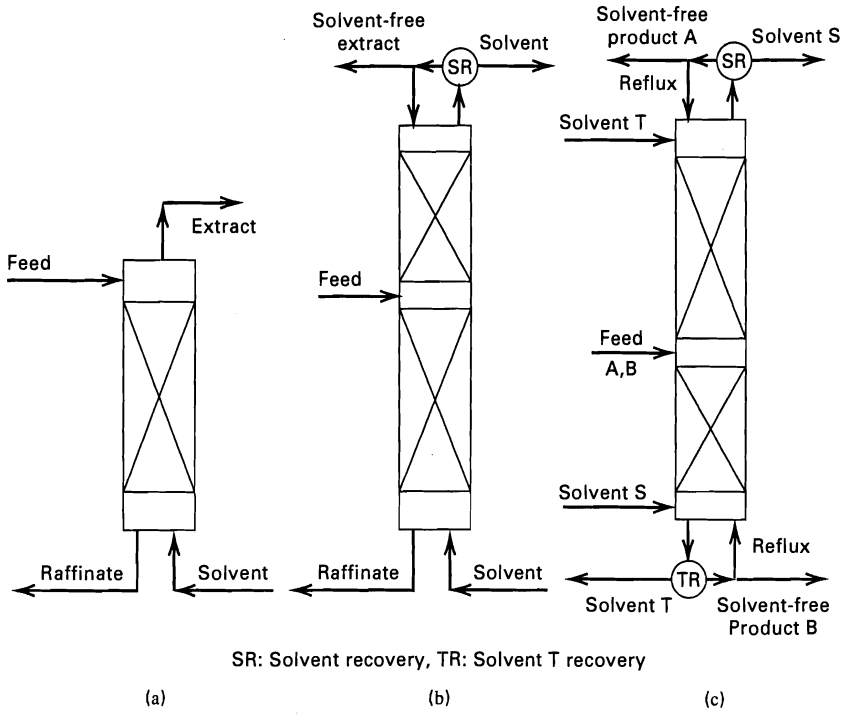

Figure 8.9 Common liquid–liquid extraction cascade configurations: (a) single-section cascade; (b) two-section cascade; (c) dual solvent with two-section cascade.

6. Operating temperature
7. Operating pressure (greater than the bubble point of the system)
8. Minimum-solvent flow rate and actual solvent flow rate as a multiple of the minimum rate for one-section cascades or reflux rate and minimum reflux ratio for two-section cascades
9. Number of equilibrium stages
10. Emulsification and scum-formation tendency
11. Interfacial tension
12. Phase-density difference
13. Type of extractor
14. Extractor size and horsepower requirement

The ideal solvent has:

1. A high selectivity for the solute relative to the carrier, so as to minimize the need to recover carrier from the solvent
2. A high capacity for dissolving the solute, so as to minimize the solvent-to-feed ratio
3. A minimal solubility in the carrier
4. A volatility sufficiently different from the solute that recovery of the solvent can be achieved by distillation, but the vapor pressure should not be so high that a high extractor pressure is needed or so low that a high temperature is needed if the solvent is recovered by distillation
5. Stability to maximize the solvent life and minimize the solvent make-up requirement
6. Inertness to permit use of common materials of construction
7. A low viscosity to promote phase separation, minimize pressure drop, and provide a high solute mass-transfer rate
8. Nontoxic and nonflammable characteristics to facilitate its safe use
9. Availability at a relatively low cost
10. A moderate interfacial tension to balance the ease of dispersion and the promotion of phase separation
11. A large difference in density relative to the carrier to achieve a high capacity in the extractor
12. Compatibility with the solute and carrier to avoid contamination
13. A lack of tendency to form a stable rag or scum layer at the phase interface
14. Desirable wetting characteristics with respect to extractor internals

Solvent selection is frequently a compromise among all the properties listed above. However, initial consideration is usually given first to selectivity and environmental concerns, and second to capacity. From (2-20) in Chapter 2, the distribution coefficient for solute A between solvent S and carrier C is given by:

$$(K_A)_D = (x_A)^{II}/(x_A)^{I} = (\gamma_A)^{I}/(\gamma_A)^{II} \qquad (8\text{-}1)$$

where II is the extract phase, rich in S, and I is the raffinate phase, rich in C. Similarly, for the carrier and the solvent, respectively,

$$(K_C)_D = (x_C)^{II}/(x_C)^{I} = (\gamma_C)^{I}/(\gamma_C)^{II} \qquad (8\text{-}2)$$

$$(K_S)_D = (x_S)^{II}/(x_S)^{I} = (\gamma_S)^{I}/(\gamma_S)^{II} \qquad (8\text{-}3)$$

From (2-22), the relative selectivity of the solute with respect to the carrier is obtained by taking the ratio of (8-1)

Table 8.4 Group Interactions for Solvent Selection

Group	Solute	Solvent 1	2	3	4	5	6	7	8	9
1	Acid, aromatic OH (phenol)	0	−	−	−	−	0	+	+	+
2	Paraffinic OH (alcohol), water, imide or amide with active H	−	0	+	+	+	+	+	+	+
3	Ketone, aromatic nitrate, tertiary amine, pyridine, sulfone, trialkyl phosphate, or phosphine oxide	−	+	0	+	+	−	0	+	+
4	Ester, aldehyde, carbonate, phosphate, nitrite or nitrate, amide without active H; intramolecular bonding, e.g., *o*-nitrophenol	−	+	+	0	+	−	+	+	+
5	Ether, oxide, sulfide, sulfoxide, primary and secondary amine or imine	−	+	+	+	0	−	0	+	+
6	Multihaloparaffin with active H	0	+	−	−	−	0	0	+	0
7	Aromatic, halogenated aromatic, olefin	+	+	0	+	0	0	0	0	0
8	Paraffin	+	+	+	+	+	+	0	0	0
9	Monohaloparaffin or olefin	+	+	+	+	+	0	0	+	0

(+) Plus sign means that compounds in the column group tend to raise activity coefficients of compounds in the row group.

(−) Minus sign means a lowering of activity coefficients.

(0) Zero means no effect.

Choose a solvent that lowers the activity coefficient.

Source: Cusack, R.W., P. Fremeaux, and D. Glate, *Chem Eng.*, **98**(2), 66–76 (1991).

to (8-2), giving

$$\beta_{AC} = (K_A)_D/(K_C)_D = \frac{(x_A)^{II}/(x_A)^{I}}{(x_C)^{II}/(x_C)^{I}} = \frac{(\gamma_A)^{I}/(\gamma_A)^{II}}{(\gamma_C)^{I}/(\gamma_C)^{II}} \tag{8-4}$$

For high selectivity, the value of β_{AC} should be high, that is, at equilibrium there should be a high concentration of A and a low concentration of C in the solvent. A first estimate of β_{AC} is made from available values or predictions of the activity coefficients $(\gamma_A)^{I}$, $(\gamma_A)^{II}$, and $(\gamma_C)^{II}$, at infinite dilution where $(\gamma_C)^{I} = 1$, or by using liquid–liquid equilibrium data for the lowest tie line on a triangular diagram of the type discussed in Chapter 4. If A and C form a nearly ideal solution, the value of $(\gamma_A)^{I}$ in (8-4) can also be taken as 1.

For high solvent capacity, the value of $(K_A)_D$ should be high. From (8-2) it is seen that this is difficult to achieve if A and C form nearly ideal solutions, such that $(\gamma_A)^{I} = 1.0$, unless A and S have a great affinity for each other, which would result in a negative deviation from Raoult's law to give $(\gamma_A)^{II} < 1$. Unfortunately, such systems are rare.

For ease in solvent recovery, $(K_S)_D$ should be as large as possible and $(K_C)_D$ as small as possible to minimize the presence of solvent in the raffinate and carrier in the extract. This will generally be the case if activity coefficients $(\gamma_S)^{I}$ and $(\gamma_C)^{II}$ at infinite dilution are large.

If a water-rich feed is to be separated, it is common to select an organic solvent; for an organic-rich feed, an aqueous solvent is often selected. In either case, it is desirable to select a solvent that lowers the activity coefficient of the solute. Consideration of molecule group interactions can help narrow the search for such a solvent before activity coefficients are estimated or liquid–liquid equilibrium data are sought. A table of interactions for solvent-screening purposes, as given by Cusack et al. [21], based on a modification of the work of Robbins [22], is shown as Table 8.4, where the solute and solvent each belong to any of nine different chemical groups. In this table, a minus (–) sign for a given solute–solvent pair means that the solvent will desirably lower the value of the activity coefficient of the solute relative to its value in the feed solution. For example, suppose it is desired to extract acetone from water. Acetone, the solute, is a ketone. Thus, in Table 8.4, group 3 applies for the solute, and desirable solvents are of the type given in groups 1 and 6. In particular, trichloroethane, a group 6 compound, is known to be a highly selective solvent with high capacity for acetone over a wide range of feed compositions. However, if the compound is environmentally objectionable, it must be rejected. A more sophisticated solvent-selection method, based on the UNIFAC group-contribution method for estimating activity coefficients and utilizing a computer-aided constrained optimization approach, has been developed by Naser and Fournier [23].

In Chapter 4, ternary diagrams were introduced for representing liquid–liquid equilibrium data for three-component systems at constant temperature. Such diagrams are available for a large number of systems, as discussed by

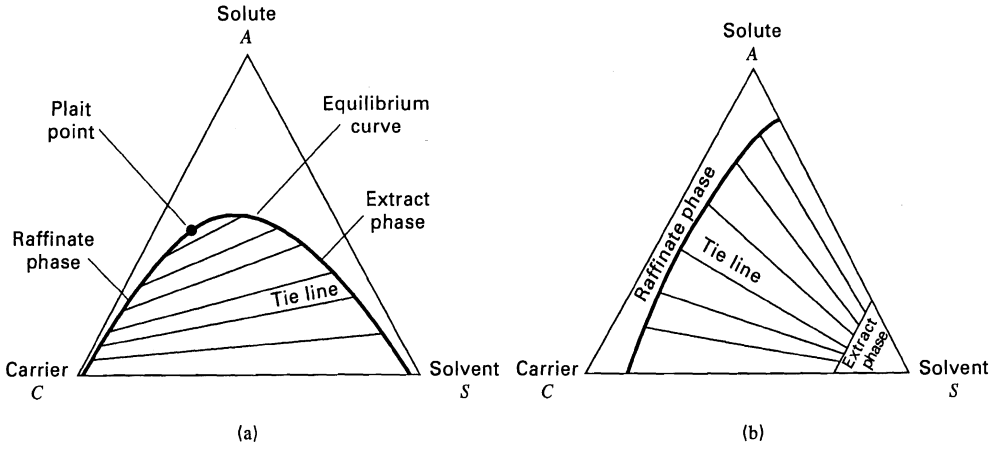

Figure 8.10 Most common classes of ternary systems: (a) type I, one immiscible pair; (b) type II, two immiscible pairs.

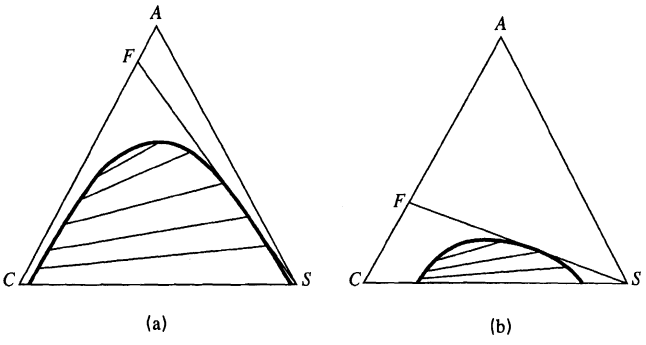

Figure 8.11 Effect of solubility on range of feed composition that can be extracted.

Humphrey et al. [6]. For liquid–liquid extraction with ternary systems, the most common diagram is Type I, shown in Figure 8.10a; much less common is Type II, shown in Figure 8.10b. Examples of Type II systems are (1) *n*-heptane/aniline/methyl cyclohexane, (2) styrene/ethylbenzene/diethylene glycol, and (3) chlorobenzene/water/methylethyl ketone. For Type I, the solute and solvent are miscible in all proportions, while in Type II they are not. For Type I systems, the greater the two-phase region on line $\overline{CS}$, the greater will be the immiscibility of carrier and solvent. The closer the top of the two-phase region is to apex A, the greater will be the range of feed composition, along line $\overline{AC}$, that can be separated with solvent *S*. In Figure 8.11, it is possible to separate feed solutions only in the composition range from *C* to *F* because, regardless of the amount of solvent added, two liquid phases are not formed in the feed composition range of $\overline{FA}$ (i.e., $\overline{FS}$ does not pass through the two-phase region).

The system in Figure 8.11a has a wider range of feed composition than the system in Figure 8.11b. For Type II systems, a high degree of insolubility of *S* in *C* and *C* in *S* will produce a desirable high relative selectivity, but at the expense of solvent capacity. Thus, solvents that result in Type I systems are more desirable.

Whether a ternary system is of Type I or Type II often depends on the temperature. For example, data of Darwent and Winkler [24] for the ternary system *n*-hexane (H)/methylcyclopentane (M)/aniline (A) for temperatures of 25, 34.5, and 45°C are shown in Figure 8.12. At the lowest temperature, 25°C, we have a Type II system because both H and M are only partially miscible in the aniline solvent. As the temperature increases, the solubility of M in aniline increases more rapidly than the solubility of H in aniline until at 34.5°C, the critical solution temperature for M in aniline is reached. At this temperature, the system is at the border of Type II and Type I. At 45°C, the system is clearly of type I, with aniline more selective for M than H. Type I systems have a plait point (*P* in Figure 8.10a); type II systems do not.

Except in the near-critical region, pressure has little if any effect on liquid-phase activity coefficients and, therefore, on liquid–liquid equilibrium. It is only necessary to select an operating pressure of at least ambient, and greater than the bubble-point pressure of the two-liquid-phase mixture at any location in the extractor. Most extractors operate at near-ambient temperature. If feed and solvent enter the extractor at the same temperature, the operation will be nearly isothermal because the only thermal effect is the heat of mixing, which is usually small.

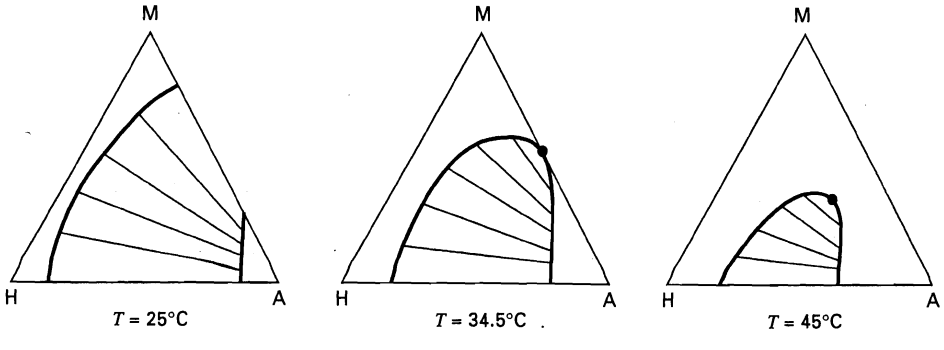

Figure 8.12 Effect of temperature on solubility for the system *n*-hexane (H)/methylcyclopentane (M)/aniline (A).

Laboratory or pilot-plant work, using actual or expected plant feed and solvent, is almost always necessary to ascertain dispersion and coalescence properties of the liquid–liquid system. Although rapid coalescence of drops is desirable, this reduces interfacial area, leading to reduced mass-transfer rates. Thus, compromises are necessary. Coalescence is enhanced when the solvent phase is continuous and mass transfer of solute is from the droplets. This phenomenon, called the *Marangoni effect,* is due to a lowering of interfacial tension by a significant presence of the solute in the interfacial film. When the solvent is the dispersed phase, the interfacial film is depleted of solute, causing an increase in interfacial tension and inhibition of coalescence.

For a given (1) feed liquid, (2) degree of solute extraction, (3) operating pressure and temperature, and (4) choice of solvent for a single-section cascade, a minimum solvent-to-feed flow-rate ratio exists that corresponds to an infinite number of countercurrent, equilibrium contacts. As with absorption and stripping, a trade-off then exists between the number of equilibrium stages and the solvent-to-feed flow-rate ratio. For a two-section cascade, as for distillation, the trade-off involves the reflux ratio and the number of stages. Algebraic methods, similar to those for absorption and stripping described in Chapter 6, for computing the minimum ratios and the trade-off are rapid, but are useful only for very dilute solutions, where values of the solute activity coefficients are essentially those at infinite dilution. When the carrier and the solvent are mutually insoluble, the algebraic method of Sections 5.3 and 5.4 can be used. For more general applications, use of the graphical methods described in this chapter is preferred for ternary systems. Computer-aided methods discussed in Chapter 10 are necessary for higher-order multicomponent systems.

8.3 HUNTER–NASH GRAPHICAL EQUILIBRIUM-STAGE METHOD

Stagewise extraction calculations for ternary systems of Type I and Type II (Figure 8.10) are most conveniently carried out with equilibrium diagrams [25]. In this section, procedures are developed and illustrated, using mainly triangular diagrams. The use of other diagrams is covered in the next section.

Consider a countercurrent-flow, N-equilibrium-stage contactor for liquid–liquid extraction of a ternary system operating under isothermal, continuous, steady-state flow conditions at a pressure sufficient to prevent vaporization, as shown in Figure 8.13. Stages are numbered from the feed end. Thus, the final extract is E_1 and the final raffinate is R_N. Equilibrium is assumed to be achieved at each stage, so that for any stage, n, the extract, E_n, and the raffinate, R_n, are in equilibrium with all three components. Mass transfer of all components occurs at each stage. The feed, F, contains the carrier, C, and the solute, A, and can also contain solvent, S, up to the solubility limit. The entering solvent, S, can contain C and A, but preferably contains little of either, if any. Because most liquid–liquid equilibrium data are given in mass rather than mole concentrations, let:

F = mass flow rate of feed to the cascade

S = mass flow rate of solvent to the cascade

E_n = mass flow rate of extract leaving stage n

R_n = mass flow rate of raffinate leaving stage n

$(y_i)_n$ = mass fraction of species i in extract leaving stage n

$(x_i)_n$ = mass fraction of species i in raffinate leaving stage n

Although Figure 8.13 might seem to imply that the extract is the light phase, either phase can be the light phase. Phase equilibrium may be represented, as discussed in Chapter 4, on an equilateral-triangle diagram, as proposed by Hunter and Nash [26], or on a right-triangle diagram as proposed by Kinney [27]. Assume, for illustration purposes, that the ternary system is A (solute), C (carrier), and S (solvent) at a particular temperature, T, such that the liquid–liquid equilibrium data are represented on the equilateral-triangle diagram of Figure 8.14, where the bold line is the equilibrium curve and the dashed lines are the tie lines that connect equilibrium phases of the equilibrium curve (also called the *binodal curve* because the plait point separates the curve into an extract and a raffinate). The equilibrium tie lines slope upward from the C side of the diagram toward the S side. Therefore, at equilibrium A has a concentration higher in S than in C. Thus, S is an effective solvent for extracting A from a mixture with C. On the other hand, because the tie lines slope downward from the S side toward the C side, C is not an effective solvent for extracting A from S.

Some ternary systems, such as isopropanol–water–benzene, exhibit a phenomenon called *solutropy,* wherein moving from the plait point, the tie lines first slope in one direction. However, the slope diminishes until an intermediate tie line becomes horizontal. Below that tie line, the remaining tie lines slope in the other direction. Sometimes, the solutropy phenomenon disappears if mole-fraction coordinates, rather than mass-fraction coordinates, are used.

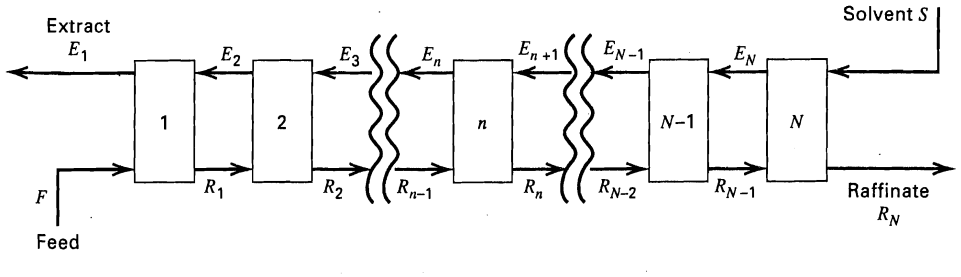

Figure 8.13 Countercurrent-flow, N-equilibrium-stage liquid–liquid extraction cascade.

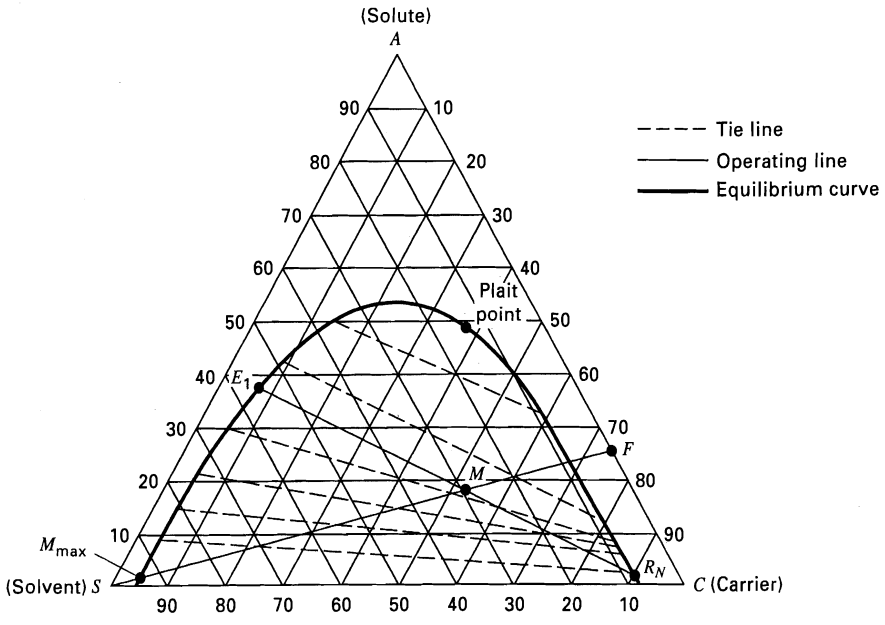

Figure 8.14 Construction 1: Location of product points.

Number of Equilibrium Stages

From the degrees-of-freedom discussion in Chapters 4 and 5, the following sets of specifications, for the cascade of Figure 8.13 with a ternary system, can be made, where all sets include the specification of F, $(x_i)_F$, $(y_i)_S$, and T:

Set 1. S and $(x_i)_{R_N}$	Set 4. N and $(x_i)_{R_N}$
Set 2. S and $(y_i)_{E_1}$	Set 5. N and $(y_i)_{E_1}$
Set 3. $(x_i)_{R_N}$ and $(y_i)_{E_1}$	Set 6. S and N

where values of $(x_i)_{R_N}$ and $(y_i)_{E_1}$ and all exiting phases must lie on the equilibrium curve.

Calculations for sets 1 to 3, which involve the determination of N, are made directly using the triangular diagram. Sets 4 to 6, which involve a specified N, require an iterative procedure. We first consider the calculational procedure for Set 1, with the procedures for Sets 2 and 3 being just minor modifications. The procedure, sometimes referred to as the *Hunter–Nash method* [26], involves three kinds of construction on the triangular diagram and is somewhat more difficult than the McCabe–Thiele staircase-type construction for distillation. Although the procedure is illustrated only for the Type I system, the principles are readily extended to a Type II system. The constructions are shown in Figure 8.14, where A is the solute, C is the carrier, and S is the solvent. On the binodal curve, all extract compositions lie on the equilibrium curve to the left of the plait point, while all raffinate compositions lie to the right. To determine the number of stages, given the flow rates and compositions of the feed and solvent, and the desired raffinate composition, the constructions are as follows:

Construction 1 (Product Points)

First, on Figure 8.14, we locate mixing point M, which represents the overall composition of the combination of feed, F, and entering solvent, S. Assume the following feed and solvent specifications, as plotted in Figure 8.14, where pure S is the solvent:

Feed	Solvent
$F = 250$ kg	$S = 100$ kg
$(x_A)_F = 0.24$	$(x_A)_S = 0.00$
$(x_C)_F = 0.76$	$(x_C)_S = 0.00$
$(x_S)_F = 0.00$	$(x_S)_S = 1.00$

The overall composition M for combined F and S is obtained from the following material balances:

$$M = F + S = 250 + 100 = 350 \text{ kg}$$

$$(x_A)_M M = (x_A)_F F + (x_A)_S S$$
$$= 0.24(250) + 0(100) = 60 \text{ kg}$$
$$(x_A)_M = 60/350 = 0.171$$

$$(x_C)_M M = (x_C)_F F + (x_C)_S S$$
$$= 0.76(250) + 0(100) = 190 \text{ kg}$$
$$(x_C)_M = 190/350 = 0.543$$

$$(x_S)_M M = (x_S)_F F + (x_S)_S S$$
$$= 0(250) + 1(100) = 100 \text{ kg}$$
$$(x_S)_M = 100/350 = 0.286$$

From any two of these $(x_i)_M$ values, point M is located, as shown, in Figure 8.14. Based on the properties of the triangular diagram, presented in Chapter 4, point M must be located somewhere on the straight line connecting F and S. Therefore, M can be located knowing just one value of $(x_i)_M$, say $(x_S)_M$. Also, the ratio S/F is given by the inverse-lever-arm rule as

$$S/F = \overline{MF}/\overline{MS} = 100/250 = 0.400$$

or

$$S/M = \overline{MF}/\overline{SF} = 100/350 = 0.286$$

Thus, point M can be located by two points or by measurement, employing either of these ratios.

With point M located, the composition of extract, E_1, exiting from a countercurrent, multistage extractor, can be determined from overall material balances:

$$M = R_N + E_1 = 350 \text{ kg}$$
$$(x_A)_M M = 60 = (x_A)_{R_N} R_N + (x_A)_{E_1} E_1$$
$$(x_C)_M M = 190 = (x_C)_{R_N} R_N + (x_C)_{E_1} E_1$$
$$(x_S)_M M = 100 = (x_S)_{R_N} R_N + (x_S)_{E_1} E_1$$

Because the raffinate, R_N, is assumed to be at equilibrium, its composition must lie on the equilibrium curve of Figure 8.14. Therefore, if we specify the value $(x_A)_{R_N} = 0.025$, we can locate the point R_N, and the values of $(x_C)_{R_N}$ and $(x_S)_{R_N}$ can be read from Figure 8.14. A straight line drawn from R_N through M will locate E_1 at the intersection of the equilibrium curve, from which, in Figure 8.14, the composition of E_1 can be read. Values of the flow rates R_N and E_1 can then be determined from the overall material balances above or from Figure 8.14 by the inverse-lever-arm rule:

$$E_1/M = \overline{MR_N}/\overline{E_1R_N}$$
$$R_N/M = \overline{ME_1}/\overline{E_1R_N}$$

with $M = 350$ kg for this illustration. By either method, we find:

Raffinate Product	Extract Product
$R_N = 198.6$ kg	$E_1 = 151.4$ kg
$(x_A)_{R_N} = 0.025$	$(x_A)_{E_1} = 0.364$
$(x_C)_{R_N} = 0.90$	$(x_C)_{E_1} = 0.075$
$(x_S)_{R_N} = 0.075$	$(x_S)_{E_1} = 0.561$

Also included in Figure 8.14 is the point $M_{\max}$, which lies on the equilibrium curve along the straight line connecting F to S. $M_{\max}$ corresponds to the maximum possible solvent addition. If more solvent were added, two liquid phases could not exist.

Construction 2 (Operating Point and Lines)

In Chapters 6 and 7, we learned that an operating line is the locus of passing streams in a cascade. Referring to Figure 8.13, material balances around groups of stages from the feed end are

$$F - E_1 = \cdots = R_{n-1} - E_n = \cdots = R_N - S = P \quad (8\text{-}5)$$

Because the passing streams are differenced, P defines a *difference point* rather than a *mixing point*. From the same geometric considerations as apply to a mixing point, a difference point also lies on a straight line drawn through the points involved. However, while the mixing point always lies inside the triangular diagram and between the two end points, the difference point usually lies outside the triangular diagram along an extrapolation of the line through two points such as F and E_1, R_N and S, and so on.

To locate the difference point, two straight lines are drawn, respectively, through the point pairs (E_1, F) and (S, R_N), which are established by Construction 1 and shown in Figure 8.15. These lines are extrapolated until they intersect at difference point P. Figure 8.15 shows these lines and the difference point, P. From (8-5), straight lines drawn through points on the triangular diagram for any other pair of passing streams, such as (E_n, R_{n-1}), must also pass through point P. Thus, we refer to the difference point as an *operating point,* and the lines drawn through pairs of points for passing streams and extrapolated to point P as *operating lines.*

The difference point has properties similar to those of the mixing point. If $F - E_1 = P$ is rewritten as $F = E_1 + P$, we see that F can be interpreted as the mixing point for P and E_1. Therefore, by the inverse-lever-arm rule, the length of line $\overline{E_1P}$ relative to the length of the line $\overline{FP}$ is given by

$$\frac{\overline{E_1P}}{\overline{FP}} = \frac{E_1 + P}{E_1} = \frac{F}{E_1} \quad (8\text{-}6)$$

Thus, point P can be located, if desired, by measurement with a ruler using either pair of feed-product passing streams.

The operating point, P, lies on the feed or raffinate side of the triangular diagram in the illustration of Figure 8.15. Depending on the relative amounts of feed and solvent and the slope of the tie lines, point P may be located on the solvent or feed side of the diagram, and inside or outside the diagram.

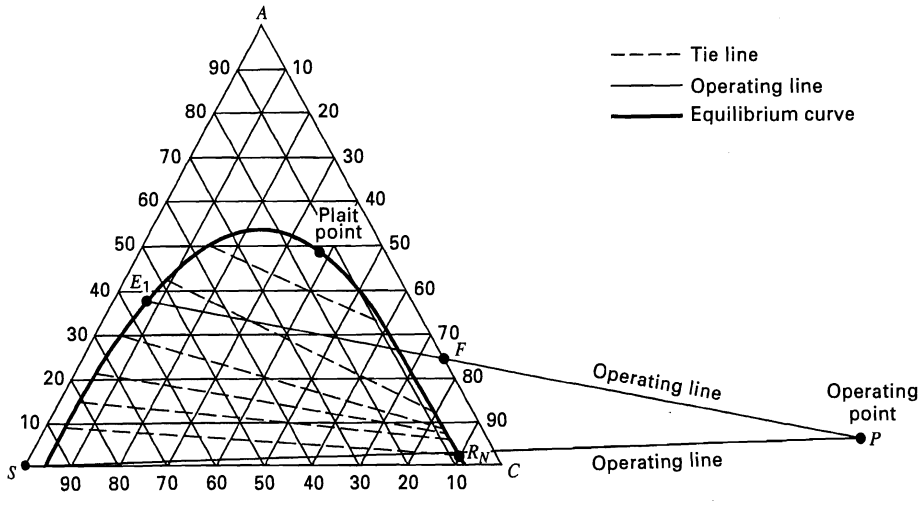

Figure 8.15 Construction 2: Location of operating point.

Construction 3 (Equilibrium Lines)

The third type of construction involves the dashed *tie lines* that connect opposite sides of the equilibrium curve, which is divided into the two sides by the plait point, which for type I diagrams is the point where the two equilibrium phases become one phase. A material balance around any stage n for any of the three components is

$$(x_i)_{n-1}R_{n-1} + (y_i)_{n+1}E_{n+1} = (x_i)_n R_n + (y_i)_n E_n \quad (8\text{-}7)$$

Because R_n and E_n are in equilibrium, their composition points are on the triangular diagram at the two ends of a tie line. Typically a diagram will not contain all the tie lines needed. Tie lines may be added by centering them between existing experimental or predicted tie lines, or by using either of two interpolation procedures illustrated in Figure 8.16. In Figure 8.16a, the conjugate line from the plait point to J is determined from four tie lines and the plait point. From tie line $\overline{DE}$, lines $\overline{DG}$ and $\overline{EF}$ are drawn parallel to triangle sides $\overline{CB}$ and $\overline{AC}$, respectively. The intersection at point H gives a second point on the conjugate curve. Subsequent intersections, using the other tie lines, establish additional points from which the conjugate curve is drawn. Then, using the curve, additional tie lines are drawn by reversing the procedure. If it is desired to keep the conjugate curve inside the two liquid-phase region of the triangular diagram, the procedure illustrated in Figure 8.16b is used, where lines are drawn parallel to triangle sides $\overline{AB}$ and $\overline{AC}$.

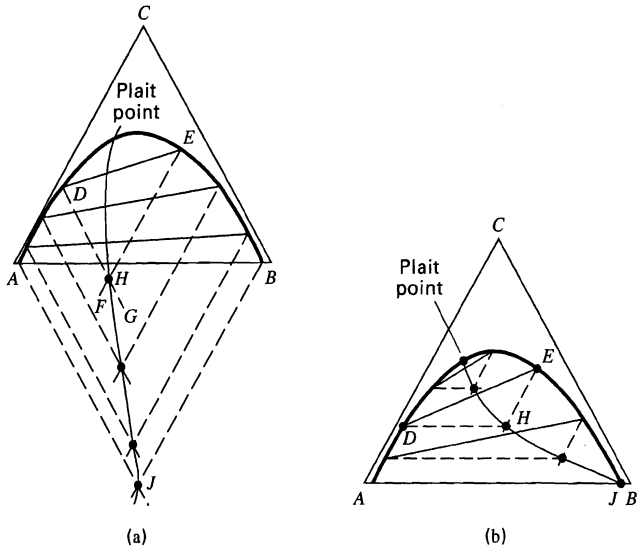

Figure 8.16 Use of conjugate curves to interpolate tie lines: (a) method of *International Critical Tables,* Vol. III, McGraw-Hill, New York, p. 393 (1928); (b) method of T.K. Sherwood, *Absorption and Extraction,* McGraw-Hill, New York, p. 242 (1937). [From R.E. Treybal, *Liquid Extraction,* 2nd ed., McGraw-Hill, New York (1963) with permission.]

Stepping off Stages

Equilibrium stages are stepped off on the triangular diagram by alternating the use of tie lines and operating lines, as shown in Figure 8.17, where Constructions 1 and 2 have already been employed to locate the five points F, E, S, R_1, and P. We start at the feed end from point E_1. Referring to Figure 8.13, we see that R_1 is in equilibrium with E_1. Therefore, by Construction 3, R_1 in Figure 8.17 must be at the opposite end of a tie line (shown as a dashed line) connecting to E_1. From Figure 8.13, R_1 passes E_2. Therefore, by Construction 2, E_2 must lie at the intersection of the straight operating line, drawn through points R_1 and P, and back to the extract side of the equilibrium curve. From E_2, we locate R_2 with a tie line by Construction 3; from R_2, we locate E_3 by Construction 2. Continuing in this fashion by alternating between equilibrium tie lines and operating lines, we finally reach or pass the specified point R_N. If the latter, a fraction of the last stage is taken. In Figure 8.17 approximately 2.8 equilibrium stages are required, where stages are counted by the number of tie lines used.

Procedures for problem specification sets 2 and 3 are very similar to that for set 1. Sets 4 and 5 can be handled by iteration on assumed values for S and following the above procedure for set 1. Set 6 can also use the procedure of set 1 by iterating on E_1.

From (8-6), we see that if the ratio F/E_1 approaches a value of 1, the operating point, P, will be located at a large distance

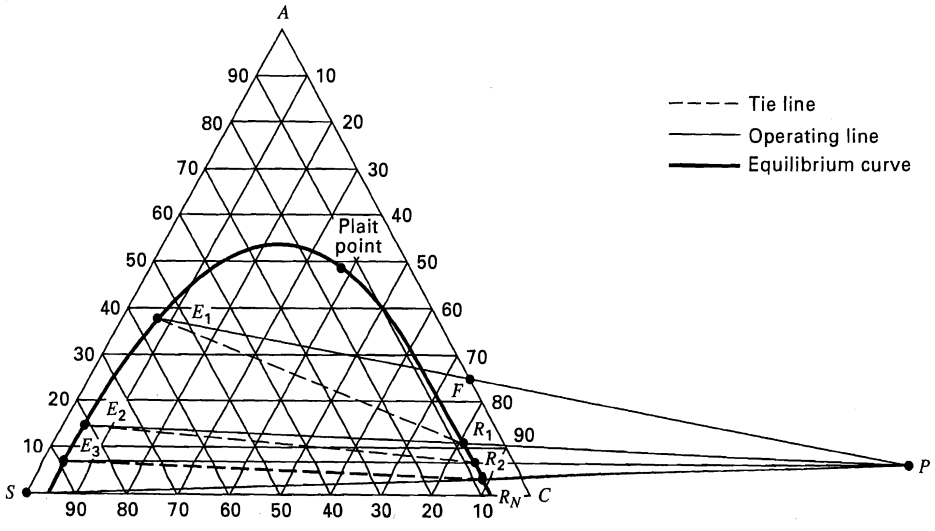

Figure 8.17 Determination of the number of equilibrium stages.

from the triangular diagram. In that case, using an arbitrary rectangular-coordinate system superimposed over the triangular diagram, the coordinates of P can be calculated from (8-6) using the equations for the two straight lines established in Construction 2. Operating lines for intermediate stages can then be located on the triangular diagram so as to pass through P. Details of this procedure are given by Treybal [25].

Minimum and Maximum Solvent-to-Feed Flow-Rate Ratios

The graphical procedure just described for determining the number of equilibrium stages to achieve a desired solute extraction for a given solvent-to-feed flow-rate ratio presupposes that this ratio is greater than the minimum ratio corresponding to the need for an infinite number of stages, but less than the maximum ratio that would prevent the formation of the required second liquid phase. In practice, one usually determines the minimum ratio before solving specification sets 1 or 2. In essence, we must solve set 4 with $N = \infty$, where, as in distillation, absorption, and stripping, the infinity of stages occurs at a pinch point of the equilibrium curve and the operating line(s). In ternary systems, the pinch point occurs when a tie line is coincident with an operating line. The calculation is somewhat involved because the location of the pinch point is not always at the feed end of the cascade. Consider the previous A–C–S system, as shown in Figure 8.18. The points F, S, and R_N are specified, but E_1 is not because the solvent rate has not yet been specified. The operating line $\overline{OL}$ is drawn through the points S and R_N and extended to the left and right of the diagram. This line is the locus of all possible material balances determined by adding S to R_N. Each tie line is then assumed to be a pinch point by extending each tie line until it intersects the line $\overline{OL}$. In this manner, a sequence of intersections, P_1, P_2, P_3, and so on, is found. If these points lie on the raffinate side of the diagram, as in Figure 8.18, the pinch point corresponds to the point $P_{\min}$ located at the greatest distance from R_N. If the triangular diagram does not have a sufficient number of tie lines to determine that point accurately, additional tie lines are introduced by a method described previously and illustrated in Figure 8.16. If we assume in Figure 8.18 that no other tie line gives a point P_i farther away from R_N than P_1, then $P_1 = P_{\min}$.

With $P_{\min}$ known, an operating line can be drawn through point F and extended to E_1 at an intersection with the extract side of the equilibrium curve. From the compositions of the four points, S, R_N, F, and E_1, the mixing point M can be found and the following material balances can then be used to solve for $S_{\min}/F$:

$$F + S_{\min} = R_N + E_1 = M \tag{8-8}$$

$$(x_A)_F F + (x_A)_S S_{\min} = (x_A)_M M \tag{8-9}$$

from which

$$\frac{S_{\min}}{F} = \frac{(x_A)_F - (x_A)_M}{(x_A)_M - (x_A)_S} \tag{8-10}$$

A solvent flow rate greater than $S_{\min}$ must be selected for the extraction to be conducted in a finite number of stages. In Figure 8.18, such a solvent rate results in an operating point P to the right of $P_{\min}$, that is, at a location farther away from R_N. A reasonable value for S might be $1.5\,S_{\min}$. From Figure 8.18, we find $(x_A)_M = 0.185$, from which, by (8-10), $S_{\min}/F = 0.30$. In our example of Figure 8.17, we used $S/F = 0.40$, giving $S/S_{\min} = 1.33$.

In Figure 8.18 the tie lines slope downward toward the raffinate side of the diagram. If the tie lines slope downward toward the extract side of the diagram, the above procedure for finding $S_{\min}/F$ must be modified. The sequence of points P_1, P_2, P_3, and so on, is now found on the other side of the diagram. However, the pinch point now corresponds to that point, $P_{\min}$, that is closest to point S and an operating point, P, must be chosen between points $P_{\min}$ and S. For a system that exhibits solutropy, intersections P_1, P_2, and so on, will be found on both sides of the diagram. Those on the extract side will determine the minimum solvent-to-feed ratio.

In Figure 8.14, the mixing point M must lie in the two-phase region. As this point is moved along the line $\overline{SF}$ toward S, the ratio S/F increases according to the inverse-lever-arm rule. In the limit, a maximum S/F ratio is reached when $M = M_{\max}$ arrives at the equilibrium curve on the

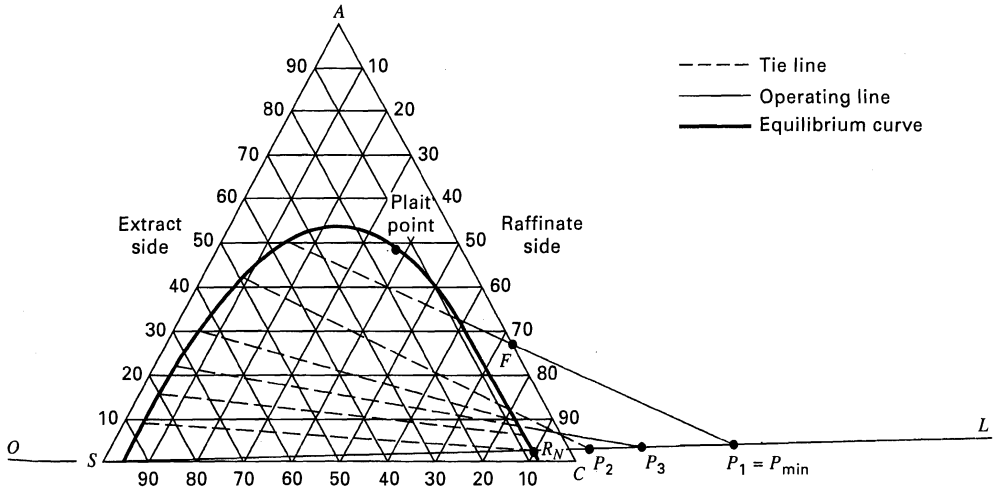

Figure 8.18 Determination of minimum solvent-to-feed ratio.

extract side. At this point, all of the feed is dissolved in the solvent, no raffinate is obtained, and only one stage is required. To avoid this impractical condition, as well as the other extreme of infinite stages, we must select a solvent ratio, S/F, such that $(S/F)_{min} < (S/F) < (S/F)_{max}$. In Figure 8.14, the mixing point M_{max} is located as shown, from which $(S/F)_{max}$ is determined to be about 16.

EXAMPLE 8.1

Acetone is to be extracted from a feed mixture of 30 wt% acetone (A) and 70 wt% ethyl acetate (C) at 30°C by using pure water (S) as the solvent by the cascade shown at the bottom of Figure 8.19. The final raffinate is to contain 5 wt% acetone on a water-free basis. Determine the minimum and maximum solvent-to-feed ratios and the number of equilibrium stages required for two intermediate S/F ratios. The equilibrium data, which are shown in Figure 8.19 and are taken from Venkataranam and Rao [28], correspond to a type I system, but with tie lines sloping downward toward the extract side of the diagram. Thus, although water is a convenient solvent, it does not have a high capacity, relative to ethyl acetate, for dissolving acetone. The flow diagram of the cascade in Figure 8.19 shows the nomenclature to be used for this example. Also, determine, for the feed, the maximum weight percent acetone that can enter the extractor. This example, as well as Example 8.2 later, are taken largely from an analysis by Sawistowski and Smith [29].

SOLUTION

Point B represents the solvent-free final raffinate. By drawing a straight line from B to S, the intersection with the equilibrium curve on the raffinate side, B', is the actual raffinate composition leaving stage N.

Minimum S/F. Because the tie lines slope downward toward the extract side of the diagram, we seek the extrapolated tie line that intersects the extrapolated line $\overline{SB}$ closest to S. This tie line, leading to P_{min}, is shown in Figure 8.20. The intersection is not shown because it occurs far to the left of the triangular diagram. Because this tie line is at the feed end of the extractor, the location of the extract composition, D'_{min}, is determined as shown in Figure 8.20. The mixing point, M_{min}, for $(S/F)_{min}$ is the intersection of lines $\overline{B'D'}$min and $\overline{SF}$. By the inverse-lever-arm rule, $(S/F)_{min} = \overline{FM}_{min}/\overline{SM}_{min} = 0.60$.

Maximum S/F. If M in Figure 8.20 is moved along line $\overline{FS}$ toward S, the intersection for $(S/F)_{max}$ occurs at the point shown on the extract side of the binodal curve. By the inverse-lever-arm rule, using line $\overline{FS}$, $(S/F)_{max} = \overline{FM}_{max}/\overline{SM}_{max} = 12$.

Equilibrium stages for other S/F ratios. First consider $S/F = 1.75$. In Figure 8.19, the composition of the saturated extract D' is obtained from a material balance about the extractor,

$$S + F = D' + B' = M$$

For $S/F = 1.75$, point M can be located such that $\overline{FM}/\overline{MS} = 1.75$. A straight line must also pass through D', B', and M. Therefore, D' can be located by extending $\overline{B'M}$ to the extract envelope.

The flow difference point P is located to the left of the triangular diagram. Therefore, $P = S - B' = D' - F$. It is located at the intersection of extensions of lines $\overline{FD'}$ and $\overline{B'S}$.

Stepping off stages poses no problem. Starting at D', we follow a tie line to L_1. Then V_2 is located by noting the intersection of the operating line $\overline{L_1P}$ with the phase envelope. Additional stages are stepped off in the same manner by alternating between the tie lines and operating lines. For the sake of clarity, only the first stage is shown; four are required.

For $S/F = 5(S/F)_{min} = 3.0$, M is determined and the stages are stepped off in a similar manner to give two equilibrium stages.

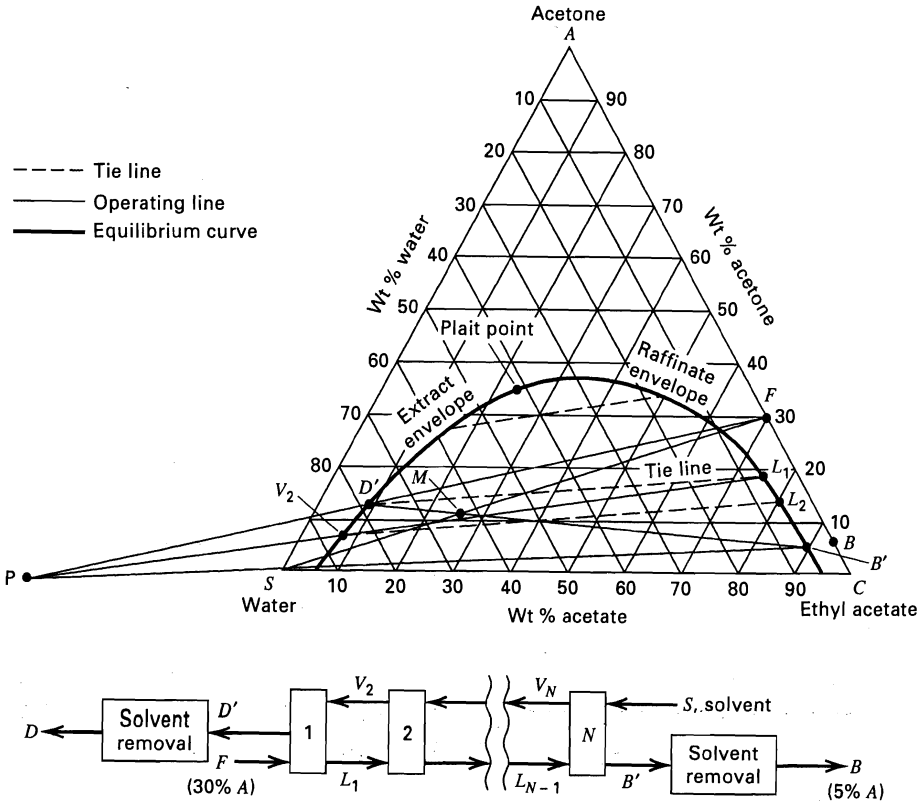

Figure 8.19 Determination of stages for Example 8.1 with $S/F = 1.75$.

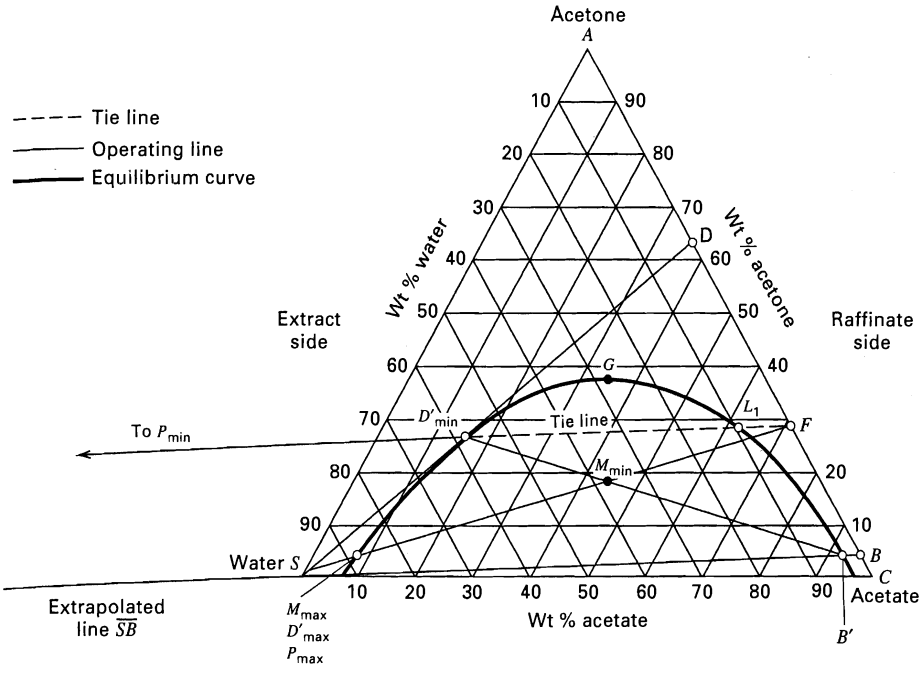

Figure 8.20 Minimum and maximum S/F for Example 8.1.

In summary, for the countercurrent cascade, we have.

S/F (solvent/feed ratio)	0.60	1.75	3	12
N (equilibrium stages)	∞	4	2	1
x_D (wt% acetone, solvent free)	64	62	50	30

If the wt% acetone in the feed mixture is increased from the base value of 30%, a feed composition will be reached that cannot be extracted because two liquid phases in equilibrium will not form (no phase splitting). This feed composition is determined by extending a line from S, tangent to the equilibrium curve, until it intersects $\overline{AC}$. This is shown as point D in Figure 8.20. The feed composition is 64 wt% acetone. Feed mixtures with a higher acetone content cannot be extracted with water.

Use of Right-Triangle Diagrams

As discussed in Chapter 4, diagrams other than the equilateral-triangle diagram are used for calculations involving ternary liquid–liquid systems. Ternary, countercurrent extraction calculations can also be made on a right-triangle diagram as shown by Kinney [27]; no new principles are involved. The disadvantage is that mass-percent compositions of only two of the components are plotted; the third being determined, when needed, by difference from 100%. The advantage of right-triangle diagrams is that ordinary rectangular-coordinates graph paper can be used and either one of the coordinates can be expanded, if necessary, to increase the accuracy of the constructions.

A right-triangle diagram can be developed from an equilateral-triangle diagram as shown in Figure 8.21a, where the coordinates in both diagrams are in mass fractions or in mole fractions. Point P on the equilibrium curve and tie line $\overline{RE}$ in the equilateral triangle become point P and tie line $\overline{RE}$ in the right-triangle diagram, which uses rectangular coordinates, x_A and x_C, where A is the solute and C is the carrier.

Consider the right-triangle diagram in Figure 8.22 for the A–C–S system of Figure 8.14. The compositions of S (the solvent) and A (the solute) are plotted in weight (mass) fractions, x_i. For example, point M represents a liquid mixture of overall composition ($x_A = 0.43$, $x_S = 0.28$). By difference, x_C, the carrier, which is not shown on the diagram, is $1 - 0.43 - 0.28 = 0.29$. Although lines of constant x_C are included on the right triangle of Figure 8.22, such lines are usually omitted because they clutter the diagram. As with the equilateral-triangle diagram, Figure 8.22 for a right triangle includes the binodal curve, with extract and raffinate sides, tie lines connecting compositions of equilibrium phases, and the plait point, at $x_A = 0.49$.

Because point M falls within the phase envelope, the mixture separates into two liquid phases, whose compositions are given by points A' and A'' at the ends of the tie line that passes through point M. In this case, the extract at A'' is richer in the solute (A) and the solvent (S) than the raffinate at A'.

Point M might be the result of mixing a feed, point F, consisting of 26,100 kg/h of 60 wt% A in C ($x_A = 0.6$, $x_S = 0$), with 10,000 kg/h of pure furfural, point S. At equilibrium, the mixture splits into the phases represented by A' and A''. The location of point M and the amounts of extract and raffinate are given by the same mixing rule and inverse-lever-arm rule used for equilateral-triangle diagrams. The mixture separates spontaneously into 11,600 kg/h of raffinate ($x_S = 0.08$, $x_A = 0.32$) and 24,500 kg/h of extract ($x_S = 0.375$, $x_A = 0.48$).

Figure 8.23 represents the portion of an n-stage, countercurrent-flow cascade, where x and y are weight fractions of solute, A, in the raffinate and extract, respectively, and L and V are total amounts of raffinate and extract, respectively. The feed to stage N is $L_{N+1} = 180$ kg of 35 wt% A in a saturated mixture with C and S ($x_{N+1} = 0.35$), and

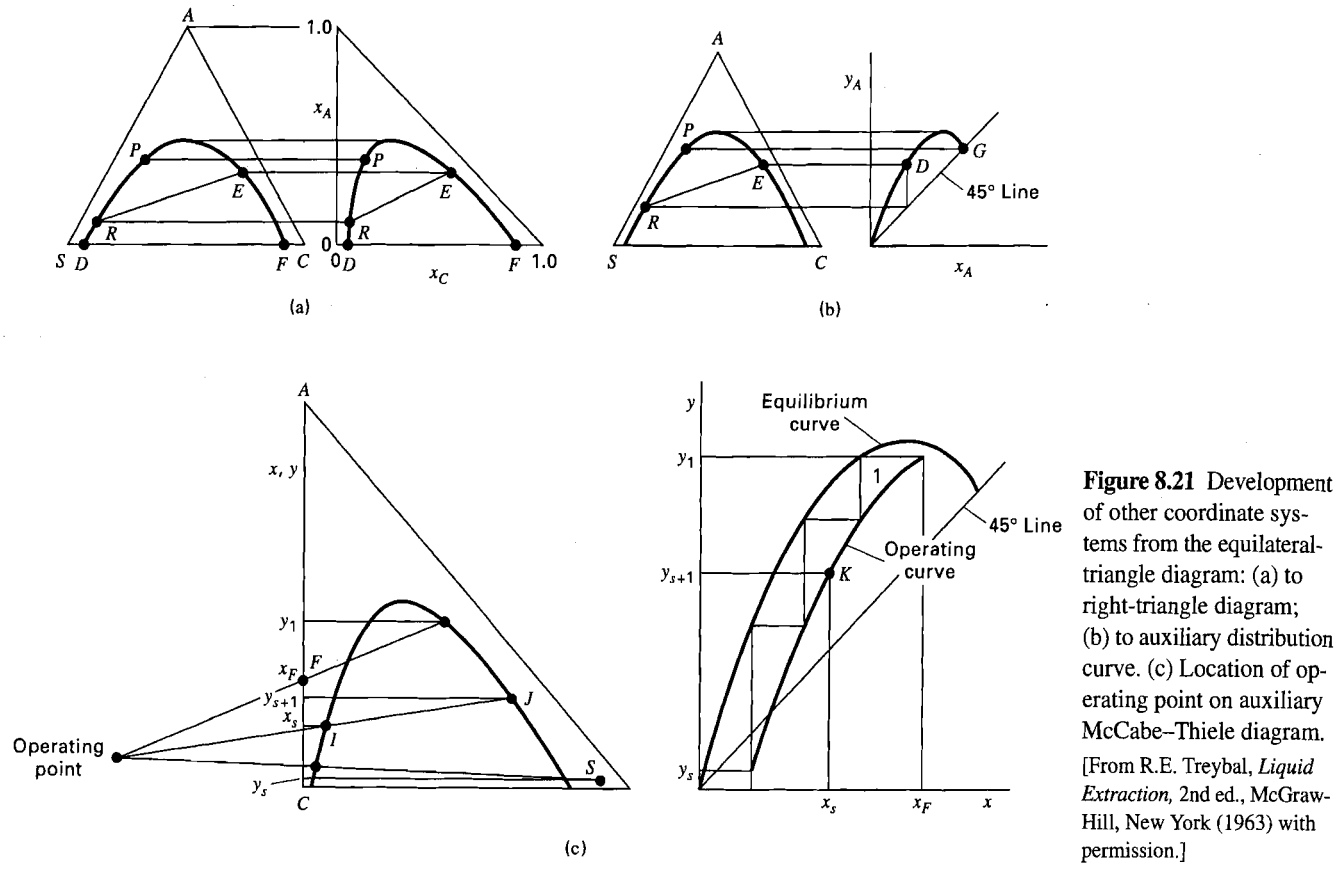

Figure 8.21 Development of other coordinate systems from the equilateral-triangle diagram: (a) to right-triangle diagram; (b) to auxiliary distribution curve. (c) Location of operating point on auxiliary McCabe–Thiele diagram. [From R.E. Treybal, *Liquid Extraction,* 2nd ed., McGraw-Hill, New York (1963) with permission.]

the solvent to stage 1 is $V_W = 100$ kg of pure S ($y_W = 0.0$). Thus, the solvent-to-feed ratio is $100/180 = 0.556$. These two points are shown on the right-triangle diagram of Figure 8.24. The mixing point for L_{N+1} and V_W is shown as point M_1, as determined by the inverse lever-arm rule. Suppose that the final raffinate, L_W, leaving stage 1 is to contain 0.05 weight-fraction glycol ($x_W = 0.05$). By an overall balance,

$$M_1 = V_W + L_{N+1} = V_N + L_W \qquad (8\text{-}11)$$

Applying the mixing rule, since V_W, L_{N+1}, and M_1 lie on a straight line, V_N, L_W, and M_1 must also lie on a straight line. Furthermore, because V_N leaves stage N at equilibrium and L_W leaves stage 1 at equilibrium, these two streams must lie on the extract and raffinate sides, respectively, of the equilibrium curve. The resulting points are shown in Figure 8.24, where it is seen that the weight fraction of glycol in the final extract is $y_N = 0.34$.

Figures 8.23b and 8.23c, and 8.24 include two additional cases of solvent-to-feed ratio, each with the same compositions for the solvent and the feed and the same

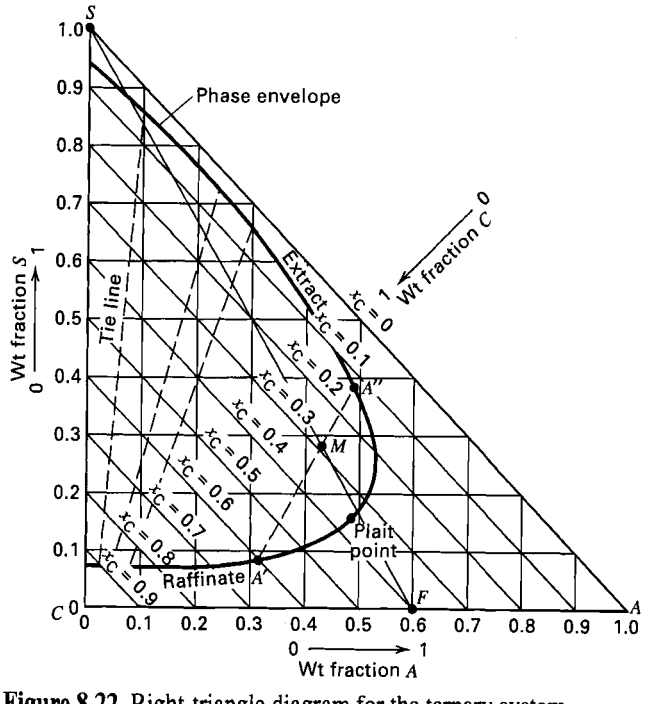

Figure 8.22 Right-triangle diagram for the ternary system of Figure 8.14.

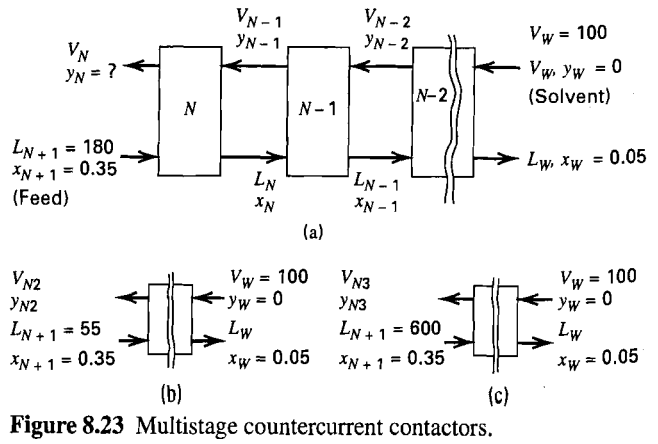

Figure 8.23 Multistage countercurrent contactors.

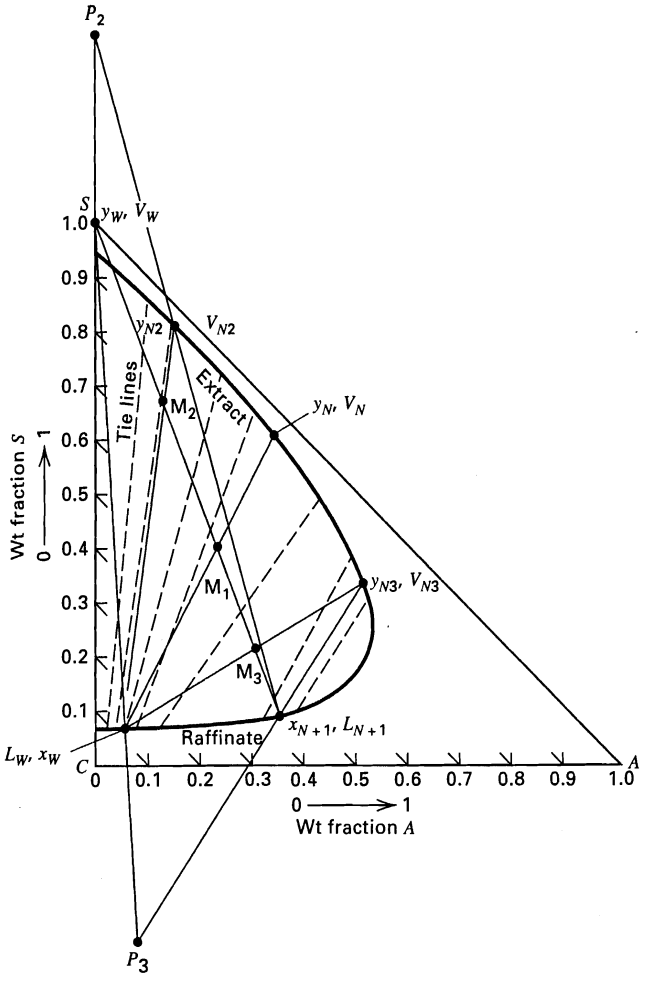

Figure 8.24 Right-triangle diagram constructions for cascade in Figure 8.23.

value for x_W:

Case	Feed L_{N+1}, kg	Solvent, V_W, kg	Solvent-to-Feed Ratio	Extract Designation	Mixing Point
1	180	100	0.556	V_N	M_1
2	55	100	1.818	V_{N2}	M_2
3	600	100	0.167	V_{N3}	M_3

For Case 2, a difference point, P_2, may be defined, as with the equilateral-triangle diagram, in terms of passing streams, as

$$P_2 = V_{N2} - L_{N+1} = V_W - L_W \qquad (8\text{-}12)$$

This point, shown in Figure 8.24, is located at the top of the diagram, where the lines $\overline{L_W V_W}$ and $\overline{L_{N+1} V_{N2}}$ intersect. For Case 3, the difference point, P_3, falls at the bottom of the diagram, where the lines $\overline{L_W V_W}$ and $\overline{L_{N+1} V_{N3}}$ intersect.

Equilibrium stages for Figure 8.24 are stepped off in a manner similar to that for an equilateral-triangle diagram by alternating use of equilibrium tie lines and operating lines passing through the difference point. For example, considering Case 2, with the high solvent-to-feed ratio of 1.818, and stepping off stages from stage N, a tie line from the point y_{N2} gives a value of $x_N = 0.04$. But this is less than the specified value of $x_w = 0.05$. Therefore, less than one equilibrium stage is required.

If we step off stages for Case 3, starting from y_{N3}, the tie line and the operating line coincide. That is, we have a pinch point. Thus, the solvent-to-feed ratio of 0.167 for this case is the minimum value corresponding to an infinite number of equilibrium stages.

For Case 1, where the solvent-to-feed ratio is in between that of Cases 2 and 3, the required number of equilibrium stages lies between 1 and ∞. Construction of the difference point and the steps for this case are not shown in Figure 8.14. The difference point is found to be located at a very large distance from the triangle because lines $\overline{L_W V_W}$ and $\overline{L_{N+1} V_N}$ are almost parallel. When the stages are stepped off, using operating lines parallel to $\overline{L_W V_W}$, it is found that between one and two stages are required.

Use of an Auxiliary Distribution Curve with a McCabe–Thiele Diagram

As the number of equilibrium stages to be stepped off on either one of the two types of triangular diagrams becomes more than a few, the diagram becomes cluttered. In that event, the use of a triangular diagram in conjunction with the McCabe–Thiele method becomes attractive. This is a method devised by Varteressian and Fenske [30]. The y–x diagram, discussed in Section 4.5 and illustrated in Figure 8.21b, is simply a plot of the tie-line data in terms of mass fractions (or mole fractions) of the solute in the extract (y_A) and equilibrium raffinate (x_A). The curve begins at the origin and terminates at the plait point where the curve intersects the 45° line. A tie line, such as $\overline{RE}$, in the triangular diagram becomes a point, in the equilibrium curve of Figure 8.25.

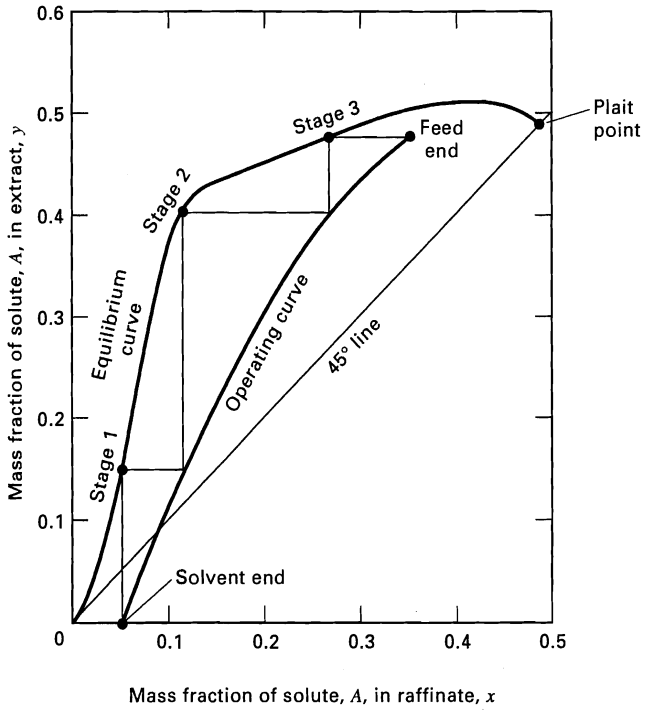

Figure 8.25 Stepping-off stages by the McCabe-Thiele method for the A–C–S system.

If an operating line is added to the equilibrium curve in Figure 8.21b, a staircase construction of the type used in the McCabe–Thiele method of Chapter 7 can rapidly determine the number of equilibrium stages. However, unlike distillation, where the operating line is straight because of the assumption of constant molar overflow, the operating line for liquid–liquid extraction in a ternary system will always be curved except in the low-solute-concentration region. Fortunately, the curved operating line is quite readily drawn using the following technique of Varteressian and Fenske [30]. In Figure 8.19 for the equilateral-triangle diagram, or in Figure 8.24 for the right-triangle diagram, the intersections of the equilibrium curve with a line drawn through a difference (operating) point represent the compositions of the passing streams. Thus, for each such operating line on the triangular diagram, one point of the operating line for the y–x plot is determined. The operating lines passing through the difference point can be drawn at random; they need not coincide with passing streams of actual equilibrium-stage operating lines. Usually five or six such fictitious operating-line intersections, covering the expected range of compositions in the extraction cascade, are sufficient to establish the curved operating line in the y–x plot. For example, in Figure 8.21c, the arbitrary operating line that intersects the equilibrium curve at I and J in the right-triangle diagram becomes a point K on the operating line of the y–x diagram. The y–x plot of Figure 8.25 for the A–C–S system includes an operating line established in this manner, based on the data of Figure 8.24, but with a solvent-to-feed ratio of 0.208, that is, $V_W = 100$, $L_{N+1} = 480$ (25% greater than the minimum ratio of 0.167). The stages are stepped off in the McCabe–Thiele manner starting from the feed end. The result is seen to be almost exactly three equilibrium stages.

Extract and Raffinate Reflux

The simple, single-section, countercurrent, equilibrium-stage extraction cascade shown in Figure 8.13 can be refluxed, as in Figure 8.26a, to resemble distillation. In Figure 8.26a, L is used for raffinate flows, V is used for extract flows, and stages are numbered from the solvent end of the process. Extract reflux, L_R, is provided by sending the extract, V_N, to a solvent-recovery step, which removes most of the solvent, to give a solute-rich solution, $L_R + D$, which is divided into extract reflux, L_R, which is returned to stage N, and solute product, D. At the other end of the cascade, a portion, B, of the raffinate, L_1, is withdrawn in a stream divider and added as raffinate reflux, V_B, to fresh solvent, S. The remaining raffinate, B, is sent to a solvent-removal step (not shown) to produce a carrier-rich raffinate product. When using extract reflux,

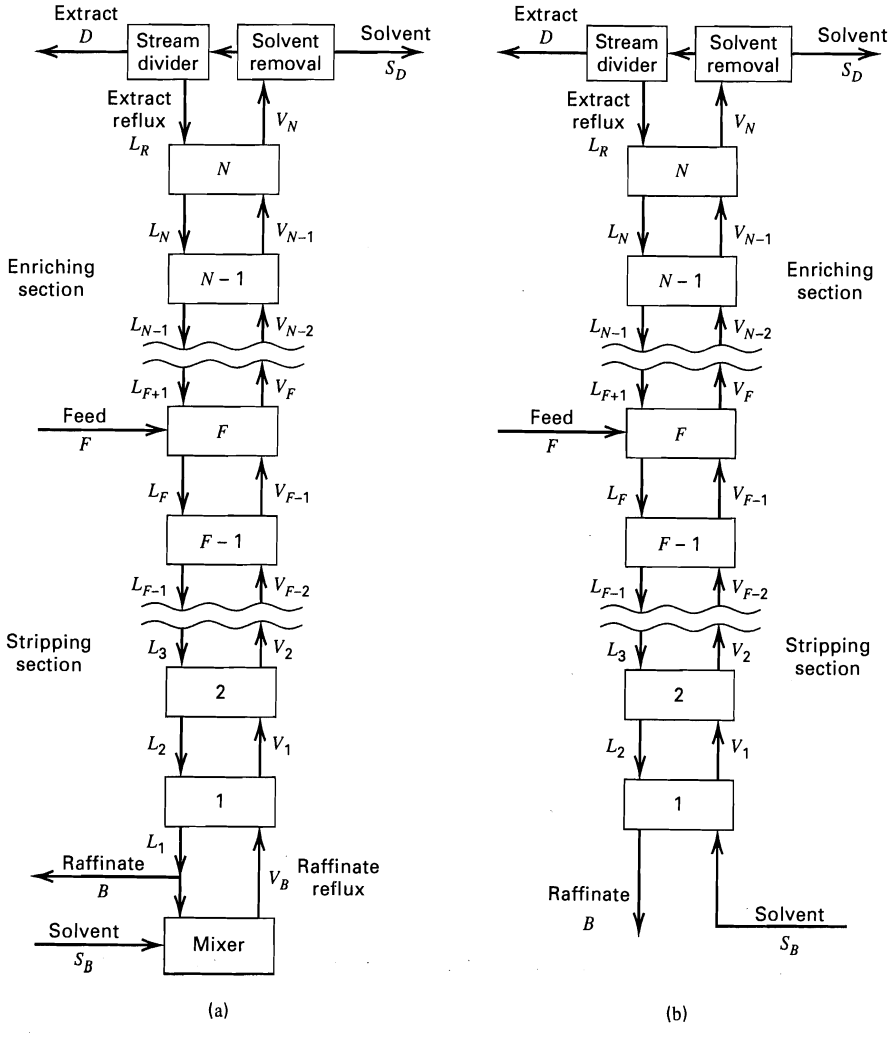

Figure 8.26 Liquid–liquid extraction with reflux: (a) with extract and raffinate reflux; (b) with extract reflux only.

Table 8.5 Analogy between Distillation and Extraction

Distillation	Extraction
Addition of heat	Addition of solvent
Reboiler	Solvent mixer
Removal of heat	Removal of solvent
Condenser	Solvent separator
Vapor at the boiling point	Solvent-rich solution saturated with solvent
Superheated vapor	Solvent-rich solution containing more solvent than that required to saturate it
Liquid below the boiling point	Solvent-lean solution, containing less solvent than that required to saturate it
Liquid at the boiling point	Solvent-lean solution saturated with solvent
Mixture of liquid and vapor	Two-phase liquid mixture
Relative volatility	Relative selectivity
Change of pressure	Change of temperature
D = distillate	D = extract product (solute on a solvent-free basis)
B = bottoms	B = raffinate (solvent-free basis)
L = saturated liquid	L = saturated raffinate (solvent-free)
V = saturated vapor	V = saturated extract (solvent-free)
A = more volatile component	A = solute to be recovered
C = less volatile component	C = carrier from which A is extracted
F = feed	F = feed
x = mole fraction A in liquid	X = mole or weight ratio of A (solvent-free), $A/(A+C)$
y = mole fraction A in vapor	$Y = S/(A+C)$

minimum- and total-reflux conditions, corresponding to infinite and minimum number of stages, bracket the optimal extract reflux ratio. Raffinate reflux is not processed through the solvent-removal unit because fresh solvent is added at this end of the cascade. It is necessary, however, to remove solvent from extract reflux at the enriching end of the cascade.

The analogy between a two-section liquid–liquid extractor with feed entering a middle stage, and distillation, is considered in some detail by Randall and Longtin [32]. Different aspects of the analogy are listed in Table 8.5. The most important analogy is that the solvent (a mass-separating agent) in extraction serves the same purpose as heat (an energy-separating agent) in distillation.

The use of raffinate reflux has been judged to be of little, if any, benefit by Skelland [31], who shows that the amount of raffinate reflux does not affect the number of stages required. Accordingly, we will consider a two-section, countercurrent cascade that includes only extract reflux, as shown in Figure 8.26b.

Analysis of a refluxed extractor, such as that of Figure 8.26b, involves relatively straightforward extensions of the procedures already developed. As will be shown, however, results for a type I system depend critically on the feed composition and the nature of the equilibrium-phase diagram, and it is very difficult to draw any general conclusions with respect to the effect (or even feasibility) of reflux.

For the two-section cascade with extract reflux shown in Figure 8.26b, a degrees-of-freedom analysis can be performed as described in Chapter 5. The result, using as elements two countercurrent cascades, a feed stage, a splitter, and a divider, is $N_D = 2N + 3C + 13$. All but four of the specifications will usually be

Variable Specification	Number of Variables
Pressure at each stage	N
Temperature for each stage	N
Feed-stream flow rate, composition, temperature, and pressure	$C+2$
Solvent composition, temperature, and pressure	$C+1$
Split of each component in the splitter (solvent removal step)	C
Temperature and pressure of the two streams leaving the splitter	4
Pressure and temperature of the divider	2
	$2N+3C+9$

The four additional specifications can be taken from one of the following sets:

Set 1	Set 2	Set 3
Solvent rate	Reflux ratio	Solvent rate
Solute concentration in extract (solvent free)	Solute concentration in extract (solvent-free)	Reflux ratio
Solute concentration in raffinate (solvent-free)	Solute concentration in raffinate (solvent-free)	Number of stages
Optimal feed-stage location	Optimal feed-stage location	Feed-stage location

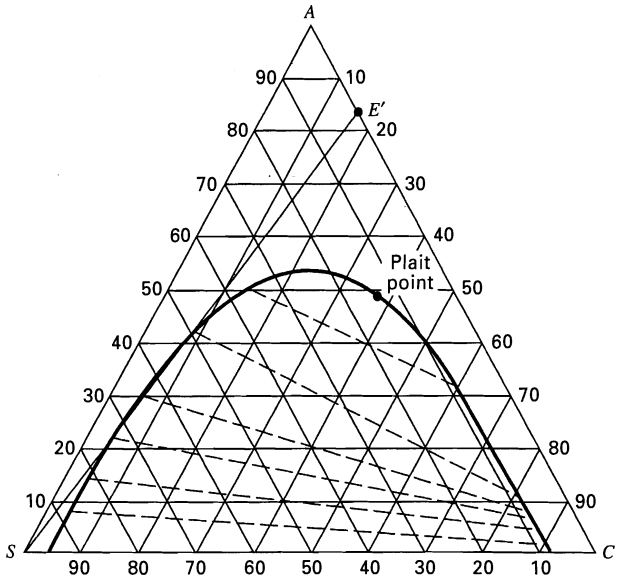

(a)

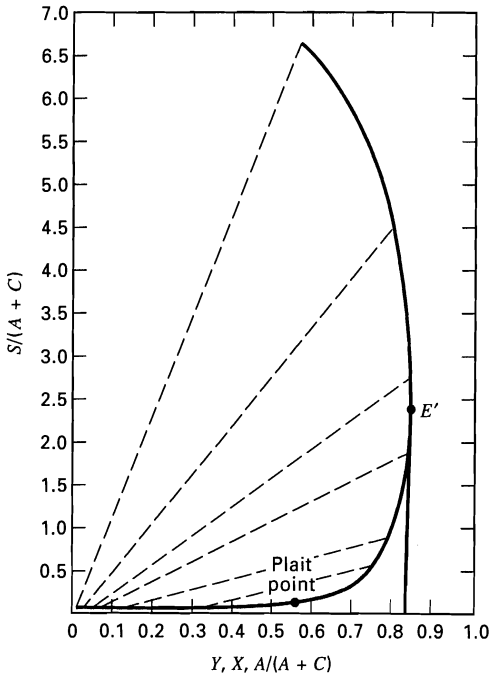

(b)

Figure 8.27 Limitation on product purity: (a) using an equilateral-triangle diagram; (b) using a Janecke diagram.

Sets 1 and 2 are of particular interest in the design of a new extractor because two of the specifications deal with the split of the feed into two products of designated purities, on a solvent-free basis. Set 2 is analogous to the design of a binary distillation column using the McCabe–Thiele graphical method, where the purities of the distillate and bottoms, the reflux ratio, and the optimal feed-stage location are specified. For a single-section cascade, it is not feasible to specify the split of the feed with respect to two key components. Instead, as in absorption and stripping, the recovery of just one component in the feed is specified.

It will be recalled for binary distillation that the purity of one of the products may be limited by the formation of an azeotrope. A similar limitation can occur for a type I system when using a two-section cascade with extract reflux, because of the plait point, which separates the two-liquid-phase region from the homogeneous, single-phase region. This limitation can be determined from a triangular diagram, but it is most readily observed on a Janecke diagram, of the type described in Chapter 4 and shown previously in Figure 4.14e. In Figure 8.27, liquid–liquid equilibrium data are repeated for the A–C–S system of Figure 8.14 where A is the solute and S is the solvent. In the triangular representation of Figure 8.27a, the maximum solvent-free solute concentration that can be achieved in the extract by a countercurrent cascade with extract reflux is determined by the intersection of line $\overline{SE'}$, drawn tangent to the binodal curve, from the pure solvent point S to the solvent-free composition line $\overline{AC}$, giving, in this case, 83 wt% solute. The same value is read from the binodal curve of the Janecke diagram of Figure 8.27b as the value of the abscissa for the point E' farthest to the right of the curve.

Without extract reflux, the maximum solvent-free solute concentration that can be achieved corresponds to an extract that is in equilibrium with the feed, when saturated with the extract. If this maximum value is close to the maximum value determined, as in Figure 8.27, then the use of extract reflux will be of little value. This is often the case for type I systems, as illustrated in the following example.

EXAMPLE 8.2

In Example 8.1, a feed mixture of 30 wt% acetone and 70 wt% ethyl acetate was extracted in a single-section, countercurrent cascade with pure water to obtain a raffinate of 5 wt% acetone on a water (solvent)-free basis. The maximum solvent-free solute concentration in the extract was found to be 64 wt%, as shown in Figure 8.20 at point D, corresponding to the condition of minimum $S/F = 0.60$ at infinite stages. For an actual $S/F = 1.75$ with four equilibrium stages, the extract contains 62 wt% acetone on a solvent-free basis. Thus, use of extract reflux for the purpose of producing a more pure (solvent-free) extract is not very attractive, given the particular phase-equilibrium diagram and feedstock composition. However, to demonstrate the technique, the calculation for extract reflux is carried out nevertheless. Also, the minimum number of equilibrium stages at total reflux and the minimum reflux ratio are determined.

SOLUTION

For the case of the single-section countercurrent cascade, the extract pinch point is at 57 wt% water, 27 wt% acetone, and 16 wt% acetate, as shown in Figure 8.20 at point D'_{min}. If stages are added above the feed point, as in the two-section, refluxed cascade of Figure 8.26b, it is possible, theoretically, to reduce the water content of the extract to about 28 wt%, as shown by point G in Figure 8.20. However, the solvent (water)-free extract would not be as rich in acetone (51 wt%), which is determined from the line drawn through points S and G and extended to where it intersects the solvent-free line $\overline{AC}$.

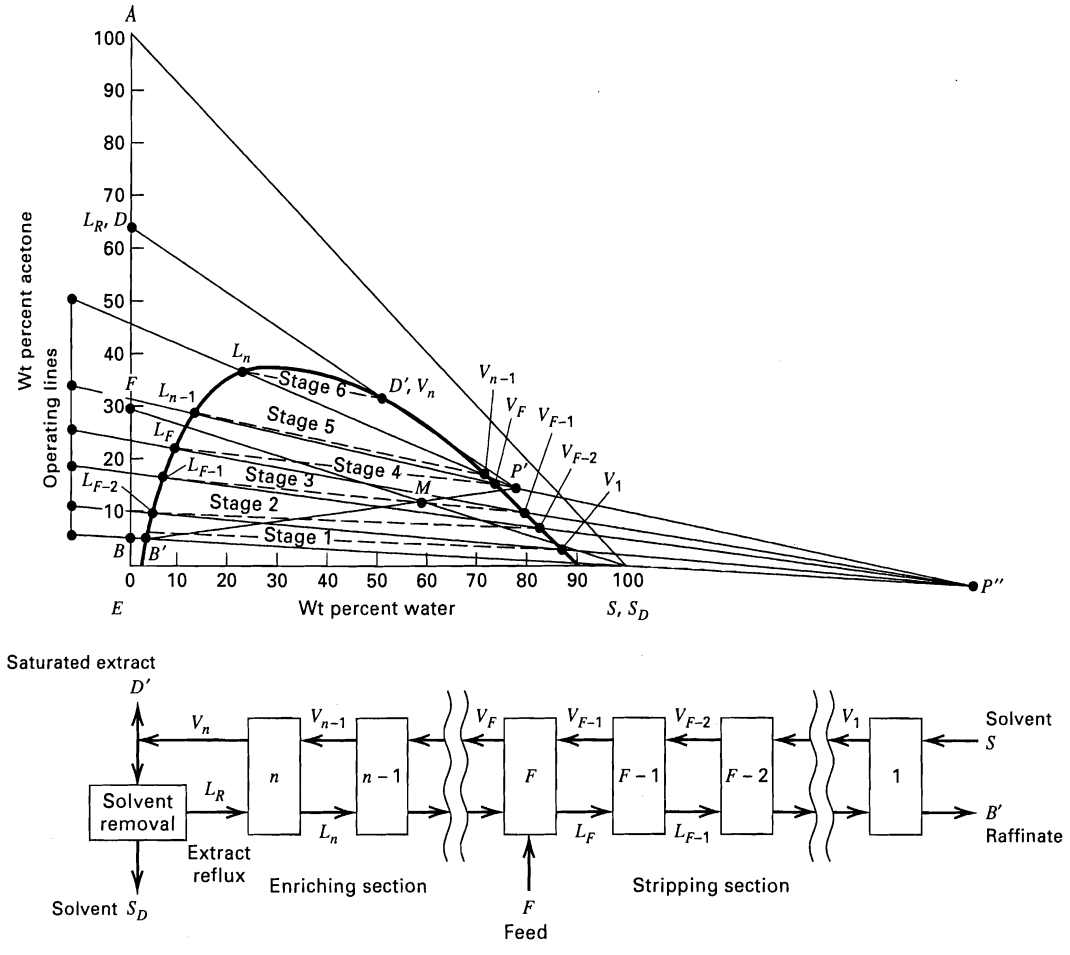

Figure 8.28 Equilibrium stages for Example 8.2.

To make this example more interesting, assume that a saturated extract containing 50 wt% water is required elsewhere in the process. Thus, the extraction cascade is that shown in Figure 8.28, rather than that of Figure 8.26b. The difference lies in the location of the solvent-removal step. This saturated-extract product is shown as point D' in Figure 8.28. Assume the ratio S/F to be 1.43, which is more than twice the minimum ratio found in Example 8.1. The desired raffinate composition is again 5 wt% acetone on a water-free basis (point B in Figure 8.28), which maps to point B' on the raffinate side of the binodal curve on a line connecting points B and S.

As with single-section cascades, the mixing point, M, in Figure 8.28, for the two streams entering the cascade, S and F, is determined by applying the inverse-lever-arm rule, using the S/F ratio, or by computing the overall composition of M, which in this case is 59 wt% water, 29 wt% acetate, and 12 wt% acetone.

The cascade in Figure 8.28 consists of an enriching section to the left of the feed point and a stripping section to the right, where extract is enriched in solute and raffinate is stripped of solute, respectively. A difference or operating point is needed for each section. We will let these be P' and P'', respectively, for the enriching and stripping sections. In the enriching section, referring to the cascade in Figure 8.28, $P' = V_n - L_R = V_{n-1} - L_n$. But, by material balance, $V_n - L_R = D' + S_D$. Therefore, $P' = D' + S_D$, that is, the total flow leaving the extract end of the cascade. Also, by overall material balance, $M = F + S = B' + D' + S_D = B' + P'$. Thus, P' must lie on a line drawn through points B' and M. To locate the position of P' on that line, we also note that V_n has the same composition as D', and L_R is simply D' with the solvent removed (point D). From above, however, $P' = V_n - L_R$ or $V_n = P' + L_R$. Thus, point P' must also lie on a line drawn through points $V_n(D')$ and $L_R(D)$. Thus, point P' is located at the intersection of the extended lines $\overline{B'M}$ and $\overline{DD'}$ as shown in Figure 8.28.

The difference point, P'', for the stripping section is located in a similar manner, if we note that $P'' = B' - S = F - D' - S_D = F - P'$. Thus, P'' must be the intersection of extended lines $\overline{FP'}$ and $\overline{B'S}$ as shown to the right of the triangular diagram of Figure 8.28.

The stages can now be stepped off in the usual manner by starting from V_n and using the difference point P' until an operating line crosses the feed line $\overline{FP'}$. From there, the stages are stepped off using the difference point P'' until the raffinate composition is reached or exceeded. In Figure 8.28, it is seen that six equilibrium stages are required, with two in the enriching section and four in the stripping section. The feed enters the third stage from the left.

The reflux ratio, defined for this example as $(V_n - D')/D' = (L_R + S_D)/D'$, can be determined as follows. From above, $P' = D' + S_D$. Therefore, by the mixing rule, $S_D/D' = \overline{D'P'}/\overline{S_DP'}$. By material balance, $V_n - D' = L_R + S_D$. Therefore,

$$\frac{V_n - D'}{S_D} = \frac{L_R + S_D}{S_D} = \frac{\overline{L_RS_D}}{\overline{L_RD'}} \quad \text{and}$$

$$\frac{V_n - D'}{D'} = \left(\frac{S_D}{D'}\right)\left(\frac{V_n - D'}{S_D}\right) = \left(\frac{\overline{D'P'}}{\overline{S_DP'}}\right)\left(\frac{\overline{L_RS_D}}{\overline{L_RD'}}\right)$$

By measurement from Figure 8.28, $(V_n - D')/D' = (1.2)(2.0) = 2.4$. The reflux ratio is valid only for the selected solvent-to-feed ratio of 1.43.

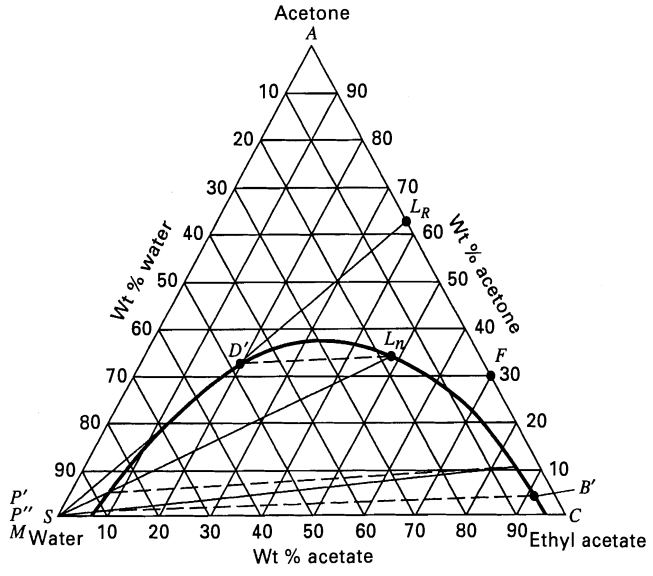

Figure 8.29 Total reflux and minimum stages for Example 8.2.

Next, we consider the case of total reflux, corresponding to the minimum number of stages. With reference to the equilateral-triangle diagram of Figure 8.29, compositions of existing streams are as previously specified or computed. With respect to acetone, we have 30 wt% in F, 4.9 wt%, in B', 33 wt%, in D', and 62 wt% in L_R. As in the case of the single-section cascade of Figure 8.20, as the solvent-to-feed ratio is increased, the mixing point $M = F + S$ moves toward the pure-solvent apex. At the maximum solvent addition, M lies at the intersection of the line through F and S with the extract side of the binodal curve. Difference points P' and P'' also move toward S because $P' = D' + S_D$ approaches S_D at total reflux and $P'' = F - P'$ approaches P', recalling that at total reflux $F = D' = 0$. As shown in Figure 8.29, the minimum number of equilibrium stages is three, as stepped off from the S apex.

Lastly, we consider the case of minimum reflux ratio at infinite stages, which also corresponds to the minimum solvent ratio. As the solvent ratio is reduced, point M moves toward the feed point, F, and point P'' moves away from the binodal curve. Also, point P' moves toward V_n. Ultimately, a value of the S/F ratio is reached where an operating line in either the enriching section or the stripping section coincides with a tie line, giving a pinch point and, therefore, an infinite number of stages. Often, this occurs for the extended tie line that passes through the feed point. Such is the case here, giving a minimum reflux ratio of about 0.6 and a corresponding minimum S/F ratio of about 0.75.

8.4 MALONEY–SCHUBERT GRAPHICAL EQUILIBRIUM-STAGE METHOD

For type II ternary systems, as shown in Figure 8.10b, use of a two-section cascade with extract reflux is particularly desirable. Without a plait point, the two-phase region extends all the way across the solute composition. Thus, while maximum solvent-free solute concentration in the extract is limited for a type I system as was shown in Figure 8.27, no such limit exists with a type II system. Accordingly, it is possible with extract reflux to achieve as sharp a separation as desired between the solute (A) and carrier (C).

When reflux is used, many stages may be required and the use of triangular diagrams is often not convenient. Instead, use can be made of a McCabe–Thiele-type diagram. Alternatively, a Janecke diagram, of the type shown earlier in Figure 4.14e, often in conjunction with a distribution diagram, has proved to be useful. In Janecke diagrams, which use convenient rectangular coordinates, solvent concentration on a solvent-free basis is plotted as the ordinate against solute concentration on a solvent-free basis as the abscissa, that is, $\%S/(\%A + \%C)$ against $\%A/(\%A + \%C)$, either with mass or mole percents. The Janecke diagram is analogous to an enthalpy–concentration diagram and is consistent with the distillation-extraction analogy of Table 8.5, where enthalpy is replaced by solvent concentration because a mass-separating agent replaces an energy-separating agent. The application of such a diagram to liquid–liquid extraction of a type II system with the use of reflux is considered in detail by Maloney and Schubert [33], who use an auxiliary distribution diagram of the McCabe–Thiele type, but on a solvent-free basis, to facilitate visualization of the stages. This method is also referred to as the *Ponchon–Savarit method for extraction.* Unlike the analogous method for distillation mentioned briefly at the end of Chapter 7 and which requires both enthalpy and vapor–liquid equilibrium data, the method for extraction requires only ternary liquid–liquid solubility data, which are far more common than combined vapor–liquid enthalpy and equilibrium data. Accordingly, despite the development of rigorous computer-aided methods, the Ponchon–Savarit method for extraction has remained useful, while the analogous method for distillation has rapidly declined in popularity. Although the Janecke diagram can also be applied to type I systems, it becomes difficult to use when the carrier and the solvent are highly immiscible, because the resulting values of the ordinate can become very large.

With the Janecke diagram, construction of tie lines, mixing points, operating points, and operating lines are all made in a manner similar to that for a triangular diagram [33]. Consider the case of extraction for a type II system with extract reflux, shown in Figure 8.26b. A representative Janecke diagram is shown in Figure 8.30, where all flow rates are on a solvent-free mass basis and the following solvent-free concentrations for both extract and raffinate phases are based on Janecke coordinates:

$$Y = \frac{\text{mass solvent}}{\text{mass of solvent-free liquid phase}}$$

$$X = \frac{\text{mass solute}}{\text{mass of solvent-free liquid phase}}$$

Values of the ordinate, Y, especially for the saturated-extract phase, can vary over a wide range depending on the solubility of the solute and carrier in the solvent. Values of the abscissa, X, vary from 0 to 1 (pure carrier to pure solute). Equilibrium tie lines relate concentrations in the saturated extract to the saturated raffinate. The Y location of the feed, F, is somewhere between zero and the saturated-raffinate curve. The extract, V_N, leaving stage N and prior to solvent

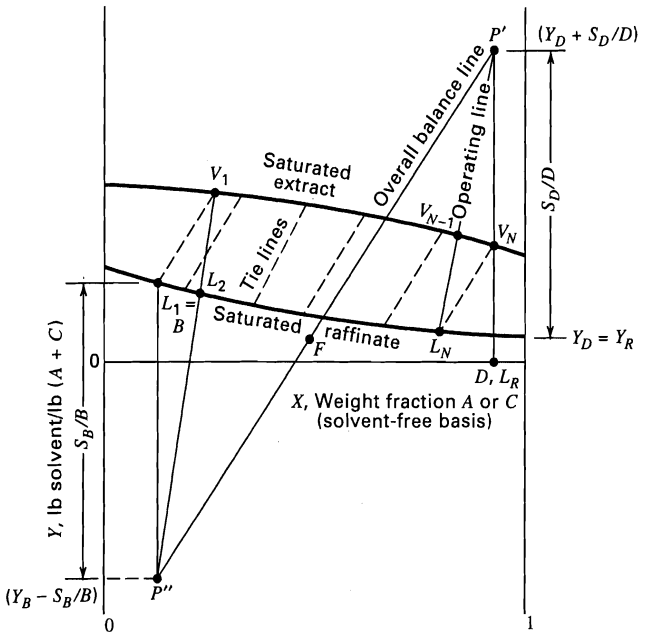

Figure 8.30 Construction of equilibrium stages on a Janecke diagram.

removal, is rich in solute and lies on the saturated extract curve. Upon solvent removal, the extract, D, and extract reflux, L_R, with identical compositions, lie on the $Y = 0$ horizontal line. The solvent removed from the cascade, S_D, is assumed to be pure. The raffinate, L_1, leaving stage 1 is rich in the carrier and lies on the saturated-raffinate line. Solvent S_B, fed to the cascade, is assumed to be pure.

Points P' and P'' are difference or operating points for the enriching and stripping sections, respectively, that are used to draw operating lines. The locations of P' and P'' are derived as follows: Referring to Figure 8.26b, solvent-free and solvent material balances around the solvent-recovery step, in terms of passing streams, are, respectively,

$$V_N - L_R = D \tag{8-13}$$

$$Y_{V_N} V_N - Y_D L_R = S_D + Y_D D \tag{8-14}$$

For a solvent difference balance around a section of top stages down to stage n, located above stage F in Figure 8.26b, we obtain

$$Y_{V_n} V_n - Y_{L_{n+1}} L_{n+1} = S_D + Y_D D \tag{8-15}$$

Thus, any solvent flow difference between passing streams in the enriching section above the feed stage is given by $S_D + Y_D D$. If (8-13) and (8-14) are combined to eliminate V_N, we obtain

$$\frac{L_R}{D} = \frac{(Y_D + S_D/D) - Y_{V_N}}{Y_{V_N} - Y_D} \tag{8-16}$$

In Figure 8.30, $(Y_{V_N} - Y_D)$ is the vertical distance between the points V_N and (D, L_R). The difference point, P', in Figure 8.30 becomes $(S_D + Y_D D)$ divided by D to give $(Y_D + S_D/D)$. That is,

$$P' = Y_D + S_D/D \tag{8-17}$$

and

$$L_R/D = \overline{P'V_N}/\overline{V_N L_R} \tag{8-18}$$

Similarly, for the stripping section, it can be shown that,

$$P'' = Y_B - S_B/B \tag{8-19}$$

$$D/B = \overline{FP''}/\overline{P'F} \tag{8-20}$$

Stages are stepped off in a manner analogous to that for the triangular diagram, starting from either the extract, D, or the raffinate, B, alternating between operating lines and tie lines. For example, in Figure 8.30, we can start from the top of the cascade at the extract D and step off stages in the enriching section. The solute compositions of D, L_R, and V_N on a solvent-free basis are identical. Thus, the operating line for passing streams L_R and V_N is a vertical line passing through the difference point P'. From point V_N on the saturated extract curve, a tie line is followed down to the equilibrium raffinate phase, L_N. An operating line connecting points P' and L_N intersects the extract curve at the passing stream V_{N-1}. Subsequent stages in the enriching section are stepped off in a similar manner until the feed stage is reached. The optimal location of this stage is determined in a manner analogous to the intersection of the rectification and stripping operating lines in the McCabe–Thiele method. On the Janecke diagram, this intersection is the line $\overline{P'P''}$, which passes through the feed point, as shown in Figure 8.30. Thus, the transition from the enriching section (where the difference point P' is used) to the stripping section (where P'' is used) is made when an equilibrium tie line for a stage crosses the line $\overline{P'P''}$. Following the location of the feed stage, the remaining stripping-section stages are stepped off until the desired product raffinate solvent-free concentration is reached or crossed over.

The Janecke diagram can also be used to determine the two limiting conditions of total reflux (minimum stages) and minimum reflux (infinite stages). For total reflux, the difference points P' and P'' lie at $Y = +\infty$ and $-\infty$, respectively, because $F = B = D = 0$. Thus, all operating lines become vertical lines and the minimum number of stages are stepped off in the manner illustrated in Figure 8.31a.

For the condition of minimum reflux, a pinch condition is sought either at the feed stage or some other stage location. In Figure 8.31b, where the pinch is assumed to be at the feed stage, an operating line is drawn coincident with a tie line and the feed point, F, to determine points P' and P''. To determine if the pinch does occur at the feed stage, tie lines to the right of the feed-stage tie line are extended to an intersection with the vertical line through D. If a higher intersection occurs, then that P' may be the correct $P'_{\min}$ difference point for minimum reflux. In a similar manner, tie lines to the left of the feed-stage tie line are extended to an intersection with the vertical line through B. If a lower intersection occurs, then that P'' may be the factor that determines the minimum reflux. The former case is shown in Figure 8.31c, where P' is higher than P'_1. Thus, $P' = P'_{\min}$. In any case, once the controlling P' or P'' is determined, a line through F determines the other difference point and the minimum reflux ratio is computed from (8-18) using $P'_{\min}$.

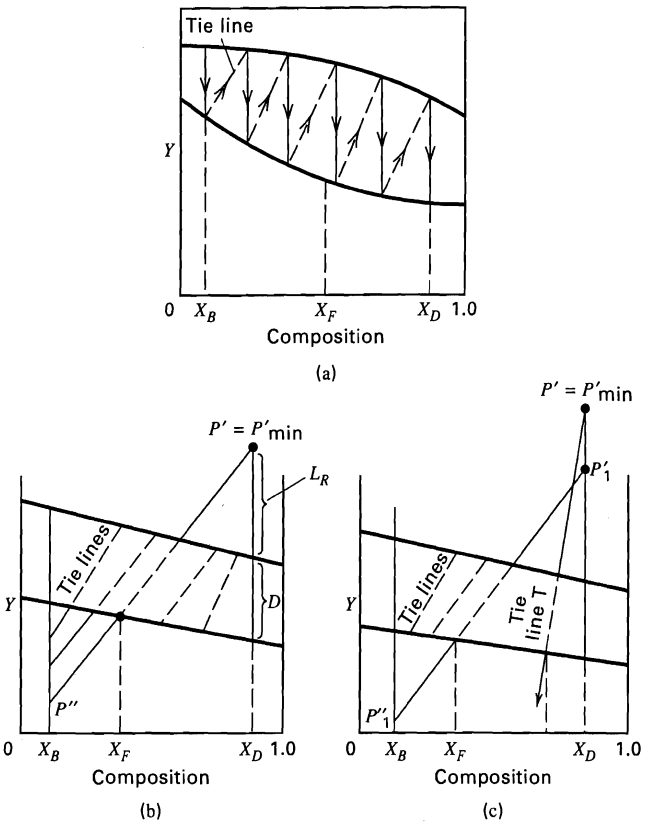

Figure 8.31 Limiting conditions on a Janecke diagram: (a) minimum number of stages at total reflux; (b) minimum reflux determined by a tie line through the feed point; (c) minimum reflux determined by a tie line to the right of the feed point.

EXAMPLE 8.3

As shown in Figure 8.32, a countercurrent, extraction cascade equipped with a perfect solvent separator to provide extract reflux is used to separate methylcyclopentane (A) and n-hexane (C) into a final extract and raffinate containing, on a solvent-free basis, 95 wt% and 5 wt% A, respectively, using aniline (S) as the solvent. The feed rate is 1,000 kg/h with 55 wt% A, and the mass ratio of solvent to feed is 4.0. The feed contains no aniline and the fresh solvent is pure. Recycle solvent is also assumed to be pure. Equilibrium curves and tie lines are given in Figure 8.33.

(a) Determine the reflux ratio and number of stages. Equilibrium data at extractor temperature and pressure are shown for mass units in the Janecke diagram of Figure 8.33. Feed is to enter at the optimal stage.

(b) Determine the minimum number of stages for the specified solvent-free extract and raffinate compositions.

(c) Determine the minimum reflux ratio for the specified feed and product compositions.

SOLUTION

(a) First, determine all product rates by material-balance calculations. An overall balance on solute plus carrier gives $D + B = 1{,}000$ kg/h

$$\text{A solute balance gives } 0.95D + 0.05B = (0.55)(1{,}000) = 550 \text{ kg/h}$$

Solving these two equations simultaneously gives $D = 556$ kg/h and $B = 444$ kg/h. Since $S_B = 4{,}000$ kg/h, $S_B/B = 9.0$. In Figure 8.30, point P'' is located at a distance of S_B/B below the raffinate composition, X_B, at point B. Since Y at point B, from Figure 8.33, is approximately 0.3, point P'' is located at $0.3 - 9.0 = -8.7$.

A line drawn through P'' and F, extended to the intersection with the vertical line through D, gives $P' = 6.7$. By measurement from Figure 8.33, using (8-16), $L_R/D = 3.7$.

In Figure 8.33, stages are stepped off starting from point D. At the third stage ($N - 2$), the tie line crosses line $\overline{P''FP'}$. Thus, this is the optimal feed stage. Three more stages are required to reach B, giving a total of six equilibrium stages.

(b) If the construction for minimum stages, shown in Figure 8.31a, is used in Figure 8.33, just less than five stages are determined.

(c) If the construction for minimum reflux, shown in Figure 8.31b for a pinch at the feed stage, is used in Figure 8.33, a value of $P' = 2.90$ is obtained. No other tie line in either section gives a larger value. Therefore, $P_{min} = 2.9$. By measurement, using (8-18), $(L_R/D)_{min} = 0.83$. Using the construction indicated in Figure 8.30, the corresponding $(S_B/B)_{min}$ is found to be 4.2. Thus, $(S_B)_{min} = 4.2(444) = 1{,}865$ kg/h or $(S_B/F)_{min} = 1{,}865/1{,}000 = 1.865$.

For this example, a relatively high reflux ratio and corresponding solvent-to-feed ratio is employed to keep the required number of equilibrium stages small. When the number of equilibrium stages is large, the Janecke diagram becomes cluttered with operating lines and tie lines. In that case, an auxiliary McCabe–Thiele-type plot of solute mass fraction in the extract layer versus solute mass fraction in the raffinate layer, both on a solvent-free basis, as in the Janecke diagram, can be drawn, with points on the enriching and stripping operating lines determined, as discussed above, from arbitrary operating lines on the Janecke diagram. Stages are

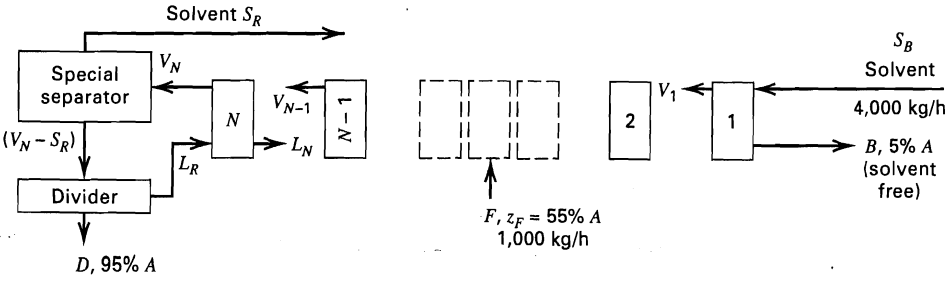

Figure 8.32 Countercurrent extraction cascade with extract reflux for Example 8.3.

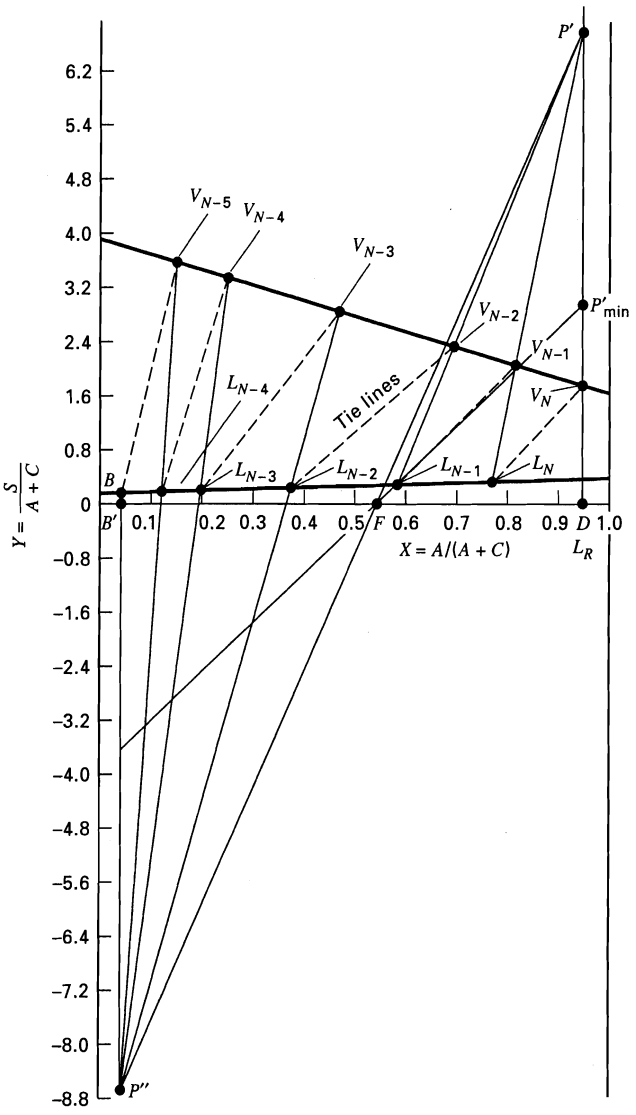

Figure 8.33 Maloney–Schubert constructions on Janecke diagram for Example 8.3.

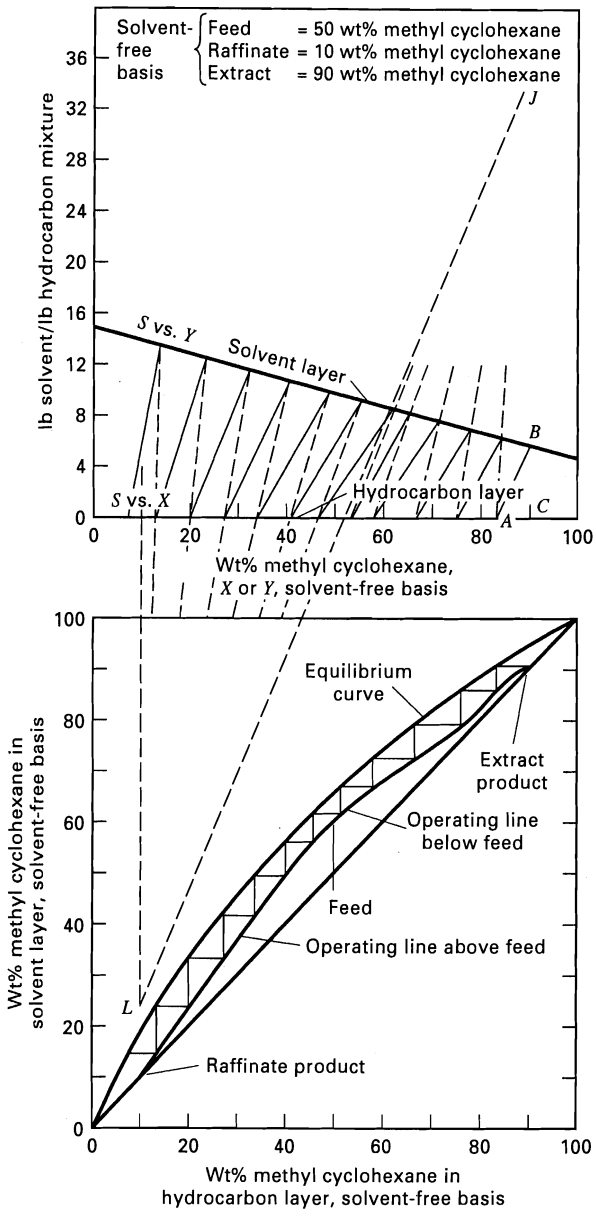

Figure 8.34 Use of Janecke diagram with auxiliary distribution diagram.

[From *Chemical Engineers' Handbook*, 5th ed., R.H. Perry and C.H. Chilton, Eds., McGraw-Hill, New York (1973).]

then stepped off in the McCabe–Thiele manner. An example of the Janecke diagram with such an auxiliary McCabe–Thiele diagram is shown in Figure 8.34, taken from Maloney and Schubert [33].

8.5 THEORY AND SCALE-UP OF EXTRACTOR PERFORMANCE

Following the estimation, by methods described in Sections 8.3 and 8.4, of the number of equilibrium stages, suitable extraction equipment can be selected using the scheme of Figure 8.8. Often, the choice is between a cascade of mixer-settler units or a multicompartment, column-type extractor with mechanical agitation, the main considerations being the number of stages required, and the floor space and head room available. Methods for estimating size and power requirements of these two general types of extractors are presented next. Column devices with no mechanical agitation are also considered.

Mixer-Settler Units

Sizing of mixer-settler units is done most accurately by scale-up from batch or continuous runs in laboratory or pilot-plant equipment. However, preliminary-sizing calculations can be made using available theory and empirical correlations. Experimental data of Flynn and Treybal [34] show that when liquid-phase viscosities are less than 5 cP and the specific-gravity difference between the two liquid phases is greater than about 0.10, the average residence time required of the two liquid phases in the mixing vessel to achieve at least 90% stage efficiency may be as low as 30 s and is usually not more than 5 min, when an agitator-power input per mixer volume of 1,000 ft-lbf/min-ft^3 (4 hp/1,000 gal) is used.

Based on experiments reported by Ryan, Daley, and Lowrie [35], the capacity of a settler vessel can be expressed in terms of C gal/min of combined extract and raffinate per square foot of phase-disengaging area. For a horizontal, cylindrical vessel of length L and diameter D_T, the economic ratio of L to D_T is approximately 4. Thus, if the phase interface is located at the middle of the vessel, the disengaging area is $D_T L$ or $4D_T^2$. A typical value of C given by Happel and Jordan [36] is about 5. Frequently, the settling vessel will be larger than the mixing vessel, as is the case in the following example.

EXAMPLE 8.4

Benzoic acid is to be continuously extracted from a dilute solution in water with a solvent of toluene in a series of discrete mixer-settler vessels operated in countercurrent flow. The flow rates of the feed and solvent are 500 and 750 gal/min, respectively. Assuming a residence time, t_{res}, of 2 min in each mixer and a settling vessel capacity of 5 gal/min-ft^2, estimate:

(a) Diameter and height of a mixing vessel, assuming $H/D_T = 1$

(b) Agitator horsepower for a mixing vessel

(c) Diameter and length of a settling vessel, assuming $L/D_T = 4$

(d) Residence time in a settling vessel in minutes

SOLUTION

(a) Q = total flow rate = 500 + 750 = 1,250 gal/min
V = volume = Qt_{res} = 1,250(2) = 2,500 gal or 2,500/7.48 = 334 ft^3

$$V = \pi D_T^2 H/4,\ H = D_T,\ \text{and}\ V = \pi D_T^3/4$$
$$D_T = (4V/\pi)^{1/3} = [(4)(334)/3.14]^{1/3}$$
$$= 7.52\ \text{ft and}\ H = 7.52\ \text{ft}$$

(b) Horsepower = 4(2,500/1,000) = 10 hp

(c) $D_T L = 1{,}250/5 = 250\ \text{ft}^2$; $D_T^2 = 250/4 = 62.5\ \text{ft}^2$

$$D_T = 7.9\ \text{ft};\ L = 4D_T = 4(7.9) = 31.6\ \text{ft}$$

(d) Volume of settler = $\pi D_T^2 L/4 = 3.14(7.9)^2(31.6)/4 = 1{,}548\ \text{ft}^3$ or 1,548(7.48) = 11,580 gal

$$t_{res} = V/Q = 11{,}580/1{,}250 = 9.3\ \text{min}$$

A typical single-compartment mixing tank for liquid–liquid extraction is shown in Figure 8.35. The vessel is closed with the two liquid phases entering at the bottom and the effluent, in the form of a two-phase emulsion, leaving at the top. Although flat tank heads are shown in Figure 8.35, rounded heads of the type in Figure 8.2 are preferred to eliminate stagnant fluid regions. Air or other gases must be evacuated from the vessel so no gas–liquid interface exists.

Mixing is accomplished by an appropriate, centrally located impeller selected from the many types available, some of which are shown in Figure 8.3. For example, a flat-blade turbine might be chosen as in Figure 8.35. A single turbine is adequate unless the vessel height is greater than the vessel diameter, in which case a compartmented vessel with two or more impellers might be employed. When the vessel is open, vertical side baffles are mandatory to prevent vortex formation at the gas–liquid interface. For closed vessels that run full of liquid, vortexing will not occur. Nevertheless, it is common to install baffles, even in closed tanks, to minimize swirling and improve circulation patterns. Although no standards exist for vessel and turbine geometry, the following, with reference to Figure 8.35, give good dispersion performance in liquid–liquid agitation:

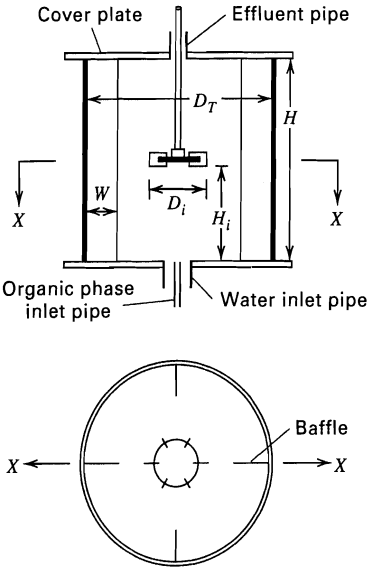

Figure 8.35 Agitated vessel with flat-blade turbine and baffles.

Number of turbine blades = 6;
Number of vertical baffles = 4

$$H/D_T = 1;\quad D_i/D_T = 1/3;$$
$$W/D_T = 1/12 \quad \text{and} \quad H_i/H = 1/2$$

To achieve a high stage efficiency for extraction in a mixing vessel—say, between 90 and 100%—it is necessary to provide fairly vigorous agitation. For a given type of impeller and vessel–impeller geometry, the agitator power, P, can be estimated from an empirical correlation in terms of a power number, N_{Po}, which depends on an impeller Reynolds number, N_{Re}, where

$$N_{Po} = \frac{P g_c}{N^3 D_i^5 \rho_M} \tag{8-21}$$

$$N_{Re} = \frac{D_i^2 N \rho_M}{\mu_M} \tag{8-22}$$

The impeller Reynolds number is the ratio of the inertial force to the viscous force:

$$\text{Inertial force} \propto (N D_i)^2 \rho_M D_i^2$$

$$\text{Viscous force} \propto \frac{\mu_M (N D_i) D_i^2}{D_i}$$

where N = rate of impeller rotation. Thus, the characteristic length in the impeller Reynolds number is the impeller diameter and the characteristic velocity is ND_i = impeller peripheral velocity.

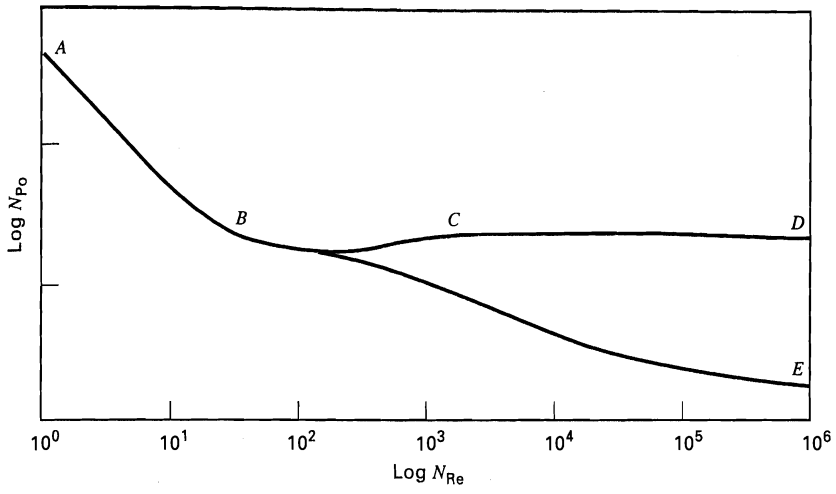

(a)

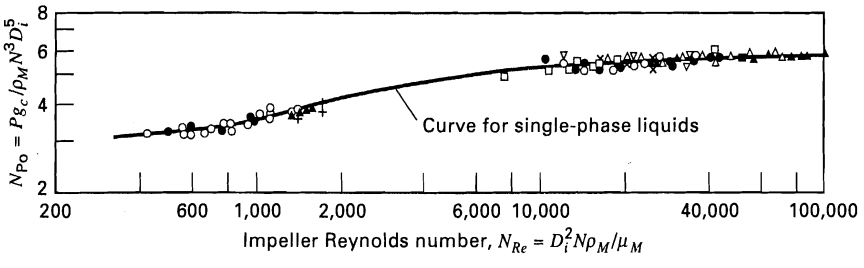

(b)

Figure 8.36 Power consumption of agitated vessels. (a) Typical power characteristics. [From J.H. Rushton and J.Y. Oldshue, *Chem. Eng. Prog.*, **49,** 161–168 (1953).] (b) Power correlation for six-bladed, flat-blade turbines with no vortex. [From D.S. Laity and R.E. Treybal, *AIChE J.*, **3,** 176–180 (1957).]

The agitator power is proportional to the product of the volumetric liquid flow produced by the impeller and the applied kinetic energy per unit volume of fluid. The result is

$$P \propto (ND_i^3)[\rho_M(ND_i)^2/2g_c]$$

which can be rewritten as (8-21), where the constant of proportionality is $2N_{Po}$. Both the impeller Reynolds number and the power number (also called the Newton number) are dimensionless groups. Thus, any consistent set of units can be used. The power number for an agitated vessel serves the same purpose as the friction factor for the flow of a fluid through a pipe. This is illustrated, over a wide range of impeller Reynolds number, for a typical mixing impeller in Figure 8.36a, taken from the work of Rushton and Oldshue [37]. The upper curve, ABCD, pertains to a vessel with baffles, while the lower curve, ABE, pertains to the same tank with no baffles. In the low-Reynolds-number region, AB, viscous forces dominate and the impeller power is proportional to $\mu_M N^2 D_i^3$. Somewhere beyond a Reynolds number of about 200, a vortex appears if no baffles are present and the power-number relation is given by curve BE. In this region, the Froude number, $N_{Fr} = N^2 D_i/g$, which is the ratio of inertial to gravitational forces, also becomes a factor. With baffles present, and the Reynolds number greater than about 1,000, a region, CD, is reached where fully developed turbulent flow exists. Now, inertial forces dominate and the power is proportional to $\rho_M N^3 D_i^5$. It is clear that the addition of baffles greatly increases power requirements in the turbulent flow region.

A correlation of experimental data for liquid–liquid mixing in baffled vessels with six-bladed, flat-blade turbines is shown in Figure 8.36b, from a study by Laity and Treybal [38]. The range of impeller Reynolds number covers only the turbulent–flow region, where efficient liquid–liquid mixing is achieved. The solid line represents batch mixing of single-phase liquids. The data points represent liquid–liquid mixing, where agreement is achieved with the single-phase curve by computing two-phase mixture properties from

$$\rho_M = \rho_C \phi_C + \rho_D \phi_D \tag{8-23}$$

$$\mu_M = \frac{\mu_C}{\phi_C}\left(1 + \frac{1.5\mu_D\phi_D}{\mu_C + \mu_D}\right) \tag{8-24}$$

where ϕ is the volume fraction of holdup in the tank, with subscripts C for the continuous phase and D the dispersed phase, such that $\phi_D + \phi_C = 1$. When measurements were made for continuous flow from inlets at the bottom of the vessel to an outlet for the emulsion from the top of the vessel and with the impeller located at a position above the liquid–liquid interface when at rest, the data were correlated with the curve of Figure 8.36b.

With fully developed turbulent flow, the volume fraction of dispersed phase in the vessel closely approximates that in the feed to the vessel; otherwise the volume fraction may be different from that in the total feed to the vessel. That is, the residence times of the two phases in the vessel may not be the same. At best, spheres of uniform size can pack tightly to

give a void fraction of 0.26. Therefore, $\phi_C > 0.26$ and $\phi_D < 0.74$ is sometimes quoted. However, some experiments have shown a 0.20–0.80 range. For continuous flow, the vessel is first filled with the phase to be continuous. Following initiation of agitation, the two-feed liquids are then introduced into the vessel in their desired volume ratio.

Based on the work of Skelland and Ramsay [39] and Skelland and Lee [40], a minimum impeller rate of rotation is required for complete and uniform dispersion of one liquid into another. For a flat-blade turbine in a baffled vessel of the type discussed above, this minimum rotation rate can be estimated from

$$\frac{N_{\min}^2 \rho_M D_i}{g\,\Delta\rho} = 1.03\left(\frac{D_T}{D_i}\right)^{2.76} \phi_D^{0.106}\left(\frac{\mu_M^2 \sigma}{D_i^5 \rho_M g^2 (\Delta\rho)^2}\right)^{0.084} \tag{8-25}$$

where $\Delta\rho$ is the absolute value of the difference in density and σ is the interfacial tension between the two liquid phases. The dimensionless group on the left-hand side of (8-25) is the two-phase Froude number. The dimensionless group at the far right of (8-25) is a ratio of forces:

$$\frac{(\text{viscous})^2(\text{interfacial tension})}{(\text{inertial})(\text{gravitational})^2}$$

EXAMPLE 8.5

Furfural is to be continuously extracted from a dilute solution in water by toluene at 25°C in an agitated vessel of the type shown in Figure 8.35. The feed enters at a flow rate of 20,400 lb/h, while the solvent enters at 11,200 lb/h. For a residence time in the vessel of 2 min, estimate for either phase as the dispersed phase:

(a) The dimensions of the mixing vessel and the diameter of the flat-blade turbine impeller

(b) The minimum rate of rotation of the impeller for complete and uniform dispersion

(c) The power requirement of the agitator at the minimum rotation rate

SOLUTION

Mass flow rate of feed = 20,400 lb/h; feed density = 62.3 lb/ft^3

Volumetric flow rate of feed = Q_F = 20,400/62.3 = 327 ft^3/h

Mass flow rate of solvent = 11,200 lb/h

Solvent density = 54.2 lb/ft^3; volumetric flow rate of solvent = Q_S = 11,200/54.2 = 207 ft^3/h

Because of the dilute concentration of solute in the feed and sufficient agitation to achieve complete and uniform dispersion, assume fractional volumetric holdups of raffinate and extract in the vessel are equal to the corresponding volume fractions in the combined feed (raffinate, R) and solvent (extract, E) entering the mixer:

$$\phi_R = 327/(327 + 207) = 0.612; \quad \phi_E = 1 - 0.612 = 0.388$$

(a) Mixer volume = $(Q_F + Q_S)t_{\text{res}} = V = (327 + 207)(2/60) = 17.8$ ft^3. Assume a cylindrical vessel with $D_T = H$ and neglect the volume of the bottom and top heads and the volume occupied by the agitator and the baffles. Then

$$V = (\pi D_T^2/4)\,H = \pi D_T^3/4$$

$$D_T = [(4/\pi)V]^{1/3} = [(4/3.14)17.8]^{1/3} = 2.83 \text{ ft}$$

$$H = D_T = 2.83 \text{ ft}$$

Make the vessel 3 ft in diameter by 3 ft high, giving a volume $V = 21.2$ ft^3 = 159 gal. Assume that

$$D_i/D_T = 1/3;\ D_i = D_T/3 = 3/3 = 1 \text{ ft.}$$

(b) *Case 1—Raffinate phase dispersed:*

$$\phi_D = \phi_R = 0.612;\ \phi_C = \phi_E = 0.388$$

$$\rho_D = \rho_R = 62.3 \text{ lb/ft}^3;\ \rho_C = \rho_E = 54.2 \text{ lb/ft}^3$$

$$\mu_D = \mu_R = 0.89 \text{ cP} = 2.16 \text{ lb/h-ft};$$

$$\mu_C = \mu_E = 0.59 \text{ cP} = 1.43 \text{ lb/h-ft}$$

$$\Delta\rho = 62.3 - 54.2 = 8.1 \text{ lb/ft}^3;$$

$$\sigma = 25 \text{ dyne/cm} = 719{,}000 \text{ lb/h}^2$$

From (8-23),

$$\rho_M = (54.2)(0.388) + (62.3)(0.612) = 59.2 \text{ lb/ft}^3$$

From (8-24),

$$\mu_M = \frac{1.43}{0.388}\left[1 + \frac{1.5(2.16)(0.612)}{1.43 + 2.16}\right] = 5.72 \text{ lb/h-ft}$$

From (8-25), using American engineering units, with $g = 4.17 \times 10^8$ ft/h^2,

$$\frac{\mu_M^2 \sigma}{D_i^5 \rho_M g^2 (\Delta\rho)^2} = \frac{(5.72)^2(719{,}000)}{(1)^5(59.2)(4.17 \times 10^8)^2(8.1)^2} = 3.47 \times 10^{-14}$$

$$N_{\min}^2 = 1.03\left(\frac{g\,\Delta\rho}{\rho_M D_i}\right)\left(\frac{D_T}{D_i}\right)^{2.76} \phi_D^{0.106}(3.47 \times 10^{-14})^{0.084}$$

$$= 1.03\left[\frac{(4.17 \times 10^8)(8.1)}{(59.2)(1)}\right]\left(\frac{3}{1}\right)^{2.76}(0.612)^{0.106}(0.0740)$$

$$= 8.56 \times 10^7 (\text{rph})^2$$

$$N_{\min} = 9{,}250 \text{ rph} = 155 \text{ rpm}$$

Case 2—Extract phase dispersed: Calculations similar to case 1 result in $N_{\min}$ = 8,820 rph = 147 rpm

(c) *Case 1—Raffinate phase dispersed:*

From (8-22), $N_{\text{Re}} = \dfrac{(1)^2(9{,}250)(59.2)}{(5.72)} = 9.57 \times 10^4$

From Figure 8.36b, it is seen that a fully turbulent flow exists, with the power number given by its asymptotic value of $N_{\text{Po}} = 5.7$.

From (8-21),

$$P = N_{\text{Po}} N^3 D_i^5 \rho_M / g_c$$

$$= (5.7)(9{,}250)^3(1)^5(59.2)/(4.17 \times 10^8)$$

$$= 640{,}000 \text{ ft-lbf/h} = 0.323 \text{ hp}$$

$$P/V = 0.323(1000)/159 = 2.0 \text{ hp/1,000 gal}$$

Case 2—Extract phase dispersed:

Calculations similar to case 1 result in P = 423,000 ft-lbf/h = 0.214 hp.

$$P/V = 0.214(1000)/159 = 1.4 \text{ hp/1,000 gal}$$

Mass-Transfer Efficiency

When dispersion is complete and uniform, the contents of the vessel are perfectly mixed with respect to both phases. In that case, the concentration of the solute in each of the two phases in the mixing vessel is uniform and equal to the concentrations in the two-phase emulsion leaving the mixing vessel. This is the so-called ideal CFSTR or CSTR (continuous-flow stirred-tank reactor) model, sometimes called the completely back-mixed or perfectly mixed model, first discussed by MacMullin and Weber [41] and widely applied to reactor design. The Murphree dispersed-phase efficiency for liquid–liquid extraction, based on the raffinate as the dispersed phase, can be expressed as the fractional approach to equilibrium. In terms of bulk molar concentrations of the solute,

$$E_{MD} = \frac{c_{D,\text{in}} - c_{D,\text{out}}}{c_{D,\text{in}} - c_D^*} \tag{8-26}$$

where c_D^* is the solute concentration in equilibrium with the bulk solute concentration in the exiting continuous phase, $c_{C,\text{out}}$. The molar rate of mass transfer of the solute, n, from the dispersed phase to the continuous phase can be expressed as

$$n = K_{OD}a(c_{D,\text{out}} - c_D^*)V \tag{8-27}$$

where the concentration driving force for mass transfer is uniform throughout the well-mixed vessel and is equal to the driving force based on the exit concentrations, a is the interfacial area for mass transfer per unit volume of liquid phases, V is the total volume of liquid phases in the vessel, and K_{OD} is the overall mass-transfer coefficient based on the dispersed phase, which is given in terms of the separate resistances of the dispersed and continuous phases by

$$\frac{1}{K_{OD}} = \frac{1}{k_D} + \frac{1}{mk_C} \tag{8-28}$$

where equilibrium is assumed at the interface between the two phases and m = the slope of the equilibrium curve for the solute plotted as c_C versus c_D:

$$m = dc_C/dc_D \tag{8-29}$$

For dilute solutions, changes in volumetric flow rates of the raffinate and extract are small, and thus the rate of mass transfer based on the change in solute concentration in the dispersed phase is given by material balance:

$$n = Q_D(c_{D,\text{in}} - c_{D,\text{out}}) \tag{8-30}$$

where Q_D is the volumetric flow rate of the dispersed phase.

To obtain an expression for E_{MD} in terms of $K_{OD}a$, (8-26), (8-27), and (8-30) are combined in the following manner. From (8-26),

$$\frac{E_{MD}}{1 - E_{MD}} = \frac{c_{D,\text{in}} - c_{D,\text{out}}}{c_{D,\text{out}} - c_D^*} \tag{8-31}$$

Equating (8-27) and (8-30), and noting that the right-hand side of (8-31) is the number of dispersed-phase transfer units for a perfectly mixed vessel with $c_D = c_{D,\text{out}}$,

$$N_{OD} = \int_{c_{D,\text{out}}}^{c_{D,\text{in}}} \frac{dc_D}{c_D - c_D^*} = \frac{c_{D,\text{in}} - c_{D,\text{out}}}{c_{D,\text{out}} - c_D^*} = \frac{K_{OD}aV}{Q_D} \tag{8-32}$$

Combining (8-31) and (8-32) and solving for E_{MD},

$$E_{MD} = \frac{K_{OD}aV/Q_D}{1 + K_{OD}aV/Q_D} = \frac{N_{OD}}{1 + N_{OD}} \tag{8-33}$$

When $N_{OD} = (K_{OD}aV/Q_D) \gg 1$, $E_{MD} = 1$.

Drop Size and Interfacial Area

From (8-33) and (8-28), it is seen that an estimate of E_{MD} requires generalized correlations of experimental data for the interfacial area for mass transfer, a, and the dispersed- and continuous-phase mass-transfer coefficients, k_D and k_C, respectively. The population of dispersed-phase droplets in an agitated vessel will cover a range of sizes and shapes. For each droplet, it is useful to define d_e, the equivalent diameter of a spherical drop, using the method of Lewis, Jones, and Pratt [42],

$$d_e = \left(d_1^2 d_2\right)^{1/3} \tag{8-34}$$

where d_1 and d_2 are the major and minor axes, respectively, of an ellipsoidal-drop image. For a spherical drop, d_e is simply the diameter of the drop. For the population of drops, it is useful to define an average or mean drop diameter. A number of different definitions are available depending on whether weight-mean, mean-volume, surface-mean, mean-surface, length-mean, or mean-length diameter is appropriate [43]. For mass-transfer calculations, the surface-mean diameter, d_{vs} (also called the *Sauter mean diameter*), is most appropriate because it is the mean drop diameter that gives the same interfacial surface area as the entire population of drops for the same mass of drops. It is determined from experimental drop-size distribution data for N drops by the definition:

$$\frac{\pi d_{vs}^2}{(\pi/6)d_{vs}^3} = \frac{\pi \sum_N d_e^2}{(\pi/6)\sum_N d_e^3}$$

which, when solved for d_{vs}, gives

$$d_{vs} = \frac{\sum_N d_e^3}{\sum_N d_e^2} \tag{8-35}$$

With this definition, the interfacial surface area per unit volume of a two-phase mixture is

$$a = \frac{\pi N d_{vs}^2 \phi_D}{\pi N d_{vs}^3/6} = \frac{6\phi_D}{d_{vs}} \tag{8-36}$$

Equation (8-36) is used to estimate the interfacial area, a, from a measurement of d_{vs} or vice versa. Early experimental investigations, such as those of Vermeulen, Williams, and

Langlois [44], found that d_{vs} is dependent on a Weber number:

$$N_{We} = \frac{\text{(inertial force)}}{\text{(interfacial tension force)}} = \frac{D_i^3 N^2 \rho_C}{\sigma} \quad (8\text{-}37)$$

High Weber numbers give small droplets and high interfacial areas. Gnanasundram, Degaleesan, and Laddha [45] correlated d_{vs} over a wide range of N_{We}. Below a critical value of $N_{We} = 10{,}000$, d_{vs} is dependent on dispersed-phase holdup, ϕ_D, because of coalescence effects. For $N_{We} > 10{,}000$, inertial forces dominate so that coalescence effects are much less prominent and d_{vs} is almost independent of holdup up to $\phi_D = 0.5$. The recommended correlations are

$$\frac{d_{vs}}{D_i} = 0.052(N_{We})^{-0.6} e^{4\phi_D}, \quad N_{We} < 10{,}000 \quad (8\text{-}38)$$

$$\frac{d_{vs}}{D_i} = 0.39(N_{We})^{-0.6}, \quad N_{We} > 10{,}000 \quad (8\text{-}39)$$

Typical values of N_{We} for industrial extractors are less than 10,000, so (8-38) applies. Values of d_{vs}/D_i are frequently in the range of 0.0005 to 0.01.

Experimental studies, for example, those of Chen and Middleman [46] and Sprow [47], show that the dispersion produced in an agitated vessel is a dynamic phenomenon. Droplet breakup by turbulent pressure fluctuations dominates in the vicinity of the impeller blades, while for reasonable dispersed-phase holdup, coalescence of drops by collisions dominates away from the impeller. Thus, a distribution of drop sizes is found in the vessel, with smaller drops in the vicinity of the impeller blades and larger drops elsewhere. Typically, when both drop breakup and coalescence occur, the drop-size distribution is such that $d_{min} \approx d_{vs}/3$ and $d_{max} \approx 3d_{vs}$. Thus, the drop size varies over about a 10-fold range, and the distribution approximates a normal Gaussian distribution.

EXAMPLE 8.6

For the conditions and results of Example 8.5, with the extract phase as the dispersed phase, estimate the Sauter mean drop diameter, the range of drop sizes, and the interfacial area.

SOLUTION

$$D_i = 1 \text{ ft}; \quad N = 147 \text{ rpm} = 8{,}820 \text{ rph}$$
$$\rho_C = 62.3 \text{ lb/ft}^3; \quad \sigma = 718{,}800 \text{ lb/h}^2$$

From (8-37),

$$N_{We} = (1)^3(8{,}820)^2(62.3)/718{,}800 = 6{,}742; \quad \phi_D = 0.388$$

From (8-38),

$$d_{vs} = (1)(0.052)(6{,}742)^{-0.6} \exp[4(0.388)] = 0.00124 \text{ ft}$$

or

$$(0.00124)(12)(25.4) = 0.38 \text{ mm}$$

$$d_{min} = d_{vs}/3 = 0.126 \text{ mm}; \quad d_{max} = 3d_{vs} = 1.134 \text{ mm}$$

From (8-36),

$$a = 6(0.388)/0.00124 = 1{,}880 \text{ ft}^2/\text{ft}^3$$

Mass-Transfer Coefficients

Experimental studies, conducted since the early 1940s, show that mass transfer in mechanically agitated liquid–liquid systems is very complex. This is true for mass transfer in (1) the dispersed-phase droplets, (2) the continuous phase, and (3) at the interface. The reasons for this complexity are many. The magnitude of k_D depends on drop diameter, solute diffusivity, and fluid motion within the drop. When drop diameter is small (less than 1 mm according to Davies [48]), interfacial tension is high (say > 15 dyne/cm), and trace amounts of surface-active agents are present, droplets are rigid (internally stagnant), and they behave like solids. As droplets become larger, interfacial tension decreases, surface-active agents become relatively ineffective, and internal toroidal fluid circulation patterns, caused by viscous drag of the continuous phase, appear within the drops. For larger-diameter drops, the shape of the drop may oscillate between spheroid and ellipsoid or other shapes.

Mass-transfer coefficients, k_C, in the continuous phase depend on the relative motion between the droplets and the continuous phase, and whether the drops are forming or breaking, or are coalescing. Interfacial movements or turbulence, called *Marangoni effects,* occur due to interfacial-tension gradients. Such effects can induce substantial increases in mass-transfer rates.

A relatively conservative estimate of the overall mass-transfer coefficient, K_{OD}, in (8-28), can be made from estimates of k_D and k_C, by assuming rigid drops, the absence of Marangoni effects, and a stable drop size (i.e., no drop forming, breaking, or coalescing). For k_D, the asymptotic steady-state solution for mass transfer in a rigid sphere with negligible resistance of the surroundings is given by Treybal [25] as

$$(N_{Sh})_D = \frac{k_D d_{vs}}{D_D} = \frac{2}{3}\pi^2 = 6.6 \quad (8\text{-}40)$$

where D_D is the diffusivity of the solute in the droplet. N_{Sh} is the Sherwood number. Exercise 3.31 in Chapter 3 for diffusion from the surface of a sphere into an infinite, quiescent fluid gives the following result for the continuous-phase Sherwood number:

$$(N_{Sh})_C = \frac{k_C d_{vs}}{D_C} = 2 \quad (8\text{-}41)$$

where D_C is the diffusivity of the solute in the continuous phase. However, if other spheres of equal diameter are located near the sphere of interest, $(N_{Sh})_C$ may decrease to a value as low as 1.386, according to Cornish [49]. In an agitated vessel, the continuous-phase Sherwood number will usually be much greater than 1.386. A reasonable estimate can be made with the semi-theoretical correlation of Skelland and Moeti [50]. They fitted 180 data points for three different solutes, three different dispersed organic solvents, and water as the continuous phase. Mass transfer was from the dispersed phase to the continuous phase, but only

for $\phi_D = 0.01$. Skelland and Moeti assumed an equation of the form

$$(N_{Sh})_C \propto (N_{Re})_C^y (N_{Sc})_C^x \tag{8-42}$$

where

$$(N_{Sh})_C = k_C d_{vs}/D_C \tag{8-43}$$

$$(N_{Sc})_C = \mu_C/\rho_C D_C \tag{8-44}$$

For the Reynolds number, they assumed that the characteristic velocity is the square root of the mean-square, local fluctuating velocity in the vicinity of the droplet, based on the theory of local isotropic turbulence of Batchelor [51]:

$$\bar{u}^2 \propto \left(\frac{Pg_c}{V}\right)^{2/3} \left(\frac{d_{vs}}{\rho_C}\right)^{2/3} \tag{8-45}$$

Thus,

$$(N_{Re})_C = \frac{(\bar{u}^2)^{1/2} d_{vs} \rho_C}{\mu_C} \tag{8-46}$$

Combining (8-45) and (8-46), with omission of the proportionality constant:

$$(N_{Re})_C = \frac{d_{vs}^{4/3} \rho_C^{2/3} (Pg_c/V)^{1/3}}{\mu_C} \tag{8-47}$$

As discussed previously in conjunction with Figure 8.36, in the turbulent-flow region,

$$Pg_c \propto \rho_M N^3 D_i^5 \quad \text{or} \quad \text{for low } \phi_D,\ Pg_c/V \propto \rho_C N^3 D_i^5/D_T^3$$

Thus,

$$(N_{Re})_C = \frac{d_{vs}^{4/3} \rho_C N D_i^{5/3}}{\mu_C D_T} \tag{8-48}$$

Skellend and Moeti correlated their mass-transfer coefficient data with

$$k_C \propto D_C^{2/3} \mu_C^{-1/3} N^{3/2} d_{vs}^0$$

The exponents in this proportionality are used to determine the exponents y and x in (8-42) as $\frac{2}{3}$ and $\frac{1}{3}$, respectively. In addition, based on the work of previous investigators, a droplet Eotvos number,

$$N_{Eo} = \rho_D d_{vs}^2 g/\sigma \tag{8-49}$$

where N_{Eo} = (gravitational force)/(surface tension force) and the dispersed-phase holdup, ϕ_D, are incorporated into the following final correlation, which predicts 180 experimental data points to an average absolute deviation of 19.71%:

$$(N_{Sh})_C = \frac{k_C d_{vs}}{D_C} = 1.237 \times 10^{-5} \left(\frac{\mu_C}{\rho_C D_C}\right)^{1/3} \times \left(\frac{D_i^2 N \rho_C}{\mu_C}\right)^{2/3} \phi_D^{-1/2} \left(\frac{D_i N^2}{g}\right)^{5/12} \times \left(\frac{D_i}{d_{vs}}\right)^2 \left(\frac{d_{vs}}{D_T}\right)^{1/2} \left(\frac{\rho_D d_{vs}^2 g}{\sigma}\right)^{5/4} \tag{8-50}$$

EXAMPLE 8.7

For the system, conditions, and results of Examples 8.5 and 8.6, with the extract as the dispersed phase, estimate:

(a) The dispersed-phase mass-transfer coefficient, k_D

(b) The continuous-phase mass-transfer coefficient, k_C

(c) The Murphree dispersed-phase efficiency, E_{MD}

(d) The fractional extraction of furfural

The molecular diffusivities of furfural in toluene (dispersed) and water (continuous) at dilute conditions are, respectively,

$$D_D = 8.32 \times 10^{-5} \text{ft}^2/\text{h} \quad \text{and} \quad D_C = 4.47 \times 10^{-5} \text{ ft}^2/\text{h}$$

The distribution coefficient for dilute conditions is $m = dc_C/dc_D = 0.0985$.

SOLUTION

(a) From (8-40), $k_D = 6.6(D_D)/d_{vs} = 6.6(8.32 \times 10^{-5})/0.00124 = 0.44$ ft/h

(b) To apply (8-50) to the estimation of k_C, first compute each of the dimensionless groups in that equation:

$$N_{Sc} = \mu_C/\rho_C D_C = 2.165/[(62.3)(4.47 \times 10^{-5})] = 777$$

$$N_{Re} = D_i^2 N \rho_C/\mu_C = (1)^2(8{,}820)(62.3)/2.165 = 254{,}000$$

$$N_{Fr} = D_i N^2/g = (1)(8{,}820)^2/(4.17 \times 10^8) = 0.187$$

$$D_i/d_{vs} = 1/0.00124 = 806; \quad d_{vs}/D_T = 0.00124/3 = 0.000413$$

$$N_{Eo} = \rho_D d_{vs}^2 g/\sigma = (54.2)(0.00124)^2(4.17 \times 10^8)/718{,}800 = 0.0483$$

From (8-50),

$$N_{Sh} = 1.237 \times 10^{-5}(777)^{1/3}(254{,}000)^{2/3}(0.388)^{-1/2}(0.187)^{5/12} \times (806)^2(0.000413)^{1/2}(0.0483)^{5/4} = 109$$

which is much greater than the value of 2 in a quiescent fluid.

$$k_C = N_{Sh} D_C/d_{vs} = (109)(4.47 \times 10^{-5})/0.00124 = 3.93 \text{ ft/h}$$

(c) From (8-28) and the results of Example 8.6,

$$K_{OD}a = \left\{\frac{1}{1/0.44 + 1/[(0.0985)(3.93)]}\right\} 1{,}880 = 387 \text{ h}^{-1}$$

From (8-32), with $V = \pi D_T^2 H/4 = (3.14)(3)^2(3)/4 = 21.2$ ft^2

$$N_{OD} = K_{OD}aV/Q_D = 387(212)/207 = 39.6$$

From (8-33),

$$E_{MD} = (N_{OD}/(1 + N_{OD}) = 39.6)/(1 + 39.6) = 0.975 = 97.5\%.$$

(d) By material balance,

$$Q_C(c_{C,\text{in}} - c_{C,\text{out}}) = Q_D c_{D,\text{out}} \tag{1}$$

From (8-26),

$$E_{MD} = c_{D,\text{out}}/c_D^* = m c_{D,\text{out}}/c_{C,\text{out}} \tag{2}$$

Combining (1) and (2) to eliminate $c_{D,\text{out}}$ gives

$$\frac{c_{C,\text{out}}}{c_{C,\text{in}}} = \frac{1}{1 + Q_D E_{MD}/(Q_C m)} \tag{3}$$

and

$$f_{\text{Extracted}} = \frac{c_{C,\text{in}} - c_{C,\text{out}}}{c_{C,\text{in}}} = 1 - \frac{c_{C,\text{out}}}{c_{C,\text{in}}} = \frac{Q_D E_{MD}/(Q_C m)}{1 + Q_D E_{MD}/(Q_C m)}$$

$$\frac{Q_D}{Q_C}\frac{E_{MD}}{m} = \frac{(207)(0.975)}{(327)(0.0985)} = 6.27$$

Thus,

$$f_{\text{Extracted}} = \frac{6.27}{1 + 6.27} = 0.862 \quad \text{or} \quad 86.2\%$$

Multicompartment Columns

Sizing extraction columns, which may or may not include mechanical agitation, involves the determination of column diameter and column height. The diameter must be sufficiently large to permit the two phases to flow countercurrently through the column without flooding. The column height must be sufficient to achieve the number of equilibrium stages corresponding to the desired degree of extraction.

For small-diameter columns, rough estimates of the diameter and height can be made using the results of a study by Stichlmair [52] with the toluene–acetone–water system for $Q_D/Q_C = 1.5$. Typical ranges of 1/HETS and the sum of the superficial phase velocities for a number of extractor types are given in Table 8.6.

Because of the large number of important variables, an accurate estimation of column diameter for liquid–liquid contacting devices is far more complex and more uncertain than for vapor–liquid contactors. These variables include individual phase flow rates, density difference between the two phases, interfacial tension, direction of mass-transfer, viscosity and density of the continuous phase, rotating or reciprocating speed, and geometry of internals. Column diameter is best determined by scale-up from tests run in standard laboratory or pilot-plant test units with a diameter of 1 in. or larger. The sum of the measured superficial velocities of the two liquid phases in the test unit can then be assumed to hold for larger commercial units. This sum is often expressed in total gallons per hour per square foot of empty column cross-section area.

In the absence of laboratory data, preliminary estimates of diameter for some columns can be made by a simplification of the theory of Logsdail, Thornton, and Pratt [53], which is compared to other procedures by Landau and Houlihan [54] in the case of the rotating-disk contactor. Because the relative motion between a dispersed droplet phase and a continuous phase is involved, this theory is based on a concept that is similar to that developed in Chapter 6 for liquid droplets dispersed in a vapor phase.

Table 8.6 Performance of Several Types of Column Extractors

Extractor Type	1/HETS, m^{-1}	$U_D + U_C$, m/h
Packed column	1.5–2.5	12–30
Pulsed packed column	3.5–6	17–23
Sieve-plate column	0.8–1.2	27–60
Pulsed-plate column	0.8–1.2	25–35
Scheibel column	5–9	10–14
RDC	2.5–3.5	15–30
Kuhni column	5–8	8–12
Karr column	3.5–7	30–40
RTL contactor	6–12	1–2

Source: J. Stichlmair, *Chemie-Ingenieur-Technik*, **52.** 253 (1980).

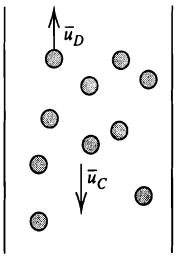

Figure 8.37 Countercurrent flows of dispersed and continuous liquid phases in a column.

Consider the case of liquid droplets of the lower-density phase rising through the denser, downward-flowing, continuous liquid phase, as shown in Figure 8.37. If the average superficial velocities of the discontinuous (droplet) phase and the continuous phase are U_D in the upward direction and U_C in the downward direction (i.e., both of these velocities are positive), respectively, the corresponding average actual velocities relative to the column wall are

$$\bar{u}_D = \frac{U_D}{\phi_D} \tag{8-51}$$

and

$$\bar{u}_C = \frac{U_C}{1 - \phi_D} \tag{8-52}$$

The average droplet rise velocity relative to the continuous phase is the sum of (8-51) and (8-52):

$$\bar{u}_r = \frac{U_D}{\phi_D} + \frac{U_C}{1 - \phi_D} \tag{8-53}$$

This relative velocity (also called *slip velocity*) can be expressed in terms of a modified form of (6-40) where the continuous-phase density in the buoyancy term is replaced by the density of the two-phase mixture, ρ_M. Thus, after noting for the case here that the drag force, F_d, and gravitational force, F_g, act downward while buoyancy, F_b, acts upward, we obtain

$$\bar{u}_r = C\left(\frac{\rho_M - \rho_D}{\rho_C}\right)^{1/2} f\{1 - \phi_D\} \tag{8-54}$$

where C is the same parameter as in (6-41) and $f\{1 - \phi_D\}$ is a factor that allows for the hindered rising effect of neighboring droplets. The density ρ_M is a volumetric mean given by

$$\rho_M = \phi_D \rho_D + (1 - \phi_D)\rho_C \tag{8-55}$$

$$\rho_M - \rho_D = (1 - \phi_D)(\rho_C - \rho_D) \tag{8-56}$$

Substitution of (8-56) into (8-54) yields

$$\bar{u}_r = C\left(\frac{\rho_C - \rho_D}{\rho_C}\right)^{1/2} (1 - \phi_D)^{1/2} f\{1 - \phi_D\} \tag{8-57}$$

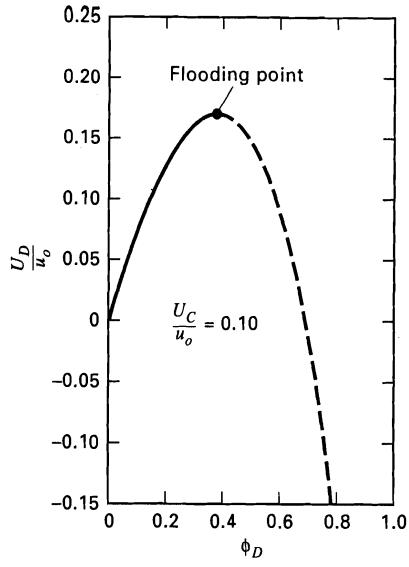

Figure 8.38 Typical holdup curve for liquid–liquid extraction column.

From experimental data, Gayler, Roberts, and Pratt [55] found that, for a given liquid–liquid system, the right-hand side of (8-57) can be expressed empirically as

$$\bar{u}_r = u_0(1 - \phi_D) \tag{8-58}$$

where u_0 is a characteristic rise velocity for a single droplet, which depends on all the variables discussed above, except those on the right-hand side of (8-53). Thus, for a given liquid–liquid system, column design, and operating conditions, the combination of (8-53) and (8-58) gives

$$\frac{U_D}{\phi_D} + \frac{U_C}{1 - \phi_D} = u_0(1 - \phi_D) \tag{8-59}$$

where u_0 is a constant. Equation (8-59) is cubic in ϕ_D, with a typical solution shown in Figure 8.38 for $U_C/u_0 = 0.1$. Thornton [56] argues that, with U_C fixed, an increase in U_D results in an increased value of the holdup ϕ_D, until the flooding point is reached, at which $(\partial U_D/\partial \phi_D)_{U_C} = 0$. Thus, in Figure 8.38, only that portion of the curve for $\phi_D = 0$ to $(\phi_D)_f$, the holdup at the flooding point, is realized in practice. Alternatively, with U_D fixed, $(\partial U_C/\partial \phi_D)_{U_D} = 0$ at the flooding point. If these two derivatives are applied to (8-59), we obtain, respectively,

$$U_C = u_0[1 - 2(\phi_D)_f][1 - (\phi_D)_f]^2 \tag{8-60}$$

$$U_D = 2u_0[1 - (\phi_D)_f](\phi_D)_f^2 \tag{8-61}$$

where the subscript f denotes flooding. Combining (8-60) and (8-61) to eliminate u_0 gives the following expression for $(\phi_D)_f$:

$$(\phi_D)_f = \frac{[1 + 8(U_C/U_D)]^{0.5} - 3}{4[(U_C/U_D) - 1]} \tag{8-62}$$

This equation predicts values of $(\phi_D)_f$ ranging from zero at $U_D/U_C = 0$ to 0.5 at $U_C/U_D = 0$. At $U_D/U_C = 1$, $(\phi_D)_f = \frac{1}{3}$. The simultaneous solution of (8-59) and (8-62) results in Figure 8.39 for the variation of total capacity as a function of phase flow ratio. The largest total capacities are achieved, as might be expected, at the smallest ratios of dispersed-phase flow rate to continuous-phase flow rate.

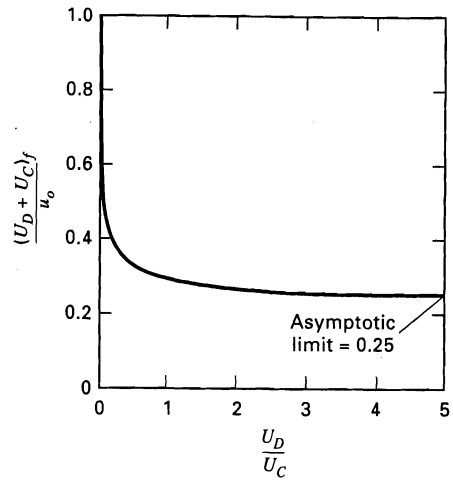

Figure 8.39 Effect of phase ratio on total capacity of liquid–liquid extraction column.

For fixed values of column geometry and rotor speed, experimental data of Logsdail et al. [53] for a laboratory-scale RDC indicate that the dimensionless group $(u_0\mu_C\rho_C/\sigma\ \Delta\rho)$ is approximately constant. Data of Reman and Olney [57] and Strand, Olney, and Ackerman [58] for well-designed and efficiently operated commercial RDC columns ranging from 8 to 42 in. in diameter indicate that this dimensionless group has a value of roughly 0.01 for systems involving water as either the continuous or dispersed phase. This value is suitable for preliminary calculations of RDC and Karr column diameters, when the sum of the actual superficial phase velocities is taken as 50% of the estimated sum at flooding conditions.

EXAMPLE 8.8

Estimate the diameter of an RDC to extract acetone from a dilute toluene–acetone solution into water at 20°C. The flow rates for the dispersed organic and continuous aqueous phases are 27,000 and 25,000 lb/h, respectively.

SOLUTION

The necessary physical properties are

$$\mu_C = 1.0 \text{ cP } (0.000021 \text{ lbf-s/ft}^2) \text{ and } \rho_C = 1.0 \text{ g/cm}^3$$

$$\Delta\rho = 0.14 \text{ g/cm}^3 \text{ and } \sigma = 32 \text{ dyne/cm } (0.00219 \text{ lbf/ft})$$

$$\frac{U_D}{U_C} = \left(\frac{27{,}000}{25{,}000}\right)\left(\frac{\rho_C}{\rho_D}\right) = \left(\frac{27{,}000}{25{,}000}\right)\left(\frac{1.0}{0.86}\right) = 1.26$$

From Figure 8.39, $(U_D + U_C)_f/u_0 = 0.29$.
Assume that $u_0\mu_C\rho_C/\sigma\Delta\rho = 0.01$.
Therefore,

$$u_0 = \frac{(0.01)(0.00219)(0.14)}{(0.000021)(1.0)} = 0.146 \text{ ft/s}$$

$$(U_D + U_C)_f = 0.29(0.146) = 0.0423 \text{ ft/s}$$

$$(U_D + U_C)_{50\% \text{ of flooding}} = \left(\frac{0.0423}{2}\right)(3{,}600) = 76.1 \text{ ft/h}$$

$$\text{Total ft}^3\text{/h} = \frac{27{,}000}{(0.86)(62.4)} + \frac{25{,}000}{(1.0)(62.4)} = 904 \text{ ft}^3\text{/h}$$

$$\text{Column cross-sectional area} = A_c = \frac{904}{76.1} = 11.88 \text{ ft}^2$$

$$\text{Column diameter} = D_T = \left(\frac{4A_c}{\pi}\right)^{0.5} = \left[\frac{(4)(11.88)}{3.14}\right]^{0.5} = 3.9 \text{ ft}$$

Note that from Table 8.6, a typical $(U_D + U_C)$ for an RDC is 15 to 30 m/h or 49 to 98.4 ft/h.

Despite their compartmentalization, mechanically assisted liquid–liquid extraction columns, such as the RDC and Karr columns, operate more nearly like differential contacting devices than like staged contactors. Therefore, it is more common to consider stage efficiency for such columns in terms of HETS (height equivalent to a theoretical stage) or as some function of mass-transfer parameters, such as HTU (height of a transfer unit). Although it is not on as sound a theoretical basis as the HTU, the HETS is preferred here because it can be applied directly to determine column height from the number of equilibrium stages.

Because of the great complexity of liquid–liquid systems and the large number of variables that influence contacting efficiency, general correlations for HETS have been difficult to develop. However, for well-designed and efficiently operated columns, the available experimental data indicate that the dominant physical properties influencing HETS are the interfacial tension, the phase viscosities, and the density difference between the phases. In addition, it has been observed by Reman [59] for RDC units and by Karr and Lo [60] for Karr columns that HETS increases with increasing column diameter because of axial mixing effects discussed in the next section.

It is preferred to obtain values of HETS by conducting small-scale laboratory experiments with systems of interest. These values are scaled to commercial-size columns by assuming that HETS varies with column diameter D_T, raised to an exponent, which may vary from 0.2 to 0.4 depending on the system.

In the absence of experimental data, the crude correlation of Figure 8.40 can be used for preliminary design if phase viscosities are no greater than 1 cP. The data points correspond to minimum reported HETS values for RDC and Karr units with the exponent on column diameter set arbitrarily to $\frac{1}{3}$. The points represent values of HETS that vary from as low as 6 in. for a 3-in.-diameter, laboratory-size column operating with a low-interfacial-tension/low-viscosity system such as methyl–isobutyl ketone/acetic acid/water, to as high as 25 in. for a 36-in.-diameter commercial column operating with a high-interfacial-tension/low-viscosity system such as xylenes–acetic acid–water. For systems having one phase of high viscosity, values of HETS can be 24 in. or more, even for a small, laboratory-size column.

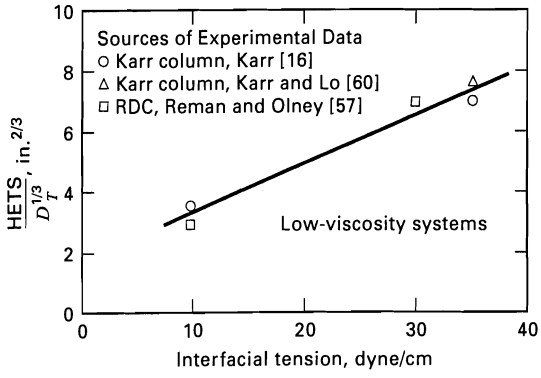

Figure 8.40 Effect of interfacial tension on HETS for RDC and Karr columns.

EXAMPLE 8.9

Estimate HETS for the conditions of Example 8.8.

SOLUTION

Because toluene has a viscosity of approximately 0.6 cP, this is a low-viscosity system. From Example 8.8, the interfacial tension is 32 dyne/cm. From Figure 8.40. $\text{HETS}/D_T^{1/3} = 6.9$. For D_T =3.9 ft, $\text{HETS} = 6.9[(3.9)(12)]^{1/3} = 24.8$ in. Note that from Table 8.6, HETS for an RDC varies from 0.29 to 0.40 m or 11.4 to 15.7 in. for a small column.

More accurate estimates of flooding and HETS are discussed in detail by Lo et al. [4] and by Thornton [61]. Packed column design is considered by Strigle [62].

Axial Dispersion

In this and previous chapters covering liquid–liquid and vapor–liquid countercurrent-flow contactors, plug flow of each phase has been assumed. Each element of a phase is assumed to have the same residence time in the contactor, while each phase may have a different residence time. Because axial concentration gradients in the direction of bulk flow are established in each phase, diffusion of a species is superimposed on the bulk flow of the species in that phase. Axial diffusion degrades the efficiency of multistage separation equipment, and in the limit, a multistage separator behaves like a single well-mixed stage. In Figure 8.41, solute concentration profiles for the extract and raffinate phases of a liquid–liquid extraction column are shown for plug flow (dashed lines) and for flow with significant axial diffusion in each of the two phases (solid lines). The continuous phase is the feed/raffinate (x subscript), which enters the contactor at the top ($z = 0$). The dispersed phase is the solvent/extract (y subscript), which enters the contactor at the bottom ($z = H$). Solute transfer is from the continuous phase to the dispersed phase. Two effects of axial diffusion are seen: (1) The concentration curves in the presence of axial diffusion are closer together than for plug flow and (2) these close proximities are due partially to concentrations at the two ends, which are different from those in the original feed and

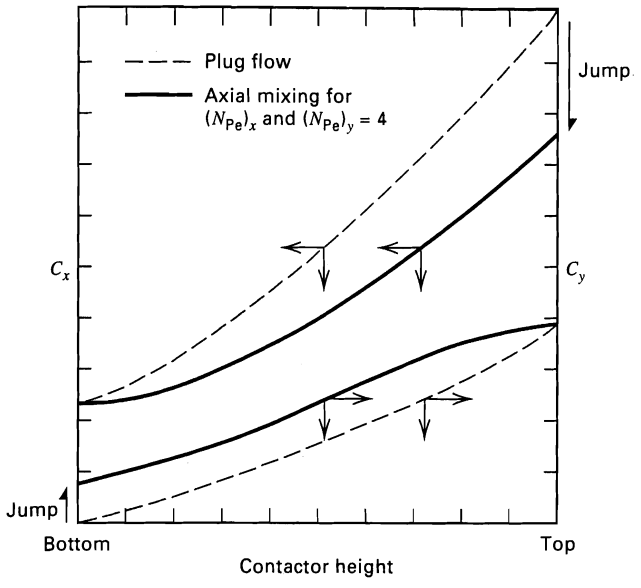

Figure 8.41 Solute concentration profiles for continuous, countercurrent extraction with and without axial mixing.

solvent. These differences are called *jumps* and are due to axial diffusion outside the region in the contactor where the two liquid phases are in contact. The jump at the top is caused by axial diffusion, superimposed on the bulk flow, in the feed liquid before it enters the contactor. This causes the concentration of solute in the feed just as it enters the contactor to be less than its concentration in the original feed liquid. Similarly, diffusion of solute into the incoming solvent causes the concentration of solute in the solvent just entering the bottom of the contactor to be greater than the concentration in the original solvent, which in Figure 8.41 is zero. The overall effect of axial diffusion is a reduction in the average driving force for mass transfer of the solute between the two phases, necessitating a taller column to accomplish the desired separation.

The effects shown in Figure 8.41 are actually due to a number of factors besides diffusion, which are lumped together into one overall effect, commonly referred to as *axial dispersion, axial mixing, longitudinal dispersion*, or *backmixing*. These factors include:

1. Molecular and turbulent diffusion of the continuous phase along concentration gradients
2. Circulatory motion of the continuous phase due to the droplets of the dispersed phase
3. Transport and shedding of the continuous phase in the wakes attached to the rear of droplets of the dispersed phase
4. Circulation of continuous and dispersed phases in mechanically agitated columns
5. Channeling and nonuniform velocity profiles leading to distributions of residence times in the two phases

In general, the effect of axial dispersion is most pronounced when (1) a high recovery of solute is necessary, (2) the contactor is short in height, (3) large circulation patterns occur, (4) a wide range of droplet sizes is present, and/or (5) the feed-to-solvent flow ratio is very small or very large. Although axial-dispersion effects are generally negligible in extractors where phase separation occurs between stages, such as in mixer-settler cascades and sieve-plate columns with downcomers, axial dispersion can be significant in spray columns, packed columns, and RDCs. Although axial dispersion can occur in packed absorbers, packed strippers, and packed distillation columns, it is significant only when operating at very high liquid-to-gas ratios. However, axial dispersion can be significant in spray and bubble columns used for absorption.

Two types of models have been developed for predicting the extent and effect of axial mixing: (1) diffusion models for differential-type contactors, due to Sleicher [63] and Miyauchi and Vermeulen [64]; and (2) backflow models for staged extractors without complete phase separation between stages, due to Sleicher [65] and Miyauchi and Vermeulen [66]. Both types are discussed by Vermeulen et al. [67]. Diffusion models, which have received the most attention and have been most applied more frequently, are convenient for studying the complex nature of axial dispersion.

Consider a differential height, dz, of a differential contactor with countercurrent two-phase flow, as shown in Figure 8.42. Feed enters the top of the column at $z = 0$, while solvent enters the bottom of the column at $z = H$. Assume that: (1) axial dispersion in each phase is characterized by a constant turbulent-diffusion coefficient, E; (2) phase superficial velocities are each uniform over the cross section and

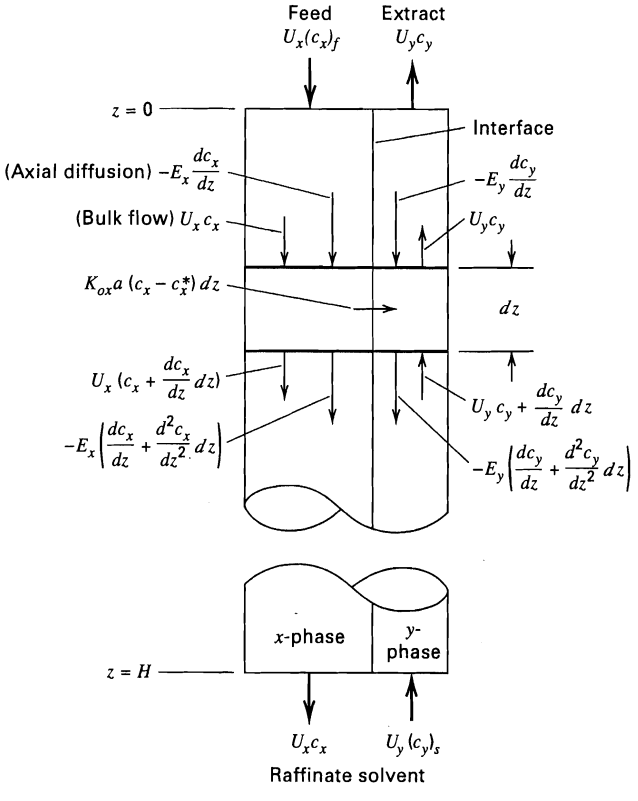

Figure 8.42 Axial dispersion in an extraction column.
[From J.D. Thornton, *Science and Practice of Liquid–Liquid Extraction*, Vol. 1, Clarendon Oxford, (1992) with permission.]

constant in the axial direction; (3) the volumetric, overall mass-transfer coefficients for the solute are constant; (4) only the solute undergoes mass transfer between the two phases; and (5) the phase equilibrium ratio for the solute is constant. Then the solute mass-balance equations for the feed/raffinate (x) and solvent/extract (y) phases, respectively, are

$$E_x \frac{d^2c_x}{dz^2} - U_x \frac{dc_x}{dz} - K_{Ox}a(c_x - c_x^*) = 0 \quad (8\text{-}63)$$

$$E_y \frac{d^2c_y}{dz^2} + U_y \frac{dc_y}{dz} + K_{Ox}a(c_x - c_x^*) = 0 \quad (8\text{-}64)$$

where c_x^* is the concentration of the solute in the raffinate that is equilibrium with the solute concentration in the bulk extract. For these two differential equations, the boundary conditions, which were first proposed by Danckwerts [68] and were further elucidated by Wehner and Wilhelm [69], are

$$\text{at } z = 0, \qquad U_x c_{x_f} - U_x c_{x_0} = -E_x \frac{dc_x}{dz} \quad (8\text{-}65)$$

and

$$dc_y/dz = 0 \quad (8\text{-}66)$$

at $z = H$,

$$U_y c_{y_H} - U_y c_{y_s} = E_y \frac{dc_y}{dz} \quad (8\text{-}67)$$

and

$$dc_x/dz = 0 \quad (8\text{-}68)$$

where:

c_{x_f} = concentration of solute in the original feed
c_{x_0} = concentration of solute in the feed at $z = 0$
c_{y_H} = concentration of solute in the solvent at $z = H$
c_{y_s} = concentration of solute in the original solvent

The two terms on the left-hand sides of (8-65) and (8-67) are the jumps shown in Figure 8.41.

It is customary to convert (8-63) and (8-64) to alternative forms in terms of pertinent dimensionless groups. This is readily done by defining

$$Z = z/H \quad (8\text{-}69)$$

$$N_{\text{Pe}_y} = U_y H/E_y = \text{axial, turbulent column Peclet number for the extract phase} \quad (8\text{-}70)$$

$$N_{\text{Pe}_x} = U_x H/E_x = \text{axial, turbulent column Peclet number for the raffinate phase} \quad (8\text{-}71)$$

$$N_{Ox} = K_{Ox}aH/U_x = K_{Ox}aV/Q_x \quad (8\text{-}72)$$

Equations (8-63) and (8-64) then become

$$\frac{d^2c_x}{dZ^2} - N_{\text{Pe}_x}\frac{dc_x}{dZ} - N_{Ox}N_{\text{Pe}_x}(c_x - c_x^*) = 0 \quad (8\text{-}73)$$

$$\frac{d^2c_y}{dZ^2} - N_{\text{Pe}_y}\frac{dc_y}{dZ} - \left(\frac{U_x}{U_y}\right)N_{Ox}N_{\text{Pe}_y}(c_x - c_x^*) = 0 \quad (8\text{-}74)$$

The boundary conditions are transformed in a similar way. For a straight equilibrium curve, $c_x^* = mc_y$. Thus, we have a coupled set of ordinary differential equations, whose solutions for c_y and c_x are functions of c_{y_f}, c_{y_s}, m, N_{Pe_x}, N_{Pe_y}, N_{Ox}, U_x/U_y, and Z.

Further algebraic manipulations involving the substitution of dimensionless solute concentrations can reduce the number of variables from 10 to 7. In either case, the solution of the axial dispersion equations as obtained by Sleicher [65] and Miyauchi and Vermeulen [66] is very difficult to display in tabular or graphical form. However, the possible importance of axial dispersion is most commonly judged by the magnitudes of the Peclet numbers. A Peclet number of 0 corresponds to complete back-mixing, such that at most only one equilibrium stage is achieved; the entire column functions like a single mixer stage. A Peclet number of ∞ corresponds to an absence of axial dispersion. Experimental data on several different types of liquid-liquid extraction columns indicate that N_{Pe} for the dispersed phase is frequently greater than 50, while N_{Pe} for the continuous phase may be in the range of 5 to 30. Thus, as a first approximation, axial dispersion in the dispersed phase can be largely ignored. This effect was observed experimentally by Geankoplis and Hixson [70] in a spray extraction column and by Gier and Hougen [71] in spray and packed extraction columns. They reported end-concentration changes of significant magnitude at the continuous-phase entrance, but not at the dispersed-phase entrance.

A number of approximate solutions to the axial dispersion equations, (8-63) to (8-68), have been published, including one by Sleicher [63]. Alternatively, if the original solvent is free of solute, a rapid and somewhat conservative estimate of the effect of axial dispersion can be made by the method of Watson and Cochran [72] from an empirical relation for the column efficiency:

$$\frac{H_{\text{plug flow}}}{H_{\text{actual}}} = \frac{(\text{HTU}_{Ox})(\text{NTU}_{Ox})}{H}$$
$$= 1 - \frac{1}{1 + N_{\text{Pe}_x}(\text{HTU}_{Ox}/H) - E + (1/\text{NTU}_{Ox})}$$
$$- \frac{E}{N_{\text{Pe}_y}(\text{HTU}_{Ox}/H) - 1 + E + (1/\text{NTU}_{Ox})} \quad (8\text{-}75)$$

where

$H_{\text{actual}} = H$ = height of column taking into account axial dispersion
HTU_{Ox} = height of an overall transfer unit based on the raffinate phase for plug flow
NTU_{Ox} = number of overall transfer units based on the raffinate phase for plug flow
E = extraction factor $= mU_x/U_y$
$m = dc_x/dc_y$

The product of HTU_{Ox} and NTU_{Ox} is the column height for plug flow, which is $< H$. Thus, the ratio on the left-hand side

of (8-75) is a column efficiency. The NTU_{Ox} is approximated by:

$$NTU_{Ox} = \ln\left(\frac{X}{XE + 1 - E}\right)\Big/(E - 1) \quad (8\text{-}76)$$

where $$X = (c_x)_{out}/(c_x)_{in} \quad (8\text{-}77)$$

The HTU_{Ox} is defined by:

$$HTU_{Ox} = U_x/K_{Ox}a \quad (8\text{-}78)$$

For given values of HTU_{Ox}, NTU_{Ox}, E, N_{Pe_x}, and N_{Pe_y}, (8-75) is solved for H. Caution must be exercised in using (8-75) because of its empirical nature. The equation is limited to $NTU_{Ox} \geq 2$, $E > 0.25$, $N_{Pe_x}(HTU_{Ox}/H) > 1.5$, and the calculated value of the column efficiency, $H_{\text{plug flow}}/H_{\text{actual}}$, must be ≥ 0.20. Within these restrictions, an extensive comparison by Watson and Cochran with the exact solution of (8-63) to (8-68) gives conservative efficiency values that deviate by no more than 0.07 (7%), with the highest accuracy for estimated efficiencies greater than 0.5 (50%).

EXAMPLE 8.10

Experiments conducted for a dilute system under laboratory conditions approximating plug flow give $HTU_{Ox} = 3$ ft. If a commercial column is to be designed for $NTU_{Ox} = 4$ and N_{Pe_x} and N_{Pe_y} are estimated to be 19 and 50, respectively, determine the necessary column height if $E = 0.5$.

SOLUTION

For plug flow, column height is $(HTU_{Ox})(NTU_{Ox})$. Substitution of the data into (8-75) gives

$$\frac{12}{H} = 1 - \frac{1}{(57/H) + 0.75} - \frac{0.5}{(180/H) - 0.25}$$

This is a nonlinear algebraic equation in H. Solving by an iterative method,

$$H = 17 \text{ ft}$$

$$\text{Efficiency} = (HTU_{Ox})(NTU_{Ox})/H = 12/17 = 0.706 \quad (70.6\%)$$

SUMMARY

1. A solvent can be used to selectively extract one or more components from a liquid mixture.

2. Although liquid–liquid extraction is a reasonably mature separation operation, considerable experimental effort is often needed to find a suitable solvent and to determine residence-time requirements or values of HETS, NTU, or mass-transfer coefficients.

3. Compared to vapor–liquid separation operations, extraction has a higher overall mass-transfer resistance. Stage efficiencies in columns are frequently low.

4. A wide variety of commercial extractors are available, as shown in Figures 8.2 to 8.7, ranging from simple columns with no mechanical agitation to centrifugal devices that may spin at several thousand revolutions per minute. A selection scheme, given in Table 8.3, is useful for choosing the most suitable extractors for a given separation.

5. Solvent selection is facilitated by consideration of a number of chemical factors given in Table 8.4 and physical factors discussed in Section 8.2.

6. For liquid–liquid extraction with ternary mixtures, phase equilibrium is conveniently represented on equilateral- or right-triangle diagrams for both type I (solute and solvent completely miscible) and the less common type II (solute and solvent not completely miscible) systems.

7. For determining equilibrium-stage requirements of single-section, countercurrent cascades for ternary systems, the graphical methods of Hunter and Nash (equilateral-triangle diagram), Kinney (right-triangle diagram), or Varteressian and Fenske (distribution diagram of McCabe–Thiele type) can be applied, as described in Section 8.3. These methods can also determine minimum and maximum solvent requirements.

8. A two-section, countercurrent cascade with extract reflux can be employed with a type II ternary system to enable a sharp separation of a binary feed mixture. The calculation of stage requirements of such a two-section cascade is conveniently carried out by the graphical method of Maloney and Schubert using a Janecke equilibrium diagram, as discussed in Section 8.4. The addition of raffinate reflux to such a cascade is of little value. The Maloney–Schubert method can also be applied to single-section cascades.

9. When only a few equilibrium stages are required, a cascade of mixer-settler units may be attractive because each mixer can be designed to closely approach an equilibrium stage. With many ternary and higher-order systems, the residence-time requirement may be only a few minutes for a 90% approach to equilibrium using an agitator input of approximately 4 hp/1,000 gal. Adequate phase-disengaging area for the settlers may be estimated from the rule of 5 gal of combined extract and raffinate per minute per square foot of disengaging area.

10. For mixers utilizing a six-flat-bladed turbine in a closed vessel with side vertical baffles, as shown in Figure 8.35, useful extractor design correlations are available for estimating, for a given extraction, the mixing-vessel dimensions, minimum impeller rotation rate for complete and uniform dispersion, impeller horsepower, mean droplet size, range of droplet sizes, interfacial area per unit volume, dispersed-phase and continuous-phase mass-transfer coefficients, and Murphree efficiency.

11. For column-type extractors, with and without mechanical agitation, correlations for determining column diameter, to avoid flooding, and column height are suitable only for very preliminary sizing calculations. For final extractor selection and design, recommendations of equipment vendors based on experimental data from pilot-size equipment are highly desirable.

12. Sizing of column-type extractors must consider axial dispersion, which can significantly reduce mass-transfer driving forces and thus increase the required column height. Axial dispersion effects are often most significant in the continuous phase.

REFERENCES

1. DERRY, T.K., and T.I. WILLIAMS, *A Short History of Technology,* Oxford University Press, New York (1961).

2. BAILES, P.J., and A. WINWARD, *Trans. Inst. Chem. Eng.,* **50,** 240–258 (1972).

3. BAILES, P.J., C. HANSON, and M.A. HUGHES, *Chem. Eng.,* **83** (2), 86–100 (1976).

4. LO, T.C., M.H.I. BAIRD, and C. HANSON, Eds., *Handbook of Solvent Extraction,* Wiley-Interscience, New York (1983).

5. REISSINGER, K.-H., and J. SCHROETER, "Alternatives to Distillation," *I. Chem. E. Symp. Ser. No. 54,* 33–48 (1978).

6. HUMPHREY, J.L., J.A. ROCHA, and J.R. FAIR, *Chem. Eng.,* **91** (19), 76–95 (1984).

7. FENSKE, M.R., C.S. CARLSON, and D. QUIGGLE, *Ind. Eng. Chem.,* **39,** 1932 (1947).

8. SCHEIBEL, E.G., *Chem. Eng. Prog.,* **44,** 681 (1948).

9. SCHEIBEL, E.G., *AIChE J.,* **2,** 74 (1956).

10. SCHEIBEL, E.G., U. S. Patent 3,389,970 (June 25, 1968).

11. OLDSHUE, J., and J. RUSHTON, *Chem. Eng. Prog.,* **48** (6), 297 (1952).

12. REMAN, G.H., *Proceedings of the 3rd World Petroleum Congress,* The Hague, Netherlands, Sec. III, 121 (1951).

13. REMAN, G.H., *Chem. Eng. Prog.,* **62** (9), 56 (1966).

14. MISEK, T., and J. MAREK, *Br. Chem. Eng.,* **15,** 202 (1970).

15. FISCHER, A.,*Verfahrenstechnik,* **5,** 360 (1971).

16. KARR, A.E., *AIChE J.,* **5,** 446 (1959).

17. KARR, A.E., and T.C. LO, *Chem. Eng. Prog.,* **72** (11), 68 (1976).

18. PROCHAZKA, J., J. LANDAU, F. SOUHRADA, and A. Heyberger, *Br. Chem. Eng.,* **16,** 42 (1971).

19. BARSON, N., and G.H. BEYER, *Chem. Eng. Prog.,* **49** (5), 243–252 (1953).

20. REISSINGER, K.-H., and J. SCHROETER, "Liquid–Liquid Extraction, Equipment Choice," in J.J. McKetta and W.A. Cunningham, Eds., *Encyclopedia of Chemical Processing and Design,* Vol. 21, Marcel Dekker, New York (1984).

21. CUSACK, R.W., P. FREMEAUX, and D. GLATZ, *Chem. Eng.,* **98** (2), 66–76 (1991).

22. ROBBINS, L.A., *Chem. Eng. Prog.,* **76** (10), 58–61 (1980).

23. NASER, S.F., and R.L. FOURNIER, *Comput. Chem. Eng.,* **15,** 397–414 (1991).

24. DARWENT, B., and C.A. WINKLER, *J. Phys. Chem.,* **47,** 442–454 (1943).

25. TREYBAL, R.E., *Liquid Extraction,* 2nd ed., McGraw-Hill, New York (1963).

26. HUNTER, T.G., and A.W. NASH, *J. Soc. Chem. Ind.,* **53,** 95T–102T (1934).

27. KINNEY, G.F., *Ind. Eng. Chem.,* **34,** 1102–1104 (1942).

28. VENKATARANAM, A., and R.J. RAO, *Chem. Eng. Sci.,* **7,** 102–110 (1957).

29. SAWISTOWSKI, H., and W. SMITH, *Mass Transfer Process Calculations,* Interscience, New York (1963).

30. VARTERESSIAN, K.A., and M.R. FENSKE, *Ind. Eng. Chem.,* **28,** 1353–1360 (1936).

31. SKELLAND, A.H.P., *Ind. Eng. Chem.,* **53,** 799–800 (1961).

32. RANDALL, M., and B. LONGTIN, *Ind. Eng. Chem.,* **30,** 1063, 1188, 1311 (1938); **31,** 908, 1295 (1939); **32,** 125 (1940).

33. MALONEY, J.O., and A.E. SCHUBERT, *Trans. AIChE,* **36,** 741 (1940).

34. FLYNN, A.W. and R.E. TREYBAL, *AIChE J.,* **1,** 324–328 (1955).

35. RYON, A.D., F.L. DALEY, and R.S. LOWRIE, *Chem. Eng. Prog.,* **55** (10), 70–75 (1959).

36. HAPPEL, J., and D.G. JORDAN, *Chemical Process Economics,* 2nd ed., Marcel Dekker, New York (1975).

37. RUSHTON, J.H., and J.Y. OLDSHUE, *Chem Eng. Prog.,* **49,** 161–168 (1953).

38. LAITY, D.S., and R.E. TREYBAL, *AIChE J.,* **3,** 176–180 (1957).

39. SKELLAND, A.H.P., and G.G. RAMSEY, *Ind. Eng. Chem. Res.,* **26,** 77–81 (1987).

40. SKELLAND, A.H.P., and J.M. LEE, *Ind. Eng. Chem. Process Des. Dev.,* **17,** 473–478 (1978).

41. MACMULLIN, R.B., and M. WEBER, *Trans. AIChE,* **31,** 409–458 (1935).

42. LEWIS, J.B., I. JONES, and H.R.C. PRATT, *Trans. Inst. Chem. Eng.,* **29,** 126 (1951).

43. COULSON, J.M., and J.F. RICHARDSON, *Chemical Engineering,* Vol. 2, 4th ed., Pergamon, Oxford (1991).

44. VERMUELEN, T., G.M. WILLIAMS, and G.E. LANGLOIS, *Chem. Eng. Prog.,* **51,** 85F (1955).

45. GNANASUNDARAM, S., T.E. DEGALEESAN, and G.S. LADDHA, *Can. J. Chem. Eng.,* **57,** 141–144 (1979).

46. CHEN, H.T., and S. MIDDLEMAN, *AIChE J.,* **13,** 989–995 (1967).

47. SPROW, F.B., *AIChE J.,* **13,** 995–998 (1967).

48. DAVIES, J.T., *Turbulence Phenomena,* Academic Press, New York, p. 311 (1978).

49. CORNISH, A.R.H., *Trans. Inst. Chem. Eng.,* **43,** T332–T333 (1965).

50. SKELLAND, A.H.P., and L.T. MOETI, *Ind. Eng. Chem. Res.,* **29,** 2258–2267 (1990).

51. BATCHELOR, G.K., *Proc. Cambridge Phil. Soc.,* **47,** 359–374 (1951).

52. STICHLMAIR, J., *Chemie-Ingenieur-Technik,* **52,** 253 (1980).

53. LOGSDAIL, D.H., J.D. THORNTON, and H.R.C. PRATT, *Trans. Inst. Chem. Eng.,* **35,** 301–315 (1957).

54. LANDAU, J., and R. HOULIHAN, *Can. J. Chem. Eng.,* **52,** 338–344 (1974).

55. GAYLER, R., N.W. ROBERTS, and H.R.C. PRATT, *Trans. Inst. Chem. Eng.,* **31,** 57–68 (1953).

56. THORNTON, J.D., *Chem. Eng. Sci.,* **5,** 201–208 (1956).

57. REMAN, G.H., and R.B. OLNEY, *Chem. Eng. Prog.,* **52** (3), 141–146 (1955).

58. STRAND, C.P., R.B. OLNEY, and G.H. ACKERMAN, *AIChE J.,* **8,** 252–261 (1962).

59. REMAN, G.H., *Chem. Eng. Prog.,* **62** (9), 56–61 (1966).

60. KARR, A.E., and T.C. LO, "Performance of a 36-inch Diameter Reciprocating-Plate Extraction Column," paper presented at the 82nd National Meeting of AIChE, Atlantic City, NJ (Aug. 29–Sept. 1, 1976).

61. THORNTON, J.D., *Science and Practice of Liquid–Liquid Extraction,* Vol. 1, Clarendon Press, Oxford (1992).

62. STRIGLE, R.F., JR., *Random Packings and Packed Towers,* Gulf Publishing Company, Houston, TX (1987).

63. SLEICHER, C.A., JR., *AIChE J.,* **5,** 145–149 (1959).

64. MIYAUCHI, T., and T. VERMEULEN, *Ind. Eng. Chem. Fund.,* **2,** 113–126 (1963).

65. SLEICHER, C.A., JR., *AIChE J.,* **6,** 529–531 (1960).

66. MIYAUCHI, T., and T. VERMEULEN, *Ind. Eng. Chem. Fund.,* **2,** 304–310 (1963).

67. VERMEULEN, T., J.S. MOON, A. HENNICO, and T. MIYAUCHI, *Chem. Eng. Prog.*, **62** (9), 95–101 (1966).

68. DANCKWERTS, P.V., *Chem. Eng. Sci.*, **2,** 1–13 (1953).

69. WEHNER, J.F., and R.H. WILHELM, *Chem. Eng. Sci.*, **6,** 89–93 (1956).

70. GEANKOPLIS, C.J., and A.N. HIXSON, *Ind. Eng. Chem.*, **42,** 1141–1151 (1950).

71. GIER, T.E., and J.O. HOUGEN, *Ind. Eng. Chem.*, **45,** 1362–1370 (1953).

72. WATSON, J.S., and H.D. COCHRAN, Jr., *Ind. Eng. Chem. Process Des. Dev.*, **10,** 83–85 (1971).

EXERCISES

Section 8.1

8.1 Explain why it is preferable to separate a dilute mixture of benzoic acid in water by liquid–liquid extraction rather than distillation.

8.2 Why is liquid–liquid extraction preferred over distillation for the separation of a mixture of formic acid and water?

8.3 Based on the information in Table 8.3 and the selection scheme in Figure 8.8, is the choice of an RDC appropriate for the extraction of acetic acid from water by ethyl acetate in the process described in the introduction to this chapter and shown in Figure 8.1? What other types of extractors might be considered?

8.4 What is the major advantage of the ARD over the RDC? What is the disadvantage of the ARD compared to the RDC?

8.5 Under what conditions is a cascade of mixer-settler units probably the best choice of extraction equipment?

8.6 A petroleum reformate stream of 4,000 bbl/day is to be contacted with diethylene glycol to extract the aromatics from the paraffins. The ratio of solvent volume to reformate volume is 5. It is estimated that eight theoretical stages will be needed. Using Tables 8.2 and 8.3, and Figure 8.8, which types of extractors would be most suitable?

Section 8.2

8.7 Using Table 8.4, select possible liquid–liquid extraction solvents for separating the following mixtures: (a) water–ethyl alcohol, (b) water–aniline, and (c) water–acetic acid. For each case, indicate clearly which of the two components should be the solute.

8.8 Using Table 8.4, select possible liquid–liquid extraction solvents for removing the solute from the carrier in the following cases:

	Solute	Carrier
(a)	Acetone	Ethylene glyol
(b)	Toluene	*n*-Heptane
(c)	Ethyl alcohol	Glycerine

8.9 For the extraction of acetic acid (A) from a dilute solution in water (C) into ethyl acetate (S) at 25°C, estimate or obtain data for $(K_A)_D$, $(K_C)_D$, $(K_S)_D$, and β_{AC}. Does this system exhibit: (a) High selectivity, (b) High solvent capacity and (c) Ease in recovering the solvent? Can you select a solvent that would exhibit better factors than ethyl acetate?

8.10 Interfacial tension can be an important factor in liquid–liquid extraction. Very low values of interfacial tension result in stable emulsions that are difficult to separate, while very high values require large energy inputs to form the dispersed phase. It is best to measure the interfacial tension for the two-phase mixture of interest. However, in the absence of experimental data, propose a method for estimating the interfacial tension of a ternary system using only the compositions of the equilibrium phases and the values of surface tension in air for each of the three components.

Section 8.3

8.11 One thousand kilograms per hour of a 45 wt% acetone in-water solution is to be extracted at 25°C in a continuous, countercurrent system with pure 1,1,2-trichloroethane to obtain a raffinate containing 10 wt% acetone. Using the following equilibrium data, determine with an equilateral-triangle diagram:

(a) the minimum flow rate of solvent,

(b) the number of stages required for a solvent rate equal to 1.5 times the minimum, and

(c) the flow rate and composition of each stream leaving each stage.

	Acetone, Weight Fraction	Water, Weight Fraction	Trichloroethane, Weight Fraction
Extract	0.60	0.13	0.27
	0.50	0.04	0.46
	0.40	0.03	0.57
	0.30	0.02	0.68
	0.20	0.015	0.785
	0.10	0.01	0.89
Raffinate	0.55	0.35	0.10
	0.50	0.43	0.07
	0.40	0.57	0.03
	0.30	0.68	0.02
	0.20	0.79	0.01
	0.10	0.895	0.005

The tie-line data are:

Raffinate, Weight Fraction Acetone	Extract, Weight Fraction Acetone
0.44	0.56
0.29	0.40
0.12	0.18

8.12 Solve Exercise 8.11 with a right-triangle diagram.

8.13 A distillate containing 45 wt% isopropyl alcohol, 50 wt% diisopropyl ether, and 5 wt% water is obtained from the heads column of an isopropyl alcohol finishing unit. The company desires to recover the ether from this stream by liquid–liquid extraction in a column, with water, as the solvent, entering the top and the feed entering the bottom so as to produce an ether containing no more than 2.5 wt% alcohol and to obtain the extracted alcohol at a concentration of at least 20 wt%. The unit will operate at 25°C and 1 atm. Using the method of Varteressian and Fenske with a McCabe–Thiele diagram, find how many theoretical stages are required.

Is it possible to obtain an extracted alcohol composition of 25 wt%? Equilibrium data are given below.

PHASE EQUILIBRIUM DATA AT 25°C, 1 ATM

Ether Phase			Water Phase		
Wt% Alcohol	Wt% Ether	Wt% Water	Wt% Alcohol	Wt% Ether	Wt% Water
2.4	96.7	0.9	8.1	1.8	90.1
3.2	95.7	1.1	8.6	1.8	89.6
5.0	93.6	1.4	10.2	1.5	88.3
9.3	88.6	2.1	11.7	1.6	86.7
24.9	69.4	5.7	17.5	1.9	80.6
38.0	50.2	11.8	21.7	2.3	76.0
45.2	33.6	21.2	26.8	3.4	69.8

ADDITIONAL POINTS ON PHASE BOUNDARY

Wt% Alcohol	Wt% Ether	Wt% Water
45.37	29.70	24.93
44.55	22.45	33.00
39.57	13.42	47.01
36.23	9.66	54.11
24.74	2.74	72.52
21.33	2.06	76.61
0	0.6	99.4
0	99.5	0.5

8.14 Benzene and trimethylamine (TMA) are to be separated in a three-stage liquid–liquid extraction column using water as the solvent. If the solvent-free extract and raffinate products are to contain, respectively, 70 and 3 wt% TMA, find the original feed composition and the water-to-feed ratio with a right-triangle diagram. There is no reflux and the solvent is pure water. Equilibrium data are as follows:

TRIMETHYLAMINE–WATER–BENZENE COMPOSITIONS ON PHASE BOUNDARY

Extract, wt%			Raffinate, wt%		
TMA	H_2O	Benzene	TMA	H_2O	Benzene
5.0	94.6	0.4	5.0	0.0	95.0
10.0	89.4	0.6	10.0	0.0	90.0
15.0	84.0	1.0	15.0	1.0	84.0
20.0	78.0	2.0	20.0	2.0	78.0
25.0	72.0	3.0	25.0	4.0	71.0
30.0	66.4	3.6	30.0	7.0	63.0
35.0	58.0	7.0	35.0	15.0	50.0
40.0	47.0	13.0	40.0	34.0	26.0

The tie-line data are:

Extract, wt% TMA	Raffinate, wt% TMA
39.5	31.0
21.5	14.5
13.0	9.0
8.3	6.8
4.0	3.5

8.15 The system docosane–diphenylhexane (DPH)–furfural is representative of more complex systems encountered in the solvent refining of lubricating oil. Five hundred kilograms per hour of a 40 wt% mixture of DPH in docosane are to be continuously extracted in a countercurrent system with 500 kg/h of a solvent containing 98 wt% furfural and 2 wt% DPH to produce a raffinate that contains only 5 wt% DPH. Calculate with a right-triangle diagram the number of theoretical stages required and the number of kilograms per hour of DPH in the extract at 45°C and at 80°C. Equilibrium data are as follows.

EQUILIBRIUM DATA: BINODAL CURVES IN DOCOSANE–DIPHENYLHEXANE–FURFURAL SYSTEM [*IND. ENG. CHEM.*, 35, 711 (1943)]

Wt% at 45°C			Wt% at 80°C		
Docosane	DPH	Furfural	Docosane	DPH	Furfural
96.0	0.0	4.0	90.3	0.0	9.7
84.0	11.0	5.0	50.5	29.5	20.0
67.0	26.0	7.0	34.2	35.8	30.0
52.5	37.5	10.0	23.8	36.2	40.0
32.6	47.4	20.0	16.2	33.8	50.0
21.3	48.7	30.0	10.7	29.3	60.0
13.2	46.8	40.0	6.9	23.1	70.0
7.7	42.3	50.0	4.6	15.4	80.0
4.4	35.6	60.0	3.0	7.0	90.0
2.6	27.4	70.0	2.2	0.0	97.8
1.5	18.5	80.0			
1.0	9.0	90.0			
0.7	0.0	99.3			

The tie lines in the docosane–diphenylhexane–furfural system are:

Docosane Phase Composition, wt%			Furfural Phase Composition, wt%		
Docosane	DPH	Furfural	Docosane	DPH	Furfural
Temperature, 45°C:					
85.2	10.0	4.8	1.1	9.8	89.1
69.0	24.5	6.5	2.2	24.2	73.6
43.9	42.6	13.3	6.8	40.9	52.3
Temperature, 80°C:					
86.7	3.0	10.3	2.6	3.3	94.1
73.1	13.9	13.0	4.6	15.8	79.6
50.5	29.5	20.2	9.2	27.4	63.4

8.16 For each of the ternary systems shown in Figure 8.43, indicate whether: (a) simple, countercurrent extraction, or (b) countercurrent extraction with extract reflux, or (c) countercurrent extraction with raffinate reflux, or (d) countercurrent extraction with both extract and raffinate reflux would be expected to yield the most economical process.

8.17 Two solutions, feed F at the rate of 7,500 kg/h containing 50 wt% acetone and 50 wt% water, and feed F' at the rate of 7,500 kg/h containing 25 wt% acetone and 75 wt% water, are to be extracted in a countercurrent system with 5,000 kg/h of 1,1,2-trichloroethane at 25°C to give a raffinate containing 10 wt% acetone. Calculate the number of equilibrium stages required and the stage to which each feed should be introduced, using a right-triangle diagram. Equilibrium data are given in Exercise 8.11.

8.18 The three-stage extractor shown in Figure 8.44 is used to extract the amine from a fluid consisting of 40 wt% benzene (B) and 60 wt% trimethylamine (T). The solvent (water) flow to stage 3

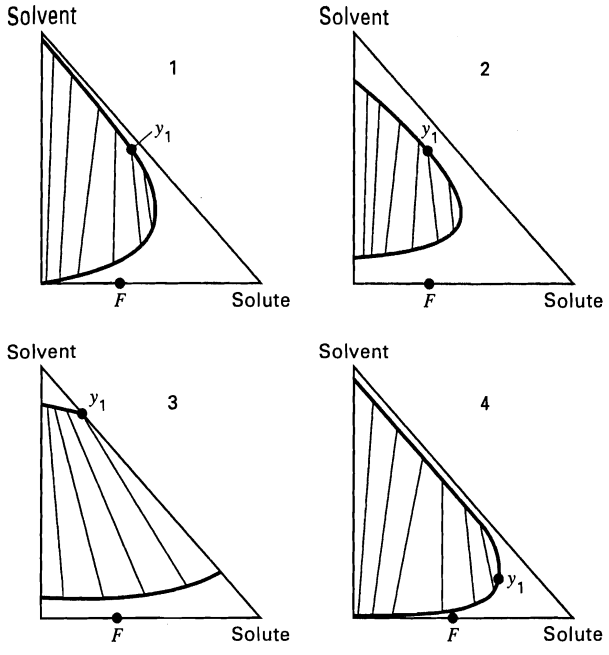

Figure 8.43 Data for Exercise 8.16.

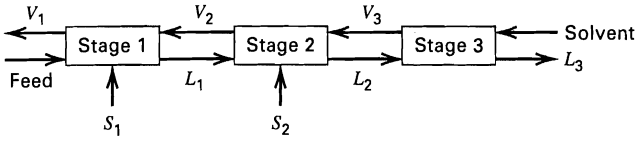

Figure 8.44 Data for Exercise 8.18.

is 5,185 kg/h and the feed flow rate is 10,000 kg/h. On a solvent-free basis V_1 is to contain 76 wt% T and L_3 is to contain 3 wt% T. Determine the required solvent flow rates S_1 and S_2 using an equilateral-triangle diagram. Equilibrium data are given in Exercise 8.14.

8.19 The extraction process shown Figure 8.45 is conducted in a multiple-feed, countercurrent unit without extract or raffinate reflux. Feed F' is composed of solvent and solute, and is an extract-phase feed. Feed F'' is composed of unextracted raffinate and solute and is a raffinate-phase feed. Derive the equations required to establish the three reference points needed to step off the theoretical stages in the extraction column. Show the graphical determination of these points on a right-triangle graph.

8.20 A mixture containing 50 wt% methylcyclohexane (MCH) in *n*-heptane is fed to a countercurrent, stage-type extractor at 25°C. Aniline is used as solvent. Reflux is used on both ends of the column.

An extract containing 95 wt% MCH and a raffinate containing 5 wt% MCH (both on solvent-free basis) are required. The minimum extract reflux ratio is 3.49. Using a right-triangle diagram with the equilibrium data of Exercise 8.22 below, calculate: (a) the raffinate reflux ratio, (b) the amount of aniline that must be removed at the separator "on top" of the column, and (c) the amount of solvent that must be added to the solvent mixer at the bottom of the column.

8.21 In its natural state, zirconium, which is an important material of construction for nuclear reactors, is associated with hafnium, which has an abnormally high neutron-absorption cross section and must be removed before the zirconium can be used. Refer to Figure 8.46 for a proposed liquid–liquid extraction process wherein tributyl phosphate (TBP) is used as a solvent for the separation of hafnium from zirconium.

One liter per hour of 5.10-N HNO_3 containing 127 g of dissolved Hf and Zr oxides per liter is fed to stage 5 of the 14-stage extraction unit. The feed contains 22,000 g Hf per million g of Zr. Fresh TBP enters stage 14, while scrub water is fed to stage 1. Raffinate is removed at stage 14, while the organic extract phase that is removed at stage 1 goes to a stripping unit. The stripping operation consists of a single contact between fresh water and the organic phase. The following table gives experimental data. (a) Use these data to fashion a complete material balance for the process. (b) Check the data for consistency in as many ways as you can. (c) What is the advantage of running the extractor as shown? Would you recommend that all the stages be used?

STAGEWISE ANALYSES OF MIXER-SETTLER RUN

	Organic Phase			Aqueous Phase		
Stage	g oxide/ liter	N HNO_3	(Hf/Zr) × (100)	g oxide/ liter	N HNO_3	(Hf/Zn) × (100)
1	22.2	1.95	<0.010	17.5	5.21	<0.010
2	29.3	2.02	<0.010	27.5	5.30	<0.010
3	31.4	2.03	<0.010	33.5	5.46	<0.010
4	31.8	2.03	0.043	34.9	5.46	0.24
5	32.2	2.03	0.11	52.8	5.15	3.6
6	21.1	1.99	0.60	30.8	5.15	6.8
7	13.7	1.93	0.27	19.9	5.05	9.8
8	7.66	1.89	1.9	11.6	4.97	20
9	4.14	1.86	4.8	8.06	4.97	36
10	1.98	1.83	10	5.32	4.75	67
11	1.03	1.77	23	3.71	4.52	110
12	0.66	1.68	32	3.14	4.12	140
13	0.46	1.50	42	2.99	3.49	130
14	0.29	1.18	28	3.54	2.56	72
Stripper		0.65		76.4	3.96	<0.01

[Data From R.P. Cox, H.C. Peterson, and C.H. Beyer, *Ind. Eng. Chem.*, **50** (2), 141 (1958). Exercise adapted from E.J. Henley and H. Bieber, *Chemical Engineering Calculations*, McGraw-Hill, New York, p. 298 (1959).]

8.22 At 45°C, 5,000 kg/h of a mixture of 65 wt% docosane, 7 wt% furfural, and 28 wt% diphenylhexane is to be extracted with pure furfural to obtain a raffinate with 12 wt% diphenylhexane in a continuous, countercurrent, multistage liquid–liquid extraction system. Phase-equilibrium data for this ternary system are given in

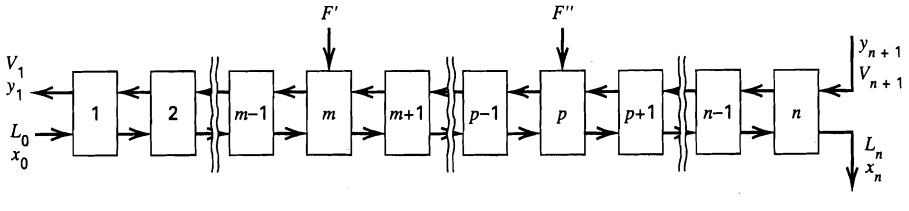

Figure 8.45 Data for Exercise 8.19.

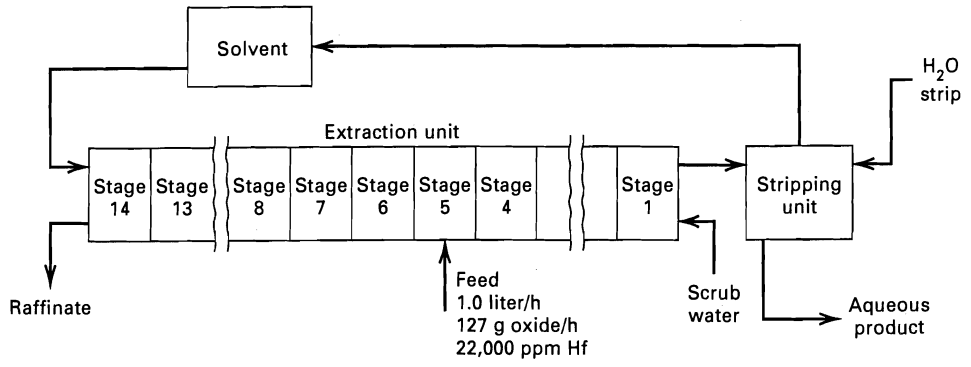

Figure 8.46 Data for Exercise 8.21.

Exercise 8.15. Determine:

(a) The minimum flow rate of solvent.

(b) The flow rate and composition of the extract at the minimum solvent flow rate.

(c) The number of equilibrium stages required if a solvent flow rate of 1.5 times the minimum is used.

8.23 At 45°C, 1,000 kg/h of a mixture of 0.80 mass fraction docosane and 0.20 mass fraction diphenylhexane is to be extracted with pure furfural to remove some of the diphenylhexane from the feed. Phase-equilibrium data for this ternary system are given in Exercise 8.15. Determine:

(a) The composition and flow rate of the extract and raffinate from a single equilibrium stage for solvent flow rates of 100, 1000, and 10000 kg/h.

(b) The minimum solvent flow rate to form two liquid phases.

(c) The maximum solvent flow rate to form two liquid phases.

(d) The composition and flow rate of the extract and raffinate if a solvent flow rate of 2000 kg/h and two equilibrium stages are used in a countercurrent flow system.

8.24 A liquid mixture of 27 wt% acetone and 73 wt% water is to be separated at 25°C into a raffinate and extract by multistage, steady-state, countercurrent liquid–liquid extraction with a solvent of pure 1,1,2-trichloroethane. Phase equilibrium data are given in Exercise 8.11. Determine:

(a) The minimum solvent-to-feed ratio to obtain a raffinate that is essentially free of acetone.

(b) The composition of extract at the minimum solvent-to-feed ratio.

(c) The composition of the extract stream leaving stage 2 (see Figure 8.13), if a large number of equilibrium stages is used with the minimum solvent rate.

Section 8.4

8.25 A feed mixture containing 50 wt% *n*-heptane and 50 wt% methylcyclohexane (MCH) is to be separated by liquid–liquid extraction into one product containing 92.5 wt% methylcyclohexane and another containing 7.5 wt% methylcyclohexane, both on a solvent-free basis. Aniline will be used as the solvent. Using the equilibrium data given below and the graphical method of Maloney and Schubert: (a) What is the minimum number of theoretical stages necessary to effect this separation? (b) What is the minimum extract reflux ratio? (c) If the reflux ratio is 7.0, how many theoretical contacts are required?

LIQUID–LIQUID EQUILIBRIUM DATA FOR THE SYSTEM *n*-HEPTANE/METHYLCYCLOHEXANE/ ANILINE AT 25°C AND AT 1 ATM (101 kPa)

Hydrocarbon Layer		Solvent Layer	
Weight Percent MCH, Solvent-Free Basis	Pounds Aniline/ Pound Solvent-Free Mixture	Weight Percent MCH, Solvent-Free Basis	Pounds Aniline/ Pound Solvent-Free Mixture
0.0	0.0799	0.0	15.12
9.9	0.0836	11.8	13.72
20.2	0.087	33.8	11.5
23.9	0.0894	37.0	11.34
36.9	0.094	50.6	9.98
44.5	0.0952	60.0	9.0
50.5	0.0989	67.3	8.09
66.0	0.1062	76.7	6.83
74.6	0.1111	84.3	6.45
79.7	0.1135	88.8	6.0
82.1	0.116	90.4	5.9
93.9	0.1272	96.2	5.17
100.0	0.135	100.0	4.92

8.26 Two liquids, A and B, which have nearly identical boiling points, are to be separated by liquid–liquid extraction with solvent C. The following data represent the equilibrium between the two liquid phases at 95°C.

EQUILIBRIUM DATA, WT%

Extract Layer			Raffinate Layer		
A, %	B, %	C, %	A, %	B, %	C, %
0	7.0	93.0	0	92.0	8.0
1.0	6.1	92.9	9.0	81.7	9.3
1.8	5.5	92.7	14.9	75.0	10.1
3.7	4.4	91.9	25.3	63.0	11.7
6.2	3.3	90.5	35.0	51.5	13.5
9.2	2.4	88.4	42.0	41.0	17.0
13.0	1.8	85.2	48.1	29.3	22.6
18.3	1.8	79.9	52.0	20.0	28.0
24.5	3.0	72.5	47.1	12.9	40.0
31.2	5.6	63.2		Plait point	

[Adapted from McCabe and Smith, *Unit Operations of Chemical Engineering*, 4th ed., McGraw-Hill, New York, p. 557 (1985).

Determine the minimum amount of reflux that must be returned from the extract product to produce an extract containing 83% A and 17% B (on a solvent-free basis) and a raffinate product containing 10% A and 90% B (solvent-free basis). The feed contains 35% A and 65% B on a solvent-free basis and is a saturated raffinate. The raffinate is the heavy liquid. Determine the number of ideal stages on both sides of the feed required to produce the same end products from the same feed when the reflux ratio of the extract, expressed as pounds of extract reflux per pound of extract product (including solvent), is twice the minimum. Calculate the masses of the various streams per 1,000 lb of feed, all on a solvent-free basis. Solve the problem using equilateral-triangle coordinates, right-triangle coordinates, and solvent-free coordinates. Which method is best for this exercise?

8.27 Solve Exercise 8.20 by the graphical method of Maloney and Schubert.

Section 8.5

8.28 Acetic acid is continuously extracted from a 3 wt% dilute solution in water with a solvent of isopropyl ether in a mixer-settler unit. The flow rates of the feed and solvent are 12,400 and 24,000 lb/h, respectively. Assuming a residence time of 1.5 min in the mixer and a settling vessel capacity of 4 gal/min-ft^2, estimate: (a) Diameter and height of the mixing vessel, assuming $H/D_T = 1$, (b) Agitator horsepower for the mixing vessel, (c) Diameter and length of the settling vessel, assuming $L/D_T = 4$, and (d) Residence time in minutes in the settling vessel.

8.29 A cascade of six mixer-settler units is available, each unit consisting of a 10-ft-diameter by 10-ft-high mixing vessel equipped with a 20-hp agitator, and a 10-ft-diameter by 40-ft-long settling vessel. If this cascade is used for the acetic acid extraction described in the introduction to this chapter, estimate the pounds per hour of feed that could be processed.

8.30 Acetic acid is to be extracted from a dilute aqueous solution with isopropyl ether at 25°C in a countercurrent cascade of mixer-settler units. In one of the units, the following conditions apply:

	Raffinate	**Extract**
Flow rate, lb/h	21,000	52,000
Density, lb/ft^3	63.5	45.3
Viscosity, cP	3.0	1.0

Interfacial tension =13.5 dyne/cm. If the raffinate is the dispersed phase and the mixer residence time is 2.5 minutes, estimate for the mixer: (a) The dimensions of a closed, baffled vessel, (b) The diameter of a flat-bladed impeller, (c) The minimum rate of rotation in revolutions per minute of the impeller for complete and uniform dispersion, and (d) The power requirement of the agitator at the minimum rate of rotation.

8.31 For the conditions of Exercise 8.30, estimate: (a) Sauter mean drop size, (b) Range of drop sizes, and (c) Interfacial area of the two-phase liquid–liquid emulsion.

8.32 For the conditions of Exercises 8.30 and 8.31, and the additional data given below, estimate: (a) The dispersed-phase mass-transfer coefficient, (b) The continuous-phase mass-transfer coefficient, (c) The Murphree dispersed-phase efficiency, and (d) The fraction of acetic acid extracted.

Additional data:

Diffusivity of acetic acid: in the raffinate, 1.3×10^{-9} m^2/s and in the extract, 2.0×10^{-9} m^2/s.

Distribution coefficient for acetic acid: $c_D/c_C = 2.7$

8.33 For the conditions and results of Example 8.4, involving the extraction of benzoic acid, from a dilute solution in water with toluene, determine the following when using a six-flat-blade turbine impeller in a closed vessel with baffles and with the extract phase dispersed, based on the physical properties given: (a) The minimum rate of rotation of the impeller for complete and uniform dispersion, (b) The power requirement of the agitator at the minimum rotation rate, (c) The Sauter mean droplet diameter, (d) The interfacial area, (e) The overall mass-transfer coefficient, K_{OD}, (f) The number of overall transfer units, N_{OD}, (g) The Murphree efficiency, E_{MD}, and (h) The fractional extraction of benzoic acid. Liquid properties are:

	Raffinate Phase	**Extract Phase**
Density, g/cm^3	0.995	0.860
Viscosity, cP	0.95	0.59
Diffusivity of benzoic acid, cm^2/s	2.2×10^{-5}	1.5×10^{-5}

Interfacial tension = 22 dyne/cm

Distribution coefficient for benzoic acid = $c_D/c_C = 21$

8.34 Estimate the diameter of an RDC column to extract acetic acid from water with isopropyl ether for the conditions and data of Exercises 8.28 and 8.30.

8.35 Estimate the diameter of a Karr column to extract benzoic acid from water with toluene for the conditions of Exercise 8.33.

8.36 Estimate the value of HETS for an RDC column operating under the conditions of Exercise 8.34.

8.37 Estimate the value of HETS for a Karr column operating under the conditions of Exercise 8.35.